INFLUENZA A VIRUS INFECTION AND UFMYLATION

by

Alina Butova

Submitted in partial fulfilment of the requirements
for the degree of Master of Science

at

Dalhousie University
Halifax, Nova Scotia
May 2024

Dalhousie University is located in Mi'kma'ki, the
ancestral and unceded territory of the Mi'kmaq.
We are all Treaty people.

Table of Contents

List of Tables

List of Figures

Abstract

This thesis investigates the interplay between UFMylation, a post-translational modification involving the conjugation of the ubiquitin-like protein Ubiquitin-fold modifier 1 (UFM1) to target proteins, and the replication of Influenza A Virus (IAV) strains PR8 and Udorn. Normally, UFMylation plays different roles in the host cell with main function in proteostasis support via stalled ribosomes degradation and ER-phagy. UFMylation also takes part in immune response and exactly antiviral one via supporting retinoic acid-inducible gene I (RIG-I) pathway activation. It was also already showed that UFMylation can affect Hepatitis A (HAV) replication and can be usurped by Epstein–Barr virus (EBV). Our study provides evidence that UFMylation exerts an antiviral effect against the PR8 strain of IAV, suggesting that the UFMylation pathway plays a crucial role in modulating host defense mechanisms against this virus. Furthermore, we demonstrate that a state of hyper-UFMylation is antiviral specifically against the Udorn strain, indicating that the degree of UFMylation can differentially influence the outcome of infections by distinct strains of IAV. Additionally, our findings reveal that IAV infection can alter the UFMylation status of host proteins, suggesting a complex virus-host interaction where the virus can manipulate host cellular pathways to facilitate its replication. Through the use of UFM1-deficient and hyper-UFMylated cell models, we have dissected the impact of UFMylation on the viral life cycle, providing insights into how modifications in the UFMylation pathway can influence the synthesis of viral proteins and, consequently, viral replication. This research not only expands our understanding of the UFMylation process but also unveils a novel aspect of the molecular battle between IAV and its host. By highlighting the antiviral capabilities of UFMylation and its manipulation by IAV, this thesis lays the groundwork for future investigations into treatment strategies that could affect the UFMylation pathway to fight IAV infections.

List of Abbreviations

2XStrep-UFM1delsc – 2XStrep-tagged preactivated UFM1

A - adenine

A549 - adenocarcinomic human alveolar basal epithelial cells

AIMP2 - aminoacyl tRNA Synthase Complex-Interacting Multifunctional Protein 2

ANOVA - analysis of variance

ASC1 - Asc-type amino acid transporter 1

ATF6 - activating transcription factor 6

Atg12 – autophagy-related 12

Atg8 - autophagy-related protein 8

BiP - binding immunoglobulin protein

BSA - bovine serum albumin

C-terminal - carboxy-terminal

Ca2+ - Calcium ions

CARD - caspase recruitment domain

CDK5RAP3 - CDK5 regulatory subunit-associated protein 3

CHIP - chromatin immunoprecipitation

CHOP - C/EBP homologous protein

CLIP-seq - cross-linking and immunoprecipitation

CMA - chaperone-mediated autophagy

CPSF30 - cleavage and polyadenylation specificity factor 30

CQ - chloroquine

CRISPR - clustered regulatory interspaced short palindromic repeats

CRL - cullin-RING ubiquitin ligase

cRNA - complementary RNA

Ct - threshold cycle

CYB5R3 - cytochrome B5 Reductase 3

Cys - Cysteine

DDRGK1 - DDRGK Domain Containing 1

DMEM - Dulbecco's modified Eagle's medium

DMSO - dimethyl sulfoxide

dsRNA - double-stranded ribonucleic acid

DTT - dithiothreitol

E1B-AP5 - E1B-55K-associated protein 5

E6-AP - E6-associated protein

EBV - Epstein-Barr virus

EDEM1 - ER degradation-enhancing alpha-mannosidase-like 1

EDEM2 - ER degradation-enhancing alpha-mannosidase-like 2

EDTA - ethylenediaminetetraacetic acid

eIF2α - eukaryotic Initiation Factor 2 α

eIF4GI - eukaryotic translation initiation factor 4GI

ER - endoplasmic reticulum

ER-Aps – endoplasmic reticulum associated proteins

ER-RQC - ER-associated ribosome-associated quality control

ERAD - ER-associated protein degradation

ERManI - endoplasmic reticulum mannosyl-oligosaccharide 1,2-alpha-mannosidase

FAT10 - human leukocyte antigen (HLA)-F adjacent transcript 10

FBS - fetal bovine serum

G - Guanosine

GCN5 - general control non-depressible 5

Gly - Glycine

GO - Gene Ontology

gRNA - guide RNA

HA - hemagglutinin

HAV - Hepatitis A virus

HDAC6 - histone deacetylase 6

HECT - homologous to the E6-AP Carboxyl Terminus

HEK293T - human embryonic kidney 293 T cells

hpi – hours post infection

HSCs - hematopoietic stem cells

Hsp40 - heat shock protein 40

IAV - Influenza A virus

IFIT2 - interferon-induced protein with tetratricopeptide repeats 2

IFN - interferon

IFNAR - interferon-α/β receptor

IKKα/β - Ikappaα/β kinase

IP - immunoprecipitation

IRE1 - inositol-requiring enzyme type 1

IRF3 - interferon regulatory factor 3

ISR - integrated-stress response

kDa - kilodalton

LE - late endosomes

LIR - LC3 interacting region

M1 - matrix-1

M2 - matrix-2

MAVS - mitochondrial antiviral-signaling protein

MDCK - Madin-Darby canine kidney cells

MDM2 - mouse double minute 2 homolog

MDVs - mitochondrial-derived vesicles

MHC-1 - major histocompatibility complex 1

MLC - myosin-light-chain phosphatase

MOI - multiplicity of infection

mRNA - messenger ribonucleic acid

MTECs - medullary thymic epithelial cells

N-terminal - amino-terminal

NA - neuraminidase

NEDD8 - neuronal precursor cell-expressed developmentally down-regulated protein 8

NEP - nuclear export protein

NF-κB - nuclear factor -κB

NLRP3 - NLR family pyrin domain containing 3

NLS - nuclear localization sequence

NP - nucleoprotein

NS1 - nonstructural protein 1

NT - not targeting

Nup98 - nucleoporin 98 And 96 Precursor

NXF1 - nuclear RNA export factor 1

NXT - nuclear Transport Factor 2 Like Export Factor 1

ORF - open reading frame

PA - polymerase acidic protein

PABII - poly(A)-binding protein II

PAP - poly(A) polymerase

PBS - phosphate-buffered saline

PCAF - P300/CBP-associated factor

PCR - polymerase chain reaction

PEI - polyethyleneimine

PERK - PKR-like ER kinase

PFA - paraformaldehyde

PFU - plaque-forming unit

pfu/ml - plaque-forming unit per milliliter

PI3K - phosphoinositide 3-kinase

PKR - protein kinase R

Pol - polymerase

PTMs – post-translational modifications

qPCR - quantitative polymerase chain reaction

Rae1 - ribonucleic Acid Export 1

RBR - Ring-between-Ring

RdRp - RNA-dependent RNA polymerase

rgPR8 - wild type PR8 obtained by reverse genetics approach

RIG-I - retinoic acid-inducible gene-I

RING - Really Interesting New Gene

RNAPII - RNA polymerase II

rNTP - ribonucleotide tri-phosphate

RFP - ribosomal footprints

RPL26 - 60S ribosomal protein L26

rpm - revolutions per minute

RQC - ribosome quality control

rRNA - ribosomal ribonucleic acid

RT - room temperature

RT-qPCR reverse transcription quantitative polymerase chain reaction

S1P - site-1 protease

S2P - site-2 protease

SCF - Skp, Cullin, F-box containing complex

SD - standard deviation

SDS - sodium dodecyl sulfate

SDS-PAGE - sodium dodecyl sulfate polyacrylamide gel electrophoresis

SEM - standard-error measurement

SenV - Sendai virus

SGs - stress granules

stPR8 - McCormick lab-stock PR8 virus

SUMO - Small Ubiquitin-like Modifier

TAP - transporter associated with antigen processing

TE - translation efficiency

Tg - thapsigargin

TLR3 - Toll-like receptor 3

TLR7 - Toll-like receptor 7

TRIM - tripartite motif

U - uracil

Ub - ubiquitin

Uba1 - ubiquitin-like modifier activating enzyme 1

Uba5 - ubiquitin like modifier activating enzyme 5

Ubl - ubiquitin like modification

UBS - UFC1-binding sequence

Ufc1 - Ubiquitin-Fold Modifier Conjugating Enzyme 1

Ufl1 - UFM1 Specific Ligase 1

Ufm1 - Ubiquitin-fold modifier 1

UFM1 KO - UFM1 knock out

UFSP1 - UFM1 specific peptidase 1

UFSP2 - UFM1 specific peptidase 2

UFSP2 KO - UFSP2 knock out

UIS - UFM1-interacting sequence

UPR - Unfolded Protein Response

UPS - ubiquitin proteasome system

Urm1 - ubiquitin-related modifier-1

USP11 - ubiquitin specific peptidase 11

UTR - untranslated gene

v - viral

v/v - volume per volume

vRNA - viral RNA

vRNP - viral ribonucleoproteins

w/v - weight per volume

XBP1 - X-box binding protein 1

XBP1s - spliced X-box binding protein 1

Xrn1 - 5′-3′ exoribonuclease 1

ZAPL - long isoform of zinc finger antiviral protein

Acknowledgments

The work here was made with the support of my supervisor, Dr. Craig McCormick. I want to thank my committee, Dr. Denys Khaperskyy, Dr. Jean Marshall, Dr. Eric Pringle. They were always supportive and helpful in their comments and suggestions. I would also like to thank my external examiner Dr. Roy Duncan.

I would also like to thank the lab that has always been supportive, but I would like to specifically thank Artem Kichydzhy, Estelle Gamage Samaraweera, Trinity Tooley-Macarandang, and Taylor Caddell.

Finally, I'd like to thank my family for love and support. I`d also like to thank my husband for all possible support that you gave me. I am also very grateful to my cats that were always near me while I were writing my thesis.

.

Chapter One - Introduction

1.1 Influenza A virus

Influenza A virus (IAV) is a member of the Orthomyxoviridae family that causes seasonal epidemics and occasional pandemics. It is a negative-sense RNA virus with a segmented genome consisting of eight RNA segments. It is classified into various subtypes based on the two major surface glycoproteins, hemagglutinin (HA) and neuraminidase (NA), which exhibit antigenic diversity. The virus is highly contagious and primarily infects avian and mammalian species, including humans, making it highly adaptable and prone to antigenic shifts and drifts (Kim et al., 2018; Webster, 1999). Antigenic drift is gradual accumulation of mutations in genes that encode HA and NA proteins that enable evasion of neutralizing antibodies. Antigenic shifts happen when two different strains of the virus infect the same cell and exchange genetic material creating a new hybrid virus with mixed properties including surface glycoproteins that can likewise evade neutralization.

The virus has an enveloped structure with a lipid bilayer derived from the host cell membrane. The surface glycoproteins HA and NA are embedded in the lipid envelope. HA promotes virus attachment to host cells through interactions with sialic acid receptors, whereas NA facilitates the release of newly formed virions from infected cells by cleaving cell surface sialic acid. The replication cycle of Influenza A virus begins with viral attachment to host cell receptors followed by endocytosis. Acidification of the endosome triggers fusion of the viral envelope with the endosomal membrane, releasing viral ribonucleoprotein complexes (vRNPs) into the cytoplasm. vRNPs include one negative-sense genomic RNA associated with nucleoproteins (NP) and one trimeric polymerase complex (includes polymerase basic 2 (PB2), polymerase basic 1 (PB1), and polymerase acidic protein (PA)). The vRNPs are then transported to the nucleus, where viral RNA transcription and replication occur. Viral RNA-dependent RNA polymerase (RdRp) does both viral transcription and genome replication in the cell nucleus. Viral genome replication occurs in two steps – firstly, complementary RNA (cRNA) is synthesized and then viral RNA (vRNA) is synthesized from the cRNA template. Viral mRNAs are exported from the nucleus to the cytosol to be translated on cytosolic ribosomes. Newly made RdRp and NP are moved back to the nucleus where they are

assembled together with viral genome. Virus assembly is happening when all viral newly synthesized proteins are transported to plasma membrane where HA and NA associate with lipid drafts that are the place of IAV budding (Matsuoka et al., 2013) (Figure 1-1).

IAV targets respiratory tract leading to symptoms that can include fever, sore throat, cough, runny nose, body pain, headache, fatigue and chills. In some cases, infection can lead to pneumonia, acute respiratory distress syndrome and death in high-risk groups such as the elderly and young children (Monto et al., 2000).

1.1.1 Discovery of IAV

IAV has had a big impact on human history. The earliest recorded accounts of influenza-like illnesses were in ancient Greece, where Hippocrates in 412 BCE identified disease remarkably similar to modern-day influenza symptoms. The initial effort to isolate and characterize influenza virus was undertaken in 1892 by Richard Pfeiffer. He attempted to extract the virus from nasal samples of influenza patients. However, he instead isolated a small rod-shaped bacterium that was named *Bacillus influenzae* (or *Pfeiffer's bacillus*). This misled scientists for some period of time and made them believe that bacteria caused influenza. During the 1918 influenza pandemic, it was discovered that the Pfeiffer`s bacillus was not the actual infectious cause of influenza. This conclusion was reached when samples from infected animals were passed through a filter fine enough to block bacteria and the filtrate was infectious and caused influenza. In 1929, there was an outbreak of disease very similar to influenza in pigs. It was called Swine Influenza and caught the attention of Richard Shope. He isolated *Pfeiffer`s bacillus* from pigs but when he injected it to healthy individuals – no disease happened. Shope obtained filtrate using the same method as before and discovered that the main causative agent of disease is in filtrate but also that when combined with Pfeiffer`s bacillus it caused even more severe illness in pigs. He concluded that the primary infectious agent was a virus. Subsequently, it was also found that serum from individuals who had influenza in 1918 could neutralize the virus. This moment marked the inception of a new era in our understanding of influenza (Potter, 2001; Mamelund, 2008).

1.2 Molecular biology of IAV

1.2.1 IAV replication cycle

The influenza virus features an enveloped structure with shapes that can vary from round to thread-like. The form of the virus is influenced by multiple factors, such as its own genetic makeup and the characteristics of the cells it infects.

The viral particle has a lipid layer that it acquires from the host cell, and within this layer are three essential proteins: HA, NA, and Matrix-2 protein (M2). HA, which exists as a trimer, facilitates attachment to cell surface sialic acid receptors and fusion with cellular membranes (Schulze, 1972; Fujiyoshi et al., 1994). On the other hand, NA, a tetramer, is responsible for breaking down receptors by splitting sialic acid molecules, thus facilitating the release of new viruses (Yoshimura et al., 1982). The M2 protein serves as an ion channel, helping to lower the pH inside the virus which is required to facilitate uncoating. Firstly, at a pH range of approximately 5.5 to 6.0, the M1 protein shell within the virus dissolves. Secondly, the acidic conditions within the endosome induce conformational changes in the influenza surface protein HA, leading to the fusion of viral and endosomal membranes. This fusion event enables the release of the vRNPs (eight segments of viral RNA are connected to the NP protein and the virus's RNA polymerases) into the perinuclear cytosol through the formation of a fusion pore (Grambas & Hay, 1992; Bui et al., 1996).

Among the proteins in the virus, NP is second only to matrix protein 1 (M1) in abundance and attaches to the vRNA in a sequence-independent manner. The RNA polymerase complex is made up of three different subunits, namely PB2, PB1, and PA. Images taken through cryo-electron microscopy showed that the vRNA within these RNP complexes forms a loop or twisted coil, with its ends in contact with the RNA polymerase (Chang et al., 2015; Chenavier et al., 2023). All proteins in vRNPs have Nuclear Localization Signals (NLS) to enter the nucleus of the host cell (Cros et al., 2005). The process of importing influenza virus ribonucleoproteins (vRNPs) into the nucleus of host cells involves interactions with key proteins involved in nuclear import, such as importin α and β (Pumroy et al., 2015). Initially, the vRNPs utilize nuclear localization sequences present on the numerous NP molecules to bind to the adapter protein importin-α. Subsequently, importin-α binds to importin-β, which serves as a transport receptor,

facilitating the movement of the vRNP-importin complex to the nuclear pore complex. Here, the vRNP is transported into the nucleoplasm (Nakada et al., 2015).

The IAV genome comprises eight segments. Messenger RNAs (mRNAs) from segments 1 and segments 3 to 6 produce a single protein each, making them monocistronic. Segment 2 of the genome encodes the polymerase basic (PB) proteins PB1, PB1-F2, and PB1-N40 through alternative translation initiation sites (Wise et al., 2009). Segment 3 encodes the PA protein variants PA and PA-X by ribosomal frameshifting and also produces two truncated forms, PA-N155 and PA-N182, using alternative translation initiation sites (Jagger et al., 2012). Lastly, segment 7 is responsible for producing M1 and the ion channel proteins M2 and M42 (Wise et al., 2012). Segment 8 encodes the nonstructural (NS) proteins NS1 and NS2/NEP (nuclear export protein), as well as NS3, through alternative mRNA splicing (Lamb & Choppin, 1979; Selman et al., 2012; O'Neill et al., 1998).

In the nucleus, the viral RNA-dependent RNA polymerase, composed of three subunits, PA, PB1, and PB2, orchestrates the transcription and replication of viral RNAs. This process involves two main steps: synthesis of complementary RNA (cRNA), followed by the synthesis of new viral RNA copies using the cRNAs as templates. cRNAs are synthesized through the complementation of free ribonucleotides (rNTPs) with the 3' end of the viral RNA template, forming an A-G dinucleotide that serves as the starting point for cRNA elongation. PB1 subunit plays role of catalytic subunit during cRNA synthesis (Nakagawa et al., 1996). These cRNAs then bind with newly formed NP molecules and viral polymerase to form cRNP complexes (Moeller et al., 2012).

Transcription of viral mRNA from vRNA templates is initiated by a priming mechanism, which enhances efficiency compared to cRNA and vRNA transcription. This process, known as cap snatching, involves the acquisition of primers by the viral polymerase through its interaction with the cellular RNA polymerase II C-terminal domain. During cap snatching, the viral polymerase, particularly the PB2 subunit, binds to 5' caps of host transcripts and cleaves downstream of the cap using the PA subunit endonuclease domain. The acquired capped primer is then utilized for mRNA extension using the vRNA as a template (Dias et al., 2009). Subsequently, each transcribed mRNA undergoes polyadenylation. Polyadenylation of viral mRNAs is distinct compared to

cellular mRNAs, as viral mRNAs lack the typical polyadenylation signal (AAUAAA). Instead, the viral RNA polymerase stochastically adds poly(A) tails to viral RNA templates, facilitated by a stretch of U residues near the 5' end of each viral segment (Poon et al., 1999; Luo et al., 1991). Additionally, the NS1 protein helping this process by inhibiting the nuclear export of cellular mRNAs (Qiu & Krug, 1994).

The virus utilizes the host cell's splicing machinery for producing multiple viral proteins while concurrently inhibiting the splicing of cellular mRNAs (Artarini et al., 2019). NP interacts with splicing factors like ATP-dependent RNA helicase uap56 (UAP56), influencing mRNA processing and nuclear export (Momose et al., 2001).

During the early stage, the virus predominantly produces NS1 and NP vRNA, thereby making these proteins the major components in infected cells at this point (Vester et al., 2010). While the specific roles of NS1 and NP in this phase are still not completely clear, they are thought to possibly be involved in regulating both viral and host cell gene expression. In the subsequent late stage, all types of vRNAs are synthesized in balanced quantities to compile the genome for new viral particles. Here, the production of NS1 protein is decreased, while there's an upsurge in the creation of HA, NA, and M1 mRNAs (Shapiro et al., 1987). The majority of the capped and polyadenylated viral mRNAs move from the cell nucleus to the cytoplasm to undergo protein synthesis. By contrast, membrane-bound proteins such as HA, NA, and M2 follow a specialized secretory route via the trans-Golgi network for further maturation (Dou et al., 2018). Both HA and NA proteins undergo additional post-translational modifications before they are integrated into the cellular membrane (Tatu et al., 1995; Ueda et al., 2008; Hogue & Nayak, 1992) (Figure 1-1).

1.2.2 Viral-host interactions: role in homeostasis and immune response

IAV are intracellular parasites that require host cell machinery to replicate its genome and produce new viral proteins. Moreover, IAV usurp host cell defensive mechanisms and use them to hide from immune response. It can be said, that virus adapt host cellular mechanisms to remodel all cellular space to facilitate infection. In this section I will discuss what exact cellular systems IAV modifies and uses for its own benefit.

1.2.2.1 How can influenza A viruses affect cellular proteostasis mechanisms?

Proteostasis is the process of maintaining cellular homeostasis of proteome via protein synthesis and turnover. It is essential for maintaining cellular function and health and when it is disrupted protein overload leads to cellular dysfunction and death (Díaz-Villanueva et al., 2015; Sala et al., 2017). Changed proteostasis is important factor that can help the virus to gain priority for its protein production and inhibit antiviral response by reduction of host cellular protein synthesis and enhanced degradation of chosen host proteins. IAV can change proteostasis in the host cell in different ways: interacting with machinery that regulates it (ubiquitin, autophagy machinery), or changing the host protein synthesis or mRNA amounts by inducing mRNA degradation (Marreiros et al., 2020; Marques et al., 2019).

1.2.2.1.1 Host mRNA synthesis and processing

Host mRNAs must be properly transcribed, post-transcriptionally modified and exported to the cytoplasm to access translation machinery. These intermediate steps in protein synthesis are attractive targets for host shutoff, a primary mechanism by which IAV gains priority access to host translation apparatus and limits host antiviral response. Significant viral components in this process are the ribonuclease PA-X and NS1 proteins (Khaperskyy & McCormick, Timing is everything: coordinated control of host shutoff by influenza A virus NS1 and PA-X proteins., 2015; Chaimayo et al., 2018).

The third segment of the influenza virus genome encodes a protein known as PA, but it also produces another protein, PA-X, through a process called ribosomal frameshifting into an alternative open reading frame, named the X ORF. PA-X is a protein with a size of 29 kDa, and it contains the endonuclease domain of PA at its N-terminus and, also, a 61-amino-acid sequence from the X ORF at its C-terminus. This protein plays significant roles in halting the synthesis of proteins in host cells by targeting the mRNAs that encode them. PA-X targets and degrades the host's cellular mRNAs and certain non-coding RNAs, without affecting the virus's own mRNAs. PA-X's selectively targets mRNAs produced by host RNA polymerase II (Pol II) while sparing those from Pol I and Pol III. Additionally, PA-X can degrade Pol II transcribed RNAs, including non-coding RNAs and transcripts with RNA hairpin structures, primarily within the cell nucleus where it predominantly resides (Hayashi et al., 2015). This nuclear concentration

of PA-X correlates with a marked reduction of its target RNAs. Following PA-X endonuclease cleavage of target mRNAs, cleaved mRNAs are rapidly degraded by the host 5′-3′ exoribonuclease 1 (Xrn1). Notably, IAV mRNAs, despite their structural parallels with host mRNAs, resist PA-X-mediated degradation. However, a deficiency of PA-X disrupts the synthesis of certain viral mRNAs, leading to decreased viral protein accumulation (Khaperskyy D. A. et al., 2016).

The huge role of PA-X in reducing host immune response was showed in study made by Hayashi and colleagues. They used WT A/California/04/09 (H1N1, Cal) and recombinant H1N1, Cal, containing mutations at the frameshift motif in the polymerase PA gene (Cal PA-XFS) which express much less PA-X. Cal WT suppressed the expression of beta interferon (IFN-β) and replicated more rapidly than Cal PA-XFS in human respiratory cells. In mice, infection with Cal PA-XFS resulted in significantly reduced viral growth and higher levels of Interferon-β (IFN-β) mRNA in their lungs compared to those infected with Cal WT. These results suggest key role of PA-X in suppressing host IFN-response (Hayashi et al., 2015).

Another IAV protein that plays important role in switching priority of expression from host mRNAs to viral one is NS1. The NS1 protein is encoded by IAV genome segment 8. NS1 typically consists of 230 amino acids, but variations in its length can occur due to mutations that either extend or shorten the protein (Hale et al., 2008). Historically, the length of the NS1 protein has changed, with human IAV NS1 proteins having additional amino acids at the end for several decades in the 20th century, while the 2009 pandemic H1N1 strain, similar to most swine H1N1 strains, has a shorter NS1 with 219 amino acids (Evseev & Magor, 2021). NS1 proteins from certain human and avian IAV strains can bind host 30 kDa subunit of cleavage and polyadenylation specificity factor (CPSF) and prevent cleavage and polyadenylation of host mRNAs. As a result, the NS1 protein can suppress host genes expression by trapping pre-mRNAs in the nucleus (Nemeroff et al., 1998). NS1 also inhibits Poly(A)-binding protein II (PABII) – a cofactor in polyA tail synthesis. Consequently, influenza-infected cells produce cellular pre-mRNAs with significantly shorter poly(A) tails, around 12 nucleotides in length, due to the NS1 protein's interference. These mRNAs that contain short poly(A) tails cannot be exported from the nucleus to cytoplasm to be translated (Chen et al., 1999).

NS1 interacts with components of the mRNA export machinery, such as Nuclear RNA export factor 1 (NXF1), NTF2-related export protein 1 (NXT), ribonucleic acid export 1 (Rae1), and Heterogeneous nuclear ribonucleoprotein U-like protein 1 (E1B-AP5), forming a complex that inhibits the normal process of mRNA transport through the nuclear pore complex. Elevated amounts of NXF1, p15, or Rae1 can counteract the blockade of mRNA export caused by NS1. Additionally, the influenza virus decreases the levels of nuclear pore complex protein 98 (Nup98), a nucleoporin that serves as a critical anchoring point for factors involved in mRNA export (Satterly et al., 2007).

However, before the polyadenylation process and export can be even started NS1 can disrupt transcription termination, at least NS1 of some IAV strains. Only NS1 RNA-binding domain and C-terminal domain are shared between multiple strains. At the same time, C-terminal domain is very divergent among strains and can bear different sites for post-translational modifications (PTMs). In the study made by Zhao and colleagues, using viruses carrying the 1918 H1N1 NS1, the researchers unveil that IAV disrupts the termination of RNAPII transcription, resulting in widespread transcriptional deregulation. This disruption is amplified by NS1 SUMOylation, which enhances the accumulation of NS1 in nuclear granules containing factors responsible for 3′-end cleavage. These termination issues lead RNAPII to traverse intergenic regions, ultimately generating abnormal mRNA and causing a global decrease in transcription (Zhao et al., 2018).

These results are important not only in the context of IAV interactions with host cell machinery but also in the context of the significant role of host post-translational modifications for viral replication cycle.

1.2.2.1.2 Host protein synthesis

IAV can manipulate not only amount of host mRNAs by degrading them or inhibiting their export from nucleus but also affect translation in the host cell in different ways. One of the studies delves into the role of NS1, a protein known to affect mRNA processing within cells, including polyadenylation, splicing, and mRNA movement. NS1 also selectively by binding to eukaryotic translation initiation factor 4 gamma 1 (eIF4GI) (Aragón et al., 2000). EIF4GI is a vital part of the eukaryotic initiation factor 4F (eIF4F) complex, crucial for cap-binding in translation initiation. This NS1-eIF4GI interaction was confirmed in both IAV infected cells and cells transfected with NS1 cDNA. In-depth

investigations revealed that NS1 binds directly to a specific region of eIF4GI, located between amino acid residues 157 and 550, and this interaction doesn't involve the Eukaryotic translation initiation factor 4E (eIF4E) subunit. Notably, this eIF4GI region hasn't been associated with any other translation components. Moreover, the binding is RNA-independent. Within NS1, the domain responsible for this binding encompasses amino acids 82 to 113. A mutation in NS1, excluding the first 81 amino acids, hinders its translation-enhancing capability. In essence, the research suggests that NS1 aids in drawing eIF4GI to the 5' untranslated region (5' UTR) of viral mRNA, prioritizing the translation of IAV mRNAs.

The RNA-dependent protein kinase, known as Protein kinase R (PKR), plays a key role in the defense against viruses by being part of the interferon signaling system. PKR is activated when it binds to viral double-stranded RNAs. Once activated, PKR phosphorylates the α-subunit of the eukaryotic translation initiation factor 2 (eIF2α), which blocks translation at the initiation step. The generation of viral dsRNAs should therefore threaten the replication of RNA viruses including IAVs. Eriko Hotada and colleagues showed that NS1protein can efficiently bind dsRNAs in vitro (Hatada & Fukuda, 1992). However, later it was shown that NS1A lacking RNA-binding domain does not affect inhibition of PKR thus it is not a mechanism by which PKR activity is inhibited during infection (Li et al., 2006). Next experiments demonstrated that NS1 binding to dsRNAs is not for inhibition IFN- β synthesis but rather for protection of IAV from the antiviral state of the cell induced by IFN- β. NS1 dsRNAs binding protect virus by inhibiting IFN-α/β-induced 2′-5′-oligo (A) synthetase (OAS)/RNase L pathway (Min & Krug, 2006).

Another interesting question that should be answered: how IAV mRNAs, generated by a viral RdRp, have structural features like host RNA Polymerase II products, are not vulnerable to regulation by eIF2α kinases, activated by stresses like viral infection? Such activation could halt the translation of both viral and host mRNAs, leading to their storage in stress granules (SGs). In cellular biology, stress granules are tiny, droplet-like clusters that form inside a cytosol when the cell experiences stress (Protter & Parker, 2016). These granules are made up of a mix of proteins and RNA molecules. Specifically, the RNA these granules is part of halted complexes that are just

starting the process of translation. These complexes include small ribosomal units (40S subunits), translation initiation factors, messenger RNAs, and proteins that bind to RNA (RNA-binding proteins or RBPs). Formation of SGs during viral infection can lead to inhibition of viral protein synthesis. The study conducted by Khaperskyy and colleagues showed no SG formation during IAV replication. It was found that three IAV proteins—NS1, NP, and PA-X—prevent SG formation and thus – viral mRNAs being trapped in the SGs. NS1 interacts with viral dsRNA, and inhibits PKR activation and subsequent eIF2α phosphorylation. NP blocks SG formation independently of eIF2α, however, the mechanism needs still to be identified. PA-X, through its endoribonuclease activity described before, curtails SG formation by decreasing cytoplasmic poly(A) RNA levels. This decrease leads to lower load of the host mRNAs and subsequent lower burden on ribosomes (Khaperskyy et al., 2014). All these together lead to increase in translation efficiency of viral proteins.

To gain priority in protein synthesis, it is important for virus to redirect ribosomes to the translation of viral mRNAs. In the study made by Panthu and colleagues it was shown that NS1 can associate with ribosomes to perform this function (Panthu et al., 2017). However, the precise mechanism by which NS1 accomplishes this has remained unclear. To gain a better understanding, a comprehensive investigation into NS1's role in translation was conducted in mentioned study. This involved a combination of influenza infection, transfection of mRNA reporters, and *in vitro* functional and biochemical assays. It revealed that NS1 has the capacity to enhance the translation of nearly all tested mRNAs, except for those carrying Internal ribosome entry segments (IRESes). This suggests that NS1 primarily influences translation initiation. It was identified that the specific domain of NS1 responsible for promoting translation is located in the amino-terminal motif of the protein, with particular emphasis on residues R38 and K41, which play a critical role in this function. While it was observed that NS1 can directly bind to mRNAs, this binding doesn't consistently correlate with its ability to boost translation. Instead, NS1's translation-enhancing activity depends on its capacity to associate with ribosomes and guide them to target mRNAs.

It was also shown that IAV can subvert some of the host factors that were known to be antiviral. Tran and colleagues used CRISPR-Cas9 technology to investigate how

host cells respond to influenza virus infection. Contrary to previous beliefs, it was found that Interferon-induced protein with tetratricopeptide repeats 2 (IFIT2), a factor activated in response to viral infections, aids the influenza virus's gene expression rather than counteracting it (Tran et al., 2020). Through CLIP-seq analysis, the study revealed that IFIT2 attaches to specific regions of both viral and host cell RNA, especially those activated during viral infections. This binding facilitates better RNA translation and promotes protein synthesis. In essence, while IFIT2 usually strengthens antiviral defenses by enhancing cellular RNA translation, the influenza virus manipulates it to support its own replication.

1.2.2.1.3 IAV host shutoff and Translation Efficiency (TE)

Host mRNAs are required to produce any protein on ribosomes, thus mRNA synthesis, mRNA transportation from nucleus to ribosomes in functional state is so important for host cell. In one of the studies, it was shown that IAV can affect the host translation efficiency (TE) during infection but not only by suppressing host mRNAs production (Bercovich-Kinori et al., 2016). In the study made by Berkovich-Kinori the researchers found that viral genes' TE was similar to host genes, suggesting that IAV doesn't prioritize its transcripts during translation. The dominant factor in host gene suppression is the overwhelming presence of viral mRNAs in the cell, with viral mRNAs constituting over 53.8% of the translation activity by 8 hours post-infection. Ribosome footprints (RFPs) were analyzed to evaluate the amount of host and viral transcripts. RFPs are segments of mRNA that are shielded by ribosomes during the process of translation. By comparing RFPs with the transcriptome, researchers can obtain a detailed view of translation activity across the entire set of mRNA molecules in a cell. In the study it was found that 74% of host transcripts had reduced RFPs, indicating a decrease in host protein synthesis. Although many genes showed reduced activity, some genes, particularly those related to antiviral defense, were upregulated, while others remained unchanged. The most affected genes were linked to DNA repair and the cell cycle, whereas the least affected were related to oxidative phosphorylation and ribosomal proteins. Using the Babel computational framework, the research identified 210 cellular mRNAs with varied translation responses to IAV. Although the study did not find

significant functional categories in the Gene Ontology (GO) enrichment analysis, there was an increased translation of certain genes linked to the phosphorylation of eIF2α at 4 hours post-infection, a stress response in cells. Western blot tests confirmed this phosphorylation, and other proteins translation patterns, reinforcing the study's findings. These results were consistent with previous studies that pointed that the main protein of host shutoff during IAV infection is not NS1 but PA-X (Khaperskyy D. A. et al., 2016). It was also found that mRNAs levels were reduced both in cytoplasm and nucleus which is consistent with PA-X strong activity in the nucleus. The fact that level of reduction of mRNAs correlate with GC content and length pointed that it is not selective degradation that depends mostly on amount of exposed ssRNA which also pointed to PA-X preference to ssRNA in earlier studies (Bavagnoli et al., 2015).

1.2.2.1.4 Host catabolic mechanisms - autophagy

Autophagy is one of the degradative pathways that cells use to degrade and recycle their own components and regulate cellular homeostasis which is the state of balance between extra- and intracellular metabolite concentrations and proteostasis which is the state of balance in proteins building and turnover. IAV is known to interact with different mechanisms of autophagy and regulate them for its own benefit. Autophagy is divided into several distinct processes including microautophagy, macroautophagy, and chaperone-mediated autophagy (CMA) (Nie et al., 2021). Microautophagy involves the direct engulfment of cytoplasmic material by the lysosome and is used to handle smaller cargo compared to macroautophagy. Macroautophagy involves the formation of a double-membrane vesicle known as an autophagosome. The autophagosome envelops damaged organelles, protein aggregates, or portions of cytoplasm, then fuses with a lysosome to form an autolysosome. CMA is a selective type of autophagy that targets specific proteins for degradation. Proteins marked for CMA contain a pentapeptide motif recognized by chaperone proteins. These chaperones escort the targeted proteins directly to the lysosome, where they bind to a receptor on the lysosomal membrane. The protein is then unfolded and translocated into the lysosome for degradation.

It was shown that IAV inhibits macroautophagy, at the point where autophagosomes merge with lysosomes. The research made by Gannagé and colleagues

identifies the viral protein M2 as the mediator of this block in autophagosome degradation. This inhibition of macroautophagy results in increased cell death among infected cells and higher release of viral antigens which is important for late stages of IAV infection (Gannagé et al., 2009). Beale et al. showed that the cytoplasmic tail of the IAV M2 protein directly interacts with microtubule-associated protein 1A/1B-light chain 3 (LC3), a critical autophagy protein, causing LC3 to relocate to the plasma membrane, an unexpected destination. This interaction is facilitated by a conserved LC3-interacting region (LIR) within M2. The presence of the M2 LIR is crucial for directing LC3 to the plasma membrane in cells infected with the virus. Alterations to the M2 protein that disrupt its ability to bind LC3 impede the process of filamentous budding, resulting in less stable viral particles (Beale et al., 2014). Thus, IAV manipulates autophagy by imitating a host protein-protein interaction motif, a tactic that likely helps the virus spread more effectively between hosts by increasing the stability of its viral offspring.

1.2.2.1.5 The place where all starts - Endoplasmic Reticulum: ER stress and Unfolded Protein Response

Besides manipulation host mRNA synthesis, protein synthesis and degradation, IAV can change cellular proteostasis in other ways. When the ER is overloaded with newly synthesized proteins that exceed folding capacity,3 transmembrane ER stress sensors are triggered – serine/threonine-protein kinase/endoribonuclease inositol-requiring enzyme 1 (IRE1), Activating transcription factor 6 (ATF6) and protein kinase R (PKR)-like endoplasmic reticulum kinase (PERK) (Hetz et al., 2020). These sensors initiate the transcriptional response called Unfolded Protein Response (UPR). IRE1α is a type I transmembrane protein that has both serine/threonine kinase and an endoribonuclease domain. It becomes active when chaperone binding immunoglobulin protein (BiP) is released from it due to an accumulation of unfolded proteins. Upon activation, IRE1α uses its endoribonuclease domain to splice the mRNA of the transcription factor X-box binding protein 1 (XBP-1). Similarly, PERK, another type I transmembrane protein after activation phosphorylates the alpha subunit of the eukaryotic translation initiation factor 2 (eIF2α) on serine 51, which leads to a reduction in protein synthesis and, consequently, fewer proteins appearing in ER. Activating transcription factor 4 (ATF4) still can be produced and plays role of transcriptional factor that controls transcription of genes that are required for apoptosis, antioxidant response, autophagy

and amino acids turnover. ATF6, a type II transmembrane protein, responds to the accumulation of unfolded proteins by moving to the Golgi, where it is cleaved by site-1 protease (S1P) and site-2 protease (S2P). This cleavage releases its N-terminal domain, which moves to the nucleus as a transcriptional factor to initiate the transcription of specific genes, including BiP, Glucose-regulated protein 94 (GRP94), and calnexin, aimed at mitigating the stress.

Accumulation of viral newly synthesized proteins (HA and NA) in ER can trigger ER stress and UPR (Frabutt et al., 2018). However, it was shown that IAV can successfully manipulate UPR for its own benefit and change proteostasis in this way (Landeras-Bueno et al., 2016; Mazel-Sanchez et al., 2021).

Prior research on HA of the IAV indicated that when misfolded viral proteins are present in the ER, they trigger the production of BiP and GRP94 (Hurtley et al., 1989). Influenza HA is initially produced as a single unit and then moves across the ER membrane, assembling into a trimer. However, certain HA mutants that cannot exit the ER have folding defects. As a result, these misfolded versions of HA stimulate the production of BiP and GRP94, unlike the properly folded HA.

Glycosylation patterns, especially in HA, significantly influence UPR. Decreased glycosylation in HA's head domain increases UPR (Hrincius et al., 2015), whereas additional glycosylation sites mitigate inflammation and reduce ER stress gene expression in infected mice (Sun et al., 2013). Similarly, variations in glycosylation correlate with differences in viral replication and virulence among IAV strains which is particularly important in the context of the current study which investigates also if different strains of IAV with different variations of HA can affect UFMylation pathway located in ER in different ways. Influenza virus HA glycoprotein also activates a strong antiviral response by inducing ER stress through ER-associated protein degradation (ERAD) that mediates HA degradation. Three critical α-mannosidases— ER Degradation Enhancing Alpha-Mannosidase Like Protein 1 (EDEM1), ER Degradation Enhancing Alpha-Mannosidase Like Protein 2 (EDEM2), and ER alpha-1, 2-mannosidase (ERManI)—are identified in this process, with gene silencing enhancing HA expression (Frabutt et al., 2018).

The role of NA in UPR is also connected with its interaction with the chaperone protein BiP across various IAV strains. It was shown that the level and specific sequence of the NA protein are vital in triggering ER stress. Most IAV strains tend to maintain a modest ER stress level, aiding glycoprotein folding and minimizing the activation of the potentially detrimental UPR. IAV has developed various strategies to keep ER stress levels low, such as modulating NA expression, generating a more foldable NA less detectable by BiP, or interfering with host protein synthesis (Mazel-Sanchez et al., 2021).

Accessory proteins, such as IAV's NS1, can suppress the UPR, especially the PERK pathway. NS1 achieves this through mentioned above interactions with double-stranded RNA (dsRNA) and by binding to pre-mRNA processing protein CPSF30. Within the UPR during IAV infection, the IRE1 pathway is predominant, with both positive and negative implications for the virus. It boosts ER chaperone levels, facilitating protein folding, but also degrades some viral proteins. The UPR also promotes a redox environment favorable for viral replication and decreases major histocompatibility complex class I molecules (MHC-1) expression, aiding immune evasion. Also, IRE1-induced Protein Kinase Inhibitor Of 58 kDa (P58IPK) inhibits eIF2α phosphorylation, supporting viral mRNA translation. At the same time, other studies pointed on the fact that in murine primary tracheal epithelial cells (MTECs), IAV infection induces ER stress through ATF6 but not C/EBP homologous protein (CHOP). This ER stress leads to apoptosis via caspase-12 (Roberson et al., 2012).

1.2.2.1.6 The role of IAV proteins in Immunity and inflammation

Limiting host immune mechanisms is a key mechanism for the successful generation of viral progeny. IAV proteins interact with various cellular pathways to limit inflammation and limit host immune response. Recent studies have linked the UFMylation pathway is linked to RIG-I-mediated antiviral immune responses that are known to respond to IAV infection. Thus, in this subsection, IAV interaction with antiviral defense and inflammation mechanisms are discussed.

Tripartite motif (TRIM) proteins are key regulators across various biological functions, particularly in modulating a broad spectrum of signaling pathways that drive immune responses. Most TRIM proteins are known for their E3 ubiquitin ligase activity,

which is central to the process of polyubiquitination of specific target proteins. Recent research underscores the pivotal role of TRIM proteins in the immune system, where they influence the function of pattern recognition receptors, crucial adaptor molecules, kinases, and transcription factors integral to immune signaling. Furthermore, the involvement of TRIM proteins in adaptive immunity, especially concerning the development and activation of T cells, is gaining recognition. TRIM proteins, especially TRIM19, TRIM5α, and TRIM25, play crucial roles in antiviral defenses (Ozato et al., 2008). NS1 impedes type I IFN production in the host by binding directly to TRIM25, consequently hindering the RIG-I-mediated IFN production. This allows the virus to sidestep immune defenses. Intriguingly, NS1 proteins from different influenza strains can all bind TRIM25, indicating a conserved evasion tactic, though sequence variations might alter the binding strength and virulence. Furthermore, NS1 deploys multiple methods to reduce IFN response: it sequesters RNA, preventing cellular sensors like RIG-I from detecting it, and curbs TRIM25's E3 ligase activity, reducing IFN production (Gack et al., 2009; Koliopoulos et al., 2018).

NS1 inhibits Interferon regulatory factor 3 (IRF3) activation, a key step in RIG-I signaling (Talon et al., 2000). IRF3 is an interferon regulatory factor 3 which is a key factor for IFN-α/β production. NS1's effectiveness in suppressing RIG-I varies among IAV strains; proteins with an E at position 196 block IRF3 more efficiently than those with K196 (Kuo et al., 2010). NS1 also disrupts the nuclear factor kappa-light-chain-enhancer of activated B cells (NF-κB) pathway which is essential for activating antiviral response (Gao et al., 2012). NS1 binds via its C-terminal effector domain to enzymes IkappaB kinase α/β (IKKα/β) and impairs its phosphorylation. It in its turn inhibits NF-κB translocation to the nucleus and subsequent upregulation of expression of its target genes. In the nucleus NS1 inhibits IKK-mediated phosphorylation of histone H3 Ser 10 which is important for expression of NF- κB target genes. All these together shield viral RNAs from the immunity sensor, 2′-5′ OAS, hindering the OAS/RNase L pathway that depends on NF-κB pathway activation.

The mitochondria's outer membrane is pivotal for Mitochondrial antiviral-signaling protein (MAVS) signaling, essential for RIG-I downstream activity. MAVS stimulates IKK proteins, which activate transcription factors NF-κB and IRF. Recent

studies show that mitochondrial PB1-F2 suppresses the immune response to viral RNA on the level of MAVS (Varga et al., 2011). Located in the mitochondrial inner membrane space, PB1-F2 reduces membrane potential and RIG-I signaling. PB1-F2 C-terminal domain binds transmembrane domain of MAVS (Varga et al., 2012). Varga and colleagues proposed that both binding to MAVS and reducing membrane potential can lead to inability of MAVS to form an active MAVS-containing protein complex or rearrange it to induce IFNs production.

All these studies taken together point to the significant role of RIG-I signaling in counteracting IAV infection and different ways how IAV can inhibit this response. It underlines important function of UFMylation pathway as antiviral one and makes a solid for investigating of its role in IAV infection.

1.2.2.2 IAV and post-translational modifications of viral proteins at different stages of infection

PTMs play a crucial role in the IAV infection. PTMs are chemical changes that occur to a protein after its initial synthesis (translation) in a cell. These modifications can alter the protein's function, localization, stability, and interactions with other molecules. For influenza viruses, several key proteins undergo post-translational modifications, significantly impacting the virus's ability to infect host cells and cause disease on different stages of viral cycle. In this section, I cover how post-translational modifications affect functionality of IAV proteins at different stages of viral infection and how they can play crucial role in interactions between virus and host defense mechanisms. Short list of modifications is presented in Table 1. Ubiquitination and Ubiquitin like modifications will be uncovered in next section.

1.2.2.2.1 Entry

IAV initiates infection through its HA protein binding to sialic acids on host cell surfaces. This binding is influenced by PTM of HA and HA's glycosylation state. Monoglycosylated HA, which binds more easily to various sialic acids, enhances infectivity across different hosts but also increases susceptibility to neutralizing antibodies. This glycosylation strikes a balance between infectivity, immune evasion, and host diversity (Gallagher et al., 1992).

One of the NP functions is to traffic between the cytoplasm and nucleus. Phosphorylation at the N-terminal impairs nuclear import, while other sites hinder

nuclear export (Neumann et al., 1997). NP's RNA-binding ability is compromised by phosphorylation at specific sites, affecting vRNPs assembly and export. This export involves sequential interactions between RNP, M1, and NEP, with NEP connecting to cellular export machinery (Li et al., 2015). At the same time, phosphorylation of residue on M1 (Y132) is essential for its nuclear import and for the export of progeny vRNPs by affecting the interaction with importin-1. A mutation in M1, increasing its phosphorylation, results in abnormal nuclear retention, impacting the formation of infectious particles. (Wang et al., 2013).

1.2.2.2.2 Transcription, translation and genome replication

During transcription, IAV employs a cap-snatching mechanism where it cleaves caps from host mRNAs to initiate viral mRNA synthesis. This requires the viral polymerase to access host mRNA by binding to phosphorylated RNA polymerase II (Martínez-Alonso et al., 2016). PTMs such as acetylation and phosphorylation of NP and other viral proteins like PB1 and NS1 are crucial in regulating this process. For example, acetylation of NP at different sites can either increase or decrease polymerase activities, while phosphorylation generally stimulates transcription (Giese et al., 2017; Kamata & Watanabe, 1977). Acetylation of the PA subunit by P300/CBP-associated factor (PCAF) and histone acetyltransferase GCN5 (GCN5) increases its endonuclease activity, crucial for IAV's RNA polymerase functionality (Hatakeyama et al., 2022).

1.2.2.2.3 Assembly and Release

The actin and microtubule cytoskeletons, regulated by myosin light chain (MLC) phosphorylation, are important for viral replication. Changes in the actin cytoskeleton, mediated by MLC phosphorylation, can impact the nuclear export of vRNPs (Haidari et al., 2011). For IAV protein trafficking, vRNPs utilize the microtubule network and vesicular transport system to move to the plasma membrane, while HA, NA, and M2 proteins are transported via the ER-Golgi secretory pathway. Microtubules, aided by PTMs like acetylation, are essential for this intracellular transport. Specifically, acetylation of α-tubulin, which is increased when tubulin deacetylase and Histone deacetylase 6 (HDAC6) activity is downregulated, facilitates virion release (Husain & Cheung, 2014).

1.2.2.2.4 PTMs influence IAV evasion of immune surveillance

The viral proteins NS1 and HA are crucial for interacting with the host's immune response. NS1 works against immune responses by hiding the virus's double-stranded RNA from host sensors and directly interacting with these sensors. NS1 regulates host translational machinery and mediates inhibition of host immune responses, particularly IFN production.

However, certain PTMs can diminish NS1's ability to counteract the host IFN response, such as phosphorylation at T49 (Kathum et al., 2016) and T80 (Zheng et al., 2017), which reduce NS1's interaction with RNA and RIG-I, and Protein kinase C α (PKCα)-mediated phosphorylation at S42 that blocks NS1 binding to dsRNA (Hsiang et al., 2012). HA, on the other hand, is the main viral protein that prompts an antibody response in the host. It's responsible for attachment and entry into host cells. Glycosylation of HA (and other viral proteins) helps the virus evade the immune system. Changing the pattern of N-linked glycosylation on HA can protect it from being detected and neutralized by antibodies. Moreover, HA glycosylation might also increase the virus's ability to spread and cause disease after evading the immune system (Ekiert et al., 2009).

Table 1 Post-translational modifications of Influenza A Virus proteins

Post-translational modification	IAV protein and location	Consequences
Glycosylation	HA (H1) N71 (Sun et al., 2013), HA (H5) N286 (Parsons et al., 2017)	Enhances infectivity across different hosts but also increases susceptibility to neutralizing antibodies, important for binding different sialic acids
Phosphorylation	NP, S9, Y10 (Zheng et al., 2015)	regulates NP nuclear import by affecting the binding affinity between NP and different isoforms of importin-α

Post-translational modification	IAV protein and location	Consequences
Phosphorylation	NP, Y78 (Cui et al., 2019)	delayed NP nuclear export through reducing the binding of NP to the cellular export receptor chromosomal region maintenance 1 (CRM1)
Phosphorylation	NP, Y296 (Zheng et al., 2015)	induces nuclear retention of NP by reducing the interaction between NP and CRM1
Phosphorylation	NP, T188 (Li et al., 2018)	controlling nuclear export signal 2 (NES2)-dependent NP nuclear export and the polymerase activity of the vRNP complex
Phosphorylation	NP, S165 (Zheng et al., 2015), S407 (Mondal et al., 2015)	blocks NP oligomerization
Phosphorylation	M1, Y132 (Wang et al., 2013)	enhances nuclear import of M1, export of progeny vRNPs by affecting the interaction with importin-1
Acetylation	PA, K19 (Hatakeyama et al., 2022)	increases PA activity as endonuclease
Acetylation	NP, K229, K113 (Giese et al., 2017)	increase or decrease polymerase activity
Acetylation	NP, K229 (Giese et al., 2017)	plays role in viral particle release

Post-translational modification	IAV protein and location	Consequences
Acetylation	NS1, K108 (Ma et al., 2020)	is important for the IFN antagonistic activity of the NS1 protein and virulence of the influenza virus
Phosphorylation	PB1, T223, S673 (Dawson et al., 2020)	is important for transcription and viral replication
Phosphorylation	NS1, S42 (Hsiang et al., 2012)	enhances viral replication
Phosphorylation	NS1, S205 (Hsiang et al., 2012)	is required for efficient NS1–DExD-Box Helicase 21 (DDX21) binding, resulting in enhanced viral polymerase activity
Palmytoilation	HA (Chlanda et al., 2017)	recruitment of M1, formation of infectious viral particles
Phosphorylation	NS1, T49 (Kathum et al., 2016), T80 (Zheng et al., 2017)	reduce NS1's interaction with RNA and RIG-I

1.3 UFMylation as a ubiquitin-like post-translational modification

1.3.1 Ubiquitin and ubiquitin-like translational post-translational modifications

Post-translational modifications such as ubiquitin (Ub) and ubiquitin-like (Ubl) one contributes to the complexity of the proteome by expanding the functional diversity of proteins without altering their genetic code. The specific PTMs and their functional consequences depend on the proteins involved, the cellular context, and signaling pathways. These PTMs play important roles in viral infections by influencing various aspects of the viral life cycle, including viral entry, replication, assembly, and evasion of host immune responses (Rajsbaum & García-Sastre, 2013; Calistri et al., 2014). PTMs

allow viruses to manipulate host cell processes, evade immune detection, and optimize viral replication. Understanding the role of PTMs in viral infections provides insights into viral pathogenesis and can aid in the development of antiviral strategies targeting these modifications.

Ub, discovered in the 1970s, is a conserved protein that forms a covalent bond with other proteins through its C-terminal glycine and the substrate's primary amine, typically a lysine residue. This process is called ubiquitination and is one of the most famous PTMs. Ubiquitin is a highly conserved, 76-residue protein found abundantly in eukaryotes. Conjugation relies on the coordinated actions of E1, E2, and E3 enzymes. Ubiquitination plays a crucial role in regulating various cellular processes, including protein degradation, signal transduction, DNA repair, and immune responses (Hershko & Ciechanover, 1998; Ciechanover, 2015).

In the 1980s, the biochemical reactions catalyzed by these enzymes were elucidated. Subsequently, in the 1990s and 2000s, additional protein families with similarities to ubiquitin, including the ubiquitin fold and the ability to be conjugated to substrates by related E1s, E2s, and E3s, were discovered and collectively termed Ubls (van der Veen & Ploegh, 2012). Ubls form a protein family that exhibits structural and evolutionary connections with ubiquitin. These proteins possess a β-grasp fold, consisting of a five-stranded β-sheet that partially encloses a central α-helix. There are 9 distinct UBLs found in humans: Interferon-stimulated gene 15 (ISG15) that was first found, neural precursor cell expressed, developmentally down-regulated 8 (NEDD8), FAU ubiquitin like and ribosomal protein S30 fusion (FUBI), Ubiquitin D (UBD/FAT10), Small Ubiquitin-like Modifier (SUMO), Autophagy-related protein 8 (Atg8), Autophagy-related protein 12 (Atg12), Ubiquitin-related modifier-1 (Urm1), and Ubiquitin-fold modifier 1 (Ufm1) (Hochstrasser, 2009). Ufm1 system was discovered recently. It has 47% amino acid sequence similarity to Ub despite being similar for all Ubls tertiary structure (Komatsu et al., 2004) (Figure 1-2). At the same time, its role in host cells during infection is still not fully understood.

1.3.2 Ubiquitination and UBLs in the IAV infection

Ubiquitination plays a significant role in the cycle of the influenza virus, influencing both viral replication and the host immune response. In the context of this

study discussing Ubiquitination is also important because Ubiquitination and UFMylation can modify the same lysines and compete for them. Here's an overview of the key aspects of ubiquitination in the context of influenza virus. Short list of modifications is presented in Table 2.

1.3.2.1 Viral entry

After internalization, the virus encounters IFITM3, a protein that inhibits viral fusion within endosomes (Su et al., 2013). The E3 ubiquitin ligase neural precursor cell expressed developmentally down-regulated protein 4 (NEDD4) can counter IFITM3 by promoting its degradation, mitigating its antiviral effects. Another such modification involves the ubiquitin proteasome system (UPS). The E3 ubiquitin ligase, Itch, modifies IAV's M1 protein, aiding its separation and degradation, which is essential for the virus's uncoating step. During this process, IAV exploits the ubiquitin chains within its virions to attract HDAC6 following viral fusion in late endosomes (LEs) (Banerjee et al., 2014). HDAC6 binds to the capsid, connecting it to cytoskeletal motors like dynein and myosin, generating forces that disassemble the capsid and release viral ribonucleoproteins (vRNPs) into the cytoplasm.

1.3.2.2 Nucleus export and import:

USP11, a deubiquitinating enzyme, interacts with and regulates IAV RNP components. It inhibits IAV RNA replication, with NP monoubiquitylation at K184 being crucial for genome replication. Ubiquitin specific protease 11 (USP11) removal of ubiquitin from NP adjusts RNA interactions, affecting replication efficiency (Liao et al., 2010). NP shuttles between the cytoplasm and nucleus, regulated by SUMOylation. SUMOylation retains NP in the nucleus, with its absence leading to premature cytoplasmic export and defective viruses (Han et al., 2014). SUMOylation of M1 impacts RNP-M1-NEP complex formation. M1 mutants lacking SUMOylation display weaker RNP interactions and export issues, reducing viral activity (Wu et al., 2011).

1.3.2.3 Viral transcription and replication:

Ubiquitination of IAV polymerase subunits, including PB1-F2, regulates their stability and functions, such as RdRp activity and IFN-beta antagonism (Kirui et al., 2016) (Košík et al., 2015). It modulates infection processes, with NP ubiquitinated at lysine 184 (K184), influencing viral RNA replication through improved RNA binding.

However, the host deubiquitinase USP11 can reverse this, reducing viral replication. Interestingly, there are instances where polyubiquitination doesn't lead to NP degradation but may have other regulatory roles (Liao et al., 2010).

PB2 and PA polyubiquitination can limit their stability and reduce the viral polymerase activity. The antiviral protein Zinc Finger Antiviral Protein Long (ZAPL) binds to PB2 and PA, inducing their proteasomal degradation. However, PB1 polymerase can prevent this degradation, suggesting a potential antiviral strategy (Liu et al., 2015). Ubiquitination of PB2 is implicated for optimal IAV infection (Karim et al., 2020). Two Cullin 4 (CRL4)-based RING-E3 ligases play a role in regulating PB2 ubiquitination and the viral cycle. Unlike typical ubiquitination processes, CRL4-induced ubiquitination primarily involves atypical K29 linkages, which don't lead to protein degradation but can affect other cellular pathways. Mutations affecting these ubiquitination sites lead to reduced virus growth, indicating the importance of this process. NEDDylation, particularly of PB2, acts as a negative regulator, impeding IAV replication. Blocking neddylation pathways also adversely affects replication. Mutations at key NEDDylation sites, like K699, result in increased replication and virulence (Zhang et al., 2017).

1.3.2.4 Virus assembly and release:

The host ubiquitin system is instrumental in IAV exit, notably in the ubiquitination of M1 protein, facilitating viral particle release (Su et al., 2018). The ubiquitination of the M2 protein, particularly at the K78 residue, plays a role in the production and spread of infectious virions. Ubiquitination at this residue potentially induces a conformational change that enhances its interaction with the viral M1 protein, leading to the efficient packaging of the viral genome into new virion particles. Mutant M2 proteins that can't be ubiquitinated at K78 produce defective virion particles with reduced viral components, resulting in lower infectivity. The ubiquitination of M2 at K78 also influences virus-induced apoptosis and the autophagy processes in host cells. These are key processes that viruses manipulate to regulate cell death and viral spreading. The K78 ubiquitination accelerates the initiation of autophagy without hindering M2's ability to halt the completion of autophagy. The M2 protein can also interact with other cellular components to regulate cell death. Viruses carrying the M2 K78R mutation, which can't be ubiquitinated at K78, trigger earlier autophagy and apoptosis, potentially leading to

suboptimal viral replication and severe consequences post-infection. M1 protein's SUMOylation play significant roles in viral RNA release and packaging. SUMOylation at K242 is essential for its nuclear export and viral morphogenesis (Wu et al., 2011). The ubiquitination state of a lysine residue (K242) on M1 can be switched to SUMOylation by the NS2-interacting protein Aminoacyl TRNA Synthetase Complex Interacting Multifunctional Protein 2 (AIMP2), which stabilizes M1 and facilitates nuclear export (Gao et al., 2015).

1.3.2.5 Evasion of Host Immune Responses by IAV modulating PTMs:

A key regulator of IFN production is the TRIM25-RIG-I signaling pathway, which senses vRNA. TRIM25's polyubiquitination of the RIG-I caspase activation and recruitment domain (CARD) leads to IFN production (Gack et al., 2007). NS1 suppresses RIG-I ubiquitination by binding to both human TRIM25 and Riplet E3 ligase, inhibiting IFN production. Instead of reducing TRIM25 expression, NS1 interacts with TRIM25's coiled-coil domain (CCD) section, preventing its multimerization and enzymatic activity essential for RIG-I ubiquitination (Gack et al., 2009). Other pathways for type I IFN production, such as Toll-like receptor 3 (TLR3) and Toll-like receptor 7 (TLR7), are affected by NS1 through its interaction with the TNF receptor-associated factor (TRAF3) E3 ubiquitin ligase (Lin et al., 2021). NS1 binds to TRAF3 and suppresses its K63-linked ubiquitination, inhibiting the expression of IFN genes. NS1's conserved FTEE motif and specific glutamate residues are crucial for its binding to TRAF3 and suppressing type I IFN production.

SUMOylation of NS1 at specific sites is essential for its maximal IFN-blocking activity, but excessive SUMOylation can impair this function (Santos et al., 2013). ISGylation, another PTM, also limits IAV virulence by modifying NS1 and interfering with its functions, such as RNA binding and homodimerization, which are critical for inhibiting IFN-β production (Zhao et al., 2010).

Table 2 Ub and Ubl modifications of IAV proteins

Ubiquitin or Ubiquitin-like modification	Location	Function
Ubiquitination	M1, K102, K104 (Hui et al., 2022)	important for M1-M2 interaction, M1 nuclear export and viral budding
Monoubiquitylation	NP, K184 (Liao et al., 2010)	improves RNA binding
SUMOylation	NP, K4, K7 (Han et al., 2014)	important for intracellular trafficking of NP
SUMOylation	M1, K242 (Wu et al., 2011)	facilitates RNP-M1-NEP complex formation, facilitates vRNP export
Polyubiquitination	PB2, K48 (Karim et al., 2020)	limits stability and reduce the viral polymerase activity through PB2 degradation
Ubiquitination	PB2, K29 (Karim et al., 2020)	necessary for an optimal influenza A virus infection
NEDDylation	PB2, K699 (Zhang et al., 2017)	inhibits viral replication

Ubiquitin or Ubiquitin-like modification	Location	Function
Ubiquitination	M2, K78 (Su et al., 2018)	induces a conformational change that enhances its interaction with the viral M1 protein, leading to the efficient packaging of the viral genome into new virion particles; accelerates the initiation of autophagy
Ubiquitination	M1, K242 (Gao et al., 2015)	proteosome-dependent degradation of M1
SUMOylation	NS1, K219, K70 (Santos et al., 2013)	essential for its maximal IFN-blocking activity
ISGylation	NS1, K41 (Zhao et al., 2010)	impairs NS1 RNA binding and homodimerization

To conclude, PTMs and exactly UBLs were shown to be very important for IAV infectious cycle and also to be a part of host cell defense system.

UFMylation is one of the UBL post-translational modification process in cells, similar to ubiquitination, but involving a different small protein called UFM1. This process is involved in a variety of cellular functions and has gained attention for its role in human diseases. It is already known that it plays role in viral infection but its connection with IAV has not been revealed yet.

1.3.3 UFM1 - key player of UFMylation cascade

UFM1, an 85-amino acid protein modifier with a molecular weight of 9.1 kDa. While UFM1 is present in various metazoans, it is absent in fungi. Initially, UFM1 is synthesized as an immature form of 85 amino acids, which matures through cleavage by the UFM1 Specific Peptidase 1 (UFSP1) protease. Structurally, UFM1 adopts a β-grasp fold similar to ubiquitin, consisting of four β-strands and α-helices (Sasakawa et al.,

2006). Despite the structural resemblance, UFM1 exhibits only 21.7% protein sequence identity and 47% similarity to ubiquitin (Komatsu et al., 2004). Nevertheless, the UFM1 sequence shows a high degree of conservation, with human and *Caenorhabditis elegans* sharing 80.6% protein sequence identity and 88.2% similarity. Unlike ubiquitin and other UBLs, like SUMO, Ufm1 possesses a single active glycine at the C-terminus, which is required for the covalent attachment to its target proteins. Depending on the species, one or two additional amino acids are attached to the C-terminal glycine. One key feature of ubiquitin is its hydrophobic patch, consisting of specific amino acids (L8, I44, and V70) crucial for its function, signaling, and activation by Ubiquitin-like modifier activating enzyme 1 (UBA1), the cognate E1 enzyme. While UFM1 partially conserves this hydrophobic patch with certain residues superimposing those in the ubiquitin - they are important for its interaction with Ubiquitin-like modifier activating enzyme 5 (UBA5) - E1 ligase, its electrostatic surface differs (Banerjee et al., 2020). As a result, Ufm1 has a significantly higher isoelectric point (pI) of 9.6, suggesting a positive charge at physiological pH, in contrast to the neutral pI of ubiquitin. While ubiquitin is known to modify target proteins by adding single ubiquitin or ubiquitin chains or even branched chains, Ufm1 has been observed to predominantly form K69-linked chains despite the presence of six lysines at positions 3, 7, 19, 34, 41, and 69. In the case of UFMylation mono-UFMylation is predominant over poly-UFMylation.

To summarize, UFM1 is a distinct ubiquitin-like protein with unique structural features and a specific C-terminal sequence. While ubiquitin exhibits versatility in modifying target proteins, including the formation of various types of ubiquitin chains, our understanding of UFM1 chain formation is limited. Mono-UFMylation has been shown to yield diverse functional outcomes, including directing proteins towards lysosomal degradation or facilitating protein-protein interactions (Gerakis et al., 2019). On the other hand, UFM1 chains have been identified to serve as molecular scaffolds. It was shown that UFM1 chains as scaffolds can facilitate the recruitment of multiple coactivators to ASC1 and can also provide protection from ubiquitination (Yoo et al., 2014).

1.3.3.1 UFMylation machinery

1.3.3.1.1 Overview

Protein ubiquitylation is a highly regulated process in cells, involving a system of enzymes. This system consists of activating enzymes (E1), conjugating enzymes (E2), and ligating enzymes (E3) (Morreale & Walden, 2016). The E1 enzyme initiates the reaction by forming a high-energy thioester bond with ubiquitin through adenylation, which requires ATP. The activated ubiquitin is then transferred to the E2 enzyme through a thioester linkage. In some cases, the E2 enzyme can directly transfer ubiquitin to substrate proteins through an isopeptide linkage. However, most E2 enzymes require the involvement of E3 enzymes to achieve substrate-specific ubiquitylation reactions. E3 enzymes are responsible for recognizing specific substrates for ubiquitylation.

UFMylation, the process of attaching UFM1 to target proteins, involves a similar enzymatic cascade comprising UFM1-activating enzyme (UBA5), UFM1-conjugating enzyme (UFC1), and UFM1-specific ligase (UFL1) (Banerjee et al., 2020) (Figure 1-4). This cascade facilitates the transfer of UFM1 to specific target proteins in an ATP-dependent manner. The attachment of UFM1 to target proteins is reversible and can be cleaved by a specific protease known as UFM1 Specific Peptidase 2 (UFSP2). Prior to activation by UBA5, the two additional amino acids at the C-terminal region of the human pro-UFM1 protein are removed, exposing the necessary Gly residue for conjugation to target molecules.

1.3.3.1.2 UFM1 activation

The activation of UFM1, facilitated by its corresponding E1 enzyme UBA5, follows a unique mechanism distinct from other Ubiquitin-like proteins (UBLs). UBA5, categorized as a non-canonical E1 enzyme, is smaller in size (404 amino acids) compared to canonical E1 enzymes, which raises questions about its functional mechanism (Oweis et al., 2016). Unlike canonical E1 enzymes that have an active site Cys within a Cys domain, UBA5 incorporates the active site Cys within its adenylation domain. The adenylation domain of UBA5 (residues 57 to 329) is responsible for binding ATP and catalyzing the attack on the C-terminal Gly of UFM1 at the alpha phosphate. This results in the formation of adenylated UFM1 (UFM1-AMP), accompanied by the release of pyrophosphate. Subsequently, C250 in UBA5's side chain attacks the C-terminal glycine

of UFM1, leading to the release of AMP and the formation of a thioester bond with UFM1.

The activation of UFM1 by UBA5 involves an additional sequence known as the UFM1-interacting sequence (UIS), located outside the adenylation domain. The UIS (amino acids 334-346) plays a vital role in mediating the interaction between UBA5 and UFM1. Experimental evidence has demonstrated that UBA5 fragments lacking the UIS fail to bind UFM1, underscoring the importance of this sequence for their interaction (Padala et al., 2017). UBA5, similar to other non-canonical E1 enzymes, functions as a homodimer, suggesting that dimeric UBA5 can simultaneously bind two UFM1 molecules. The crystal structure of UBA5 in complex with UFM1 reveals that each UIS binds to one UFM1 molecule.

1.3.3.1.3 UFM1 conjugation

To date, the sole E2 enzyme known to function in conjunction with UFM1 is UFC1, which stands out from other Ubl E2 enzymes due to its limited similarity in sequence. Nonetheless, UFC1 maintains the general E2 fold characteristic of conjugating enzymes. Notably, UFC1 possesses a unique N-terminal alpha-1 helix that contributes to its thermal stability, distinguishing it from other E2s. Additionally, the highly conserved HPN motif observed in other E2 enzymes, which includes an asparagine residue stabilizing the oxyanion hole, is replaced by the TAK motif (amino acids 106-108) in UFC1. The threonine residue at position 106 plays a role in maintaining structural stability, and any mutation to a hydrophobic residue at this position disrupts the structural integrity around the active site, leading to impaired UFM1 transfer.

The transfer of UFM1 from UBA5 to UFC1 occurs through a process called trans-thiolation, which requires the binding of UFC1 to UBA5 to bring their respective active site cysteines in close proximity. Unlike canonical E1 enzymes, UBA5 lacks a dedicated domain for interacting with UFC1 but possesses a short sequence called the UFC1-binding sequence (UBS) at its C-terminus. The precise structural mechanisms by which the UBS binds to UFC1 and facilitates the interaction between the active site cysteines are not yet fully understood. However, it has been suggested that UFC1's helix 2 plays a role in binding to the UBS. Mizushima *et al*. demonstrated that mutations at positions Q30A and K33A in UFC1's alpha helix 2 significantly affected the binding affinity with

UBA5 (Mizushima et al., 2007). Moreover, *in vitro* conjugation assays revealed that the K33A mutant greatly impaired the transfer of activated UFM1 from UBA5, underscoring the critical role of alpha-2 helix in both UBA5 binding and UFM1 transfer.

It is important to note that UBA5 functions as a homodimer, offering two binding sites for UFC1, thereby enabling it to simultaneously bind two UFC1 molecules. Studies utilizing UBA5 truncations and mutations have demonstrated that UFM1 transfer occurs through a trans-binding mechanism (Kumar et al., 2021). In this mode of transfer, UFC1 binds to the UBS of one UBA5 molecule and accepts the UFM1 moiety attached to the active site cysteine of the other UBA5 molecule. However, the precise interplay between the UFM1 intermediate site (UIS) and the UBS, both located towards the C-terminus of the adenylation domain, remains uncertain. Specifically, it is yet to be determined whether UFM1 must dissociate from the UIS before the UBS can engage with UFC1, warranting further investigation into potential crosstalk between these regions.

1.3.3.1.4 UFM1 Ligation

The final step is the transfer of UFM1 from UFC1 to the substrate. Unlike ubiquitin (Ub), which relies on a vast array of over 600 E3 ligases for this step, UFM1 utilizes a single known E3 enzyme called UFL1 (Tatsumi et al., 2010). UFL1 is a protein composed of 794 amino acids with a molecular mass of approximately 90 kDa.

1.3.3.1.4.1 Different types of E3 ligases

E3 ligases are classified into three main types based on their structural domains and mechanisms of action:

HECT (Homologous to the E6-AP Carboxyl Terminus): HECT domain-containing E3 ligases are characterized by a conserved catalytic HECT domain (Wang et al., 2020). These ligases form a thioester intermediate with ubiquitin before transferring it to the target protein. HECT E3 ligases are involved in various cellular processes, including cell cycle regulation, signal transduction, and protein degradation. Examples of HECT E3 ligases include E6-associated protein (E6-AP) and NEDD4.

RBR (Ring-between-Ring): RBR E3 ligases contain a combination of three domains: RING (Really Interesting New Gene), in-between-RING, and RING2 (Smit & Sixma, 2014). They possess both E3 ligase activity and E2-like activity, forming a thioester intermediate with ubiquitin and transferring it to the target protein. RBR ligases

are involved in diverse cellular processes, including DNA repair, mitochondrial homeostasis, and development. Notable examples of RBR E3 ligases include Parkin, HOIL-1-interacting protein (HOIP), and TRIM proteins.

RING (Really Interesting New Gene): RING domain-containing E3 ligases are the largest group and the most common type of E3 ligases (Deshaies & Joazeiro, 2009). They act as scaffolds to facilitate the transfer of ubiquitin from E2 enzymes directly to the target protein. RING E3 ligases do not form a thioester intermediate with ubiquitin but provide a platform for bringing E2 and the substrate in close proximity for efficient ubiquitylation. RING E3 ligases are involved in a wide range of cellular processes, including protein degradation, DNA repair, and immune response. Examples of RING E3 ligases include Mouse double minute 2 (MDM2), Carboxyl terminus of Hsp70-interacting protein (CHIP), and Casitas B-lineage lymphoma (c-Cbl).

U-box E3 ligases are a type of E3 ligase that possess a conserved U-box domain. The U-box domain is structurally similar to the RING (Really Interesting New Gene) domain found in RING E3 ligases but lacks the characteristic zinc-binding motif (Hatakeyama & Kei-ichi, 2003). U-box E3 ligases function as scaffold proteins that facilitate the transfer of ubiquitin from E2 conjugating enzymes to target proteins for ubiquitylation.

UFL1 cannot be included in one of the existing classes as it does not possess the typical structural features observed in other E3 ligases, such as a RING domain, a HECT-type catalytic domain, or an RBR structure. Furthermore, it remains unclear whether UFL1 contains a specific UFM1-interacting motif, unlike some atypical E3 enzymes that have well-defined motifs for interacting with UBLs. Therefore, it is possible that UFL1 exerts its E3 activity through a distinct, yet unknown mechanism that differs from canonical E3 enzymes. Alternatively, there may be other proteins involved in facilitating the ligase activity of UFL1 such as in the case of Multi-subunit RINGs. The RING-type E3 ligases can form multi-subunit assemblies, such as the Cullin RING Ligase (CRL) superfamily (Cai & Yang, 2016). CRLs exhibit remarkable flexibility in substrate specificity. Each CRL subfamily consists of a cullin protein, a small RING protein (often RING-box protein 1 (Rbx1)/ Regulator of cullins-1 (Roc1)/ RING-box protein HRT1 (Hrt1)), and either adaptor proteins or proteins that bind both the cullin protein and the

substrate (Figure 1-3). The possibility that the UFMylation cascade may demonstrate a similar mechanism for its E3 ligase complex is supported by studies investigating the UFMylation of the nuclear receptor coactivator ASC1, which demonstrated the requirement of an additional protein called DDRGK Domain Containing 1 (DDRGK1) for UFL1 to modify ASC1 with UFM1 (Yoo et al., 2014). These findings suggest that UFMylation of target proteins may involve the proposed E3 ligase, UFL1, and other unidentified factors that contribute to the process. Further exploration is necessary to fully uncover the complete set of factors involved in UFMylation.

Analysis of potential catalytic cysteine (Cys) residues in UFL1 showed that individual Cys mutations did not affect the UFMylation activity or UFMylation of substrates, indicating that UFL1 lacks a catalytic Cys (Peter et al., 2022). This suggests that the UFL1/DDRGK1 ligase complex likely operates through a scaffolding mechanism for UFM1 transfer. The complex facilitates aminolysis of UFC1~UFM1, enabling the release of UFM1 onto lysine residues. UFC1 alone is capable of assembling free UFM1 chains, with a preference for K69 linkages, and this activity is significantly enhanced in the presence of the UFL1/DDRGK1 ligase complex - which was shown in in vitro experiments with purified proteins alone. The specificity of the linkages is determined by the E2 enzyme (UFC1) and remains unchanged in the presence of the E3 ligase complex.

1.3.3.1.5 DDRGK1 and CDK5RAP3 - modifiers of UFMylation cascade

In addition to classical E1 ('Activating'), E2 ('Conjugating'), and E3 ('Ligating') enzymes, the UFMylation machinery also features regulatory proteins and adaptors. In the case of UFMylation, they are called DDRGK1 (adaptor) and CDK5 Regulatory Subunit Associated Protein 3 (CDK5RAP3) (regulator) (Peter et al., 2022). Accessory proteins were also described for the ubiquitination pathway - which means that the presence of these proteins is not a coincidence but a requirement. Three types of multisubunit E3 ligases involve such proteins. The RING finger protein, such as Rbx1, plays an important role in organizing these complexes and recruiting the corresponding E2 enzyme. Moreover, the Skp1-cullin 1-F-box (SCF) E3s recruit substrate-specific F-box proteins through the adaptor protein S-phase kinase-associated protein 1 (Skp1), while VCB utilizes Von Hippel–Lindau tumor suppressor (pVHL) as the substrate recognition subunit (Wei & Sun, 2010). The ubiquitin-like protein Nedd8/ Ubiquitin-

NEDD8-like protein RUB1 (Rub1) modifies the cullin subunits of these E3 ligases and regulates their activity. Nedd8 modification enhances substrate polyubiquitination by these E3s. The SCF E3s, in particular, employ a shared platform consisting of Cul1/Rbx1/Skp1/Cdc34, where different F-box subunits may compete for limiting concentrations of other subunits. The instability of F-box proteins allows for the rapid remodeling of SCF complexes in response to cellular changes (Stebbins et al., 1999).

DDRGK1 plays this type of adaptor role and conceptually is similar to F-box in the UFMylation cascade (Witting & Mulder, 2021). UFL1 is recruited to the ER membrane through its interaction with DDRGK1, facilitated by the ER signal peptide of DDRGK1, as UFL1 itself lacks a conventional transmembrane domain. This interaction activates the ligase activity of UFL1 and brings it close to its substrates. The deletion of DDRGK1 and the subsequent reintroduction of variants lacking the transmembrane domain have demonstrated the importance of DDRGK1 in promoting the correct localization of UFL1. The interaction between DDRGK1 and UFL1, as well as the recruitment of the UFM1-specific protease UFSP2, is facilitated by the Proteasome component (PCI) domain of DDRGK1 in a UFM1-dependent manner (Banerjee et al., 2023). Firstly, DDRGK1 was found as a binding partner of UFL1, it has also been observed to undergo UFMylation at the PCI domain at lysine 267. This modification modulates the binding affinity of DDRGK1 to UFL1, thereby stimulating the ligase activity of UFL1. DDRGK1, particularly its PCI domain, plays a crucial role in recruiting various components of the UFM1 cascade, including UFL1, CDK5RAP3, UFSP2, and ASC1, thereby promoting the formation of enzyme-protein complexes that fine-tune UFM1 modification.

Some proteins modulate the assembly and structure of polyubiquitin chains through distinct mechanisms. One such factor is encoded by the Ubiquitin Fusion Degradation 2 (UFD2) gene in yeast (Hänzelmann et al., 2010). It works together with the Ubiquitin Fusion Degradation 4 (UFD4)-encoded HECT E3 and the E2 Ubiquitin-Conjugating 4 (Ubc4) to promote the elongation of polyubiquitin chains that start at the K29 position of ubiquitin. UFD2 may recognize the product of the ubiquitin conjugation reaction itself rather than a conjugating enzyme. A contrasting mode of action has been observed in the nucleotide excision repair factor Rad23/HHR23A. This factor has the

ability to bind to short ubiquitin chains attached to substrates, thereby preventing the conjugation of additional ubiquitin molecules to these intermediates.

In the UFMylation pathway CDK5RAP3, a highly conserved protein was found to play the regulator role of di- or mono-UFMylation. CDK5RAP3 is recruited by DDRGK1. It has been shown to associate with UFL1, and DDRGK1, and contribute to the relocation of UFL1 to the ER membrane. Moreover, the formation of a complex involving UFL1, DDRGK1, and CDK5RAP3 promotes the stability of CDK5RAP3 by regulating its degradation (Ishimura et al., 2023). Moreover, recently it was found by Peter et al. that ligase complexes containing UFL1, DDRGK1, and CDK5RAP3 exist in an autoinhibited state (Peter et al., 2022). It was observed that ribosome UFMylation, although restricted to monoUFMylation, is not abolished in the presence of CDK5RAP3. This led researchers to suggest that CDK5RAP3 regulates ligase activity as follows: (i) in the absence of a substrate, CDK5RAP3 binding inhibits E3 ligase activity, and (ii) this autoinhibition is relieved upon encountering specific substrates like the 60S ribosome. The release from inhibition may involve conformational changes triggered by the recognition of structural features on the substrate by UFL1, DDRGK1, or CDK5RAP3, facilitating substrate UFMylation. Additionally, CDK5RAP3 prevents UFM1 from attaching to another UFM1 molecule, thereby restricting the formation of UFM1 chains on substrates. This multi-layered regulation likely prevents unrestrained UFMylation, ensuring ribosome UFMylation occurs only in the appropriate context.

1.3.4 UFMylation primary targets and host cell processes regulated by UFMylation

UFMylation, a post-translational modification involving the attachment of the ubiquitin-like protein UFM1 to target proteins, plays a multifaceted role in various cellular processes including, ribosome function, protein quality control and ER stress, cell death and immune response discussed below.

1.3.4.1 Regulation of Ribosome Function:

Ribosomal Protein L26 (RPL26), a ribosomal protein, is identified as crucial for the translocation of proteins into the ER during translation. It is the primary target of UFMylation, which is key to resolving translation arrest by facilitating the removal of stalled polypeptide chains (Walczak et al., 2019). While previous studies hinted that such stalled ER proteins might be tagged for degradation by ubiquitination, evidence for this in

mammalian systems was lacking. Recent findings underscore the unique role of RPL26 UFMylation as a quality control mechanism, distinct from the canonical ER-associated degradation or cytosolic ribosome quality control systems (Wang et al., 2020). When ribosomes stall, UFMylation of RPL26 is imperative for redirecting the halted polypeptides from the ER to the lysosomes for degradation, thereby preventing the buildup of defective translation products and ensuring secretory homeostasis. Cells that lack UFMylation, or specifically the UFMylation sites on RPL26, show compromised processing and elimination of these translation-arrested ER substrates (Scavone et al., 2023). UFMylation is integral to the ER-associated ribosome quality control (ER-RQC) process, with the UFMylation of RPL26 facilitating the degradation of Endoplasmic Reticulum Associated Proteins (ER-Aps) and suggesting that it collaborates with the RQC pathway in a significant capacity.

1.3.4.2 Protein Quality Control and ER Stress Response:

The ER is crucial for protein processing, folding, lipid synthesis, and calcium regulation. Maintaining ER homeostasis is vital for protein maturation, and disruptions lead to ER stress and the activation of the UPR. UFMylation is intricately involved in maintaining ER homeostasis. It plays a critical role in the degradation of misfolded proteins, particularly during the ERAD process. This is crucial in preventing the accumulation of faulty proteins, which can lead to ER stress. Proteins like DDRGK1, UFSP2, UFL1, and UFM1, forming a complex at the ER's cytosolic side, are instrumental in ER function. The UFM1 modification system plays a key role here. Stress-inducing treatments, such as with tunicamycin (Bull & Thiede, 2012) or thapsigargin (Abdullahi et al., 2017) that activate ER stress and UPR, increase UFM1 system expression in specific cell types - which support the point that UFMylation is transcriptionally regulated by the UPR. It was shown that UFMylation is regulated by the transcription factor XBP1, linking it to specifically IRE1 arm of UPR (Zhang et al., 2012).

DDRGK1 is essential for ER homeostasis and hematopoietic stem cell survival. It interacts with the ER stress sensor IRE1α, stabilizing it via an interaction that depends on UFMylation at DDRGK1's K267 (Liu et al., 2017). When K267 in DDRGK1 is mutated to Arginine, this interaction is impaired. Loss of DDRGK1 accelerates IRE1α

degradation, leading to the activation of PERK (another ER stress sensor) and consequently, cell death. DDRGK1 also plays a role in the in ER-phagy, the process which is required for selective degradation of ER parts via lysosomal degradation. The UFL1 ligase is recruited to the ER surface by DDRGK1, where it initiates UFMylation of Ribophorin-1 (RPN1) and RPL26 (Liang et al., 2020). This process selectively targets ER sheets for degradation in a manner similar to how the PTEN-induced kinase 1 (PINK1)-Parkin system regulates mitophagy. Another UFMylation substrate linked to ER homeostasis and ER-phagy is Cytochrome B5 Reductase 3 (CYB5R3), an ER membrane-localizing reductase (Ishimura et al., 2022). CYB5R3 UFMylation, induced by UFL1 and DDRGK1, is proposed as a signal for macro-ER-phagy. The UFMylated CYB5R3 interacts with DDRGK1, potentially increasing UFL1's E3-ligating activity against CYB5R3, and leading to autophagic degradation of specific ER subdomains. Under different stress conditions, CYB5R3 UFMylation might be key in ER-phagy, with both UFL1 and DDRGK1 being ER stress-inducible proteins. CDK5RAP3 is a strong link between UFMylation and ER-phagy, as it plays role of ER-phagy receptor under ER stress conditions (Stephani et al., 2020). CDK5RAP3 can interact with both UFM1 and Atg8, with ER stress reducing UFM1's affinity for CDK5RAP3 in favor of Atg8. This switch triggers macro-ER-phagy by transferring UFM1 from CDK5RAP3 to other targets. The absence of either the UFMylation machinery or CDK5RAP3 itself leads to increased ER stress in mammalian cells.

1.3.4.3 Cell death

A novel aspect of UFMylation that was discovered is its ability to modify Tumor protein P53 (p53) covalently (Liu et al., 2020). This modification of p53 by UFM1 helps stabilize the protein by counteracting its ubiquitination and subsequent degradation by the proteasome. The mechanism involves UFL1, the UFM1 ligase, which competes with MDM2 for binding to p53, thus stabilizing it. A reduction in UFL1 or DDRGK1, both key regulators of UFMylation, leads to decreased p53 stability, fostering cell growth and tumor development *in vivo*. Clinically, low levels of UFL1 and DDRGK1 are observed in a significant number of renal cell carcinomas, correlating with reduced p53 levels.

1.3.4.4 Immune response

UFMylation, mediated by the enzyme UFL1, enhances the RIG-I pathway signaling, crucial for IFN production and antiviral immune response (Snider et al., 2022). RIG-I recognizes viral dsRNA. It triggers a signaling pathway via MAVS. 14-3-3ε is crucial partner for RIG-I, forming part of a complex or "translocon" that includes RIG-I, 14-3-3ε, and the TRIM25 ubiquitin ligase. This complex is responsible for guiding RIG-I's movement from the cytosol to membrane areas, enabling MAVS-dependent signaling critical for the immune response to acute RNA virus infections. The presence of 14-3-3ε is vital for maintaining the interaction between RIG-I and TRIM25, which in turn supports the ubiquitination of RIG-I and triggers the immune defense against RNA viruses. The result of RIG-I signaling is the generation and release of primarily type I and III IFNs. UFL1 is drawn to the membrane-targeting protein 14-3-3ε, forming a complex that subsequently is recruited to activated RIG-I, thereby facilitating downstream signaling. Activation of RIG-I leads to an enhanced conjugation of UFM1 to 14–3-3ε. Furthermore, the absence of UFMylation within cells disrupts the binding between 14–3-3ε and RIG-I. This disruption effectively impedes RIG-I's interaction with MAVS, thus halting the signal transduction pathway that triggers interferon IFNs production.

1.3.5 UFMylation pathway and viral infections

At the current time, there are no studies that highlight interactions between UFMylation and IAV infection. However, some studies have begun to shed light on the role of UFMylation in viral infections (

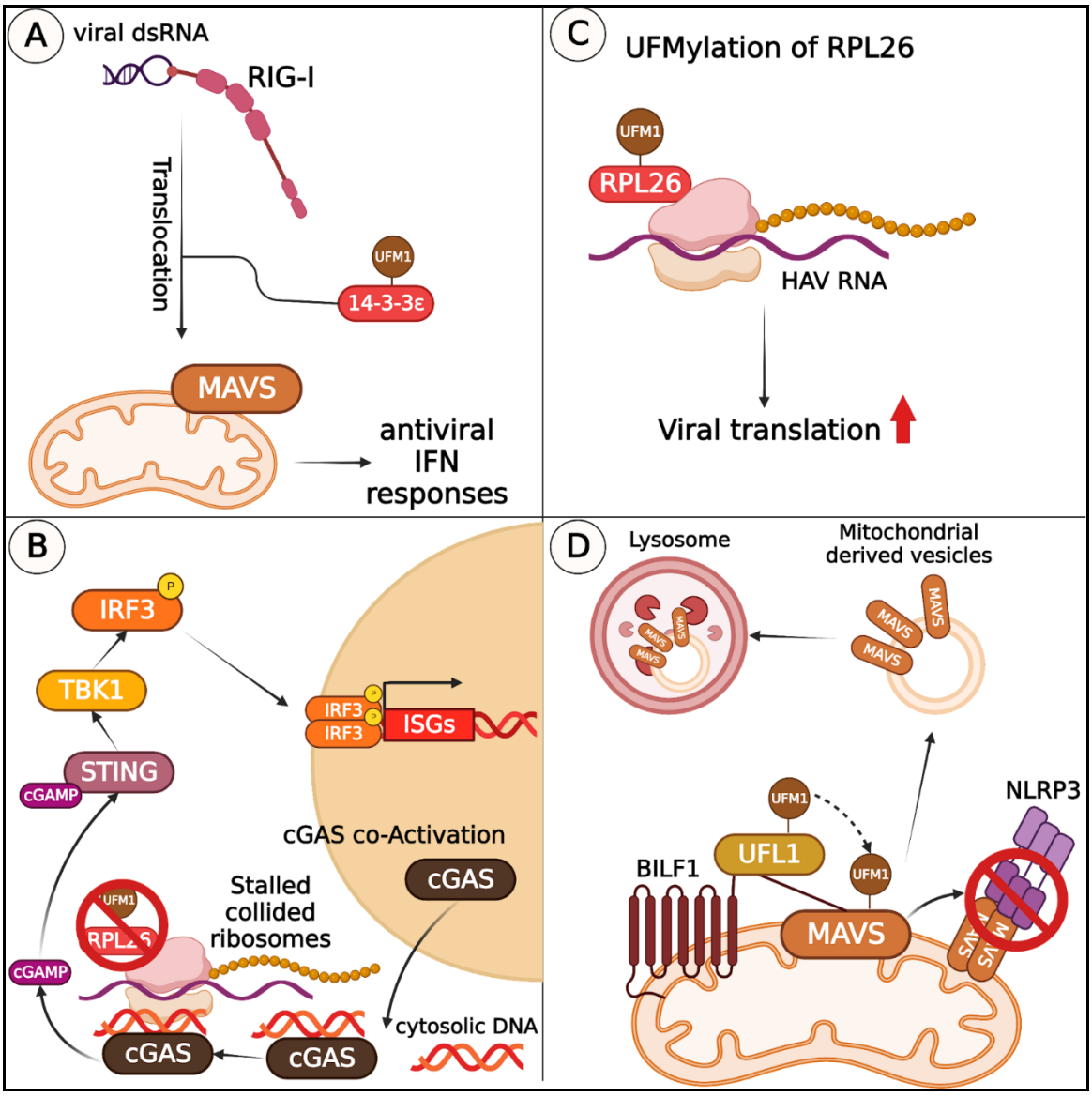

Figure 1-5).

Research from Stacy Horner's lab has demonstrated that UFMylation is essential for the effective activation and signaling of RIG-I, a receptor that detects viral RNA and triggers type 1 IFN responses, in the context of Sendai virus (SenV) infections (Snider et al., 2022) (

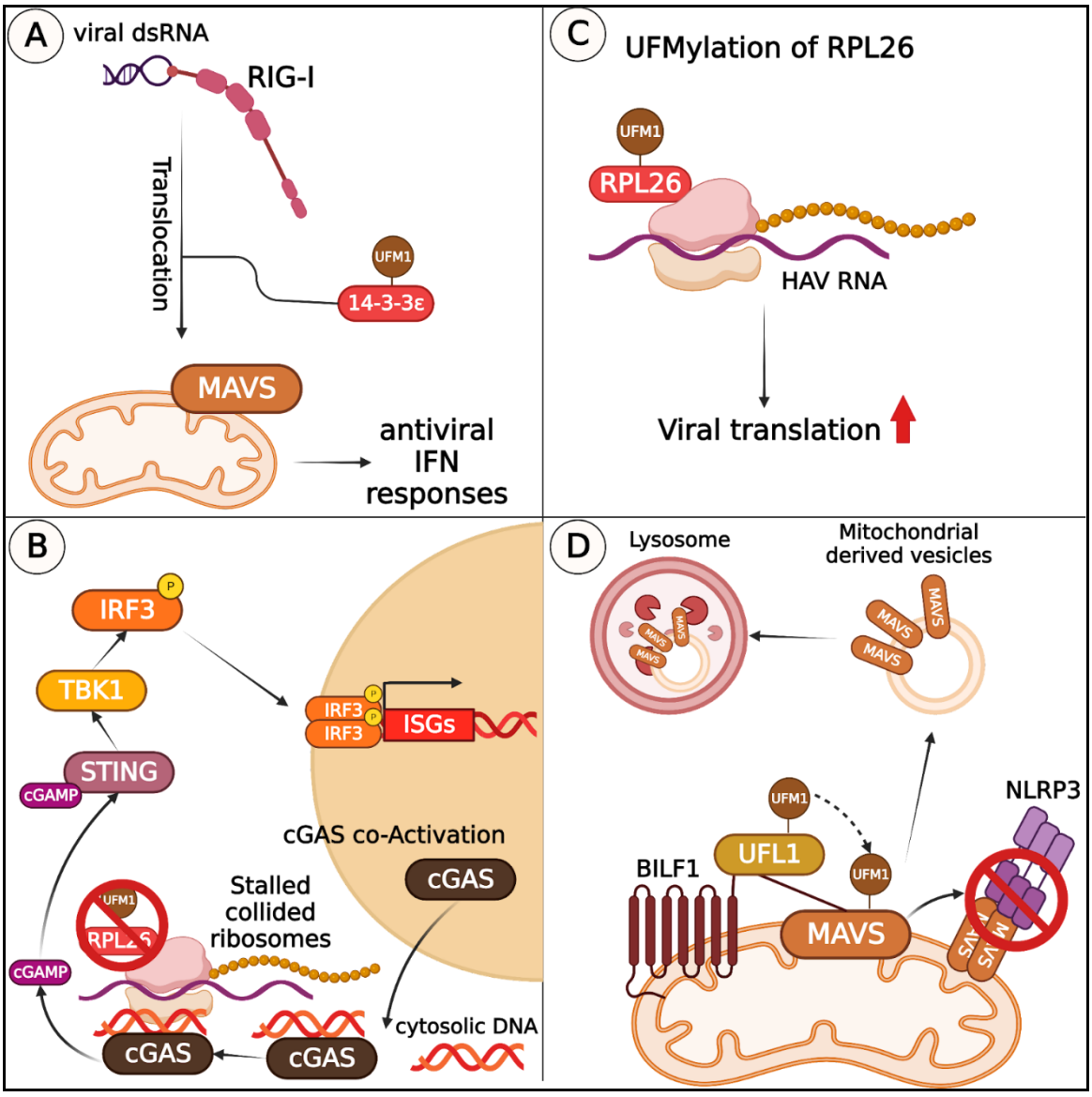

Figure 1-5 (A)). Upon RNA virus infection, such as with SenV, UFL1 increases its association with intracellular membranes, a response similar to that of RIG-I. UFL1 is also recruited to the mitochondrial-associated membrane (MAM) before the activation of MAVS, an essential adaptor in RIG-I signaling. UFL1 interacts with both 14–3-3ε, a molecular trafficking protein, and RIG-I, a pattern recognition receptor that detects viral RNA. This interaction is enhanced following RIG-I activation by SenV. RIG-I activation involves RNA binding and subsequent ubiquitination. Mutations that impair these steps significantly reduce UFL1's interaction with RIG-I, indicating that UFL1's role comes after RIG-I's RNA binding and ubiquitination. Co-expression of UFL1 with Riplet or 14–3-3ε increases IFN-β promoter activation above levels seen with each protein alone. The

study proposes two models for how UFL1 interacts with RIG-I. Experiments reveal that both 14–3-3ε and UFM1 are required for UFL1 to interact with RIG-I, supporting a model where UFL1 first interacts with 14–3-3ε and catalyzes its UFMylation or that of an associated protein, and this complex then associates with RIG-I. UFL1 is necessary for the interaction of 14–3-3ε with activated RIG-I, which is essential for RIG-I to move to intracellular membranes to interact with MAVS. Loss of UFL1 or UFM1 diminishes the SenV-induced interaction of RIG-I with 14–3-3ε and MAVS, as well as MAVS oligomerization, a key step in its activation.

Andres Puschnik's lab has shown that for hepatitis A virus (HAV), another RNA virus, to replicate efficiently, UFMylation of the host's ribosomal protein RPL26 is necessary (Kulsuptrakul et al., 2021)(

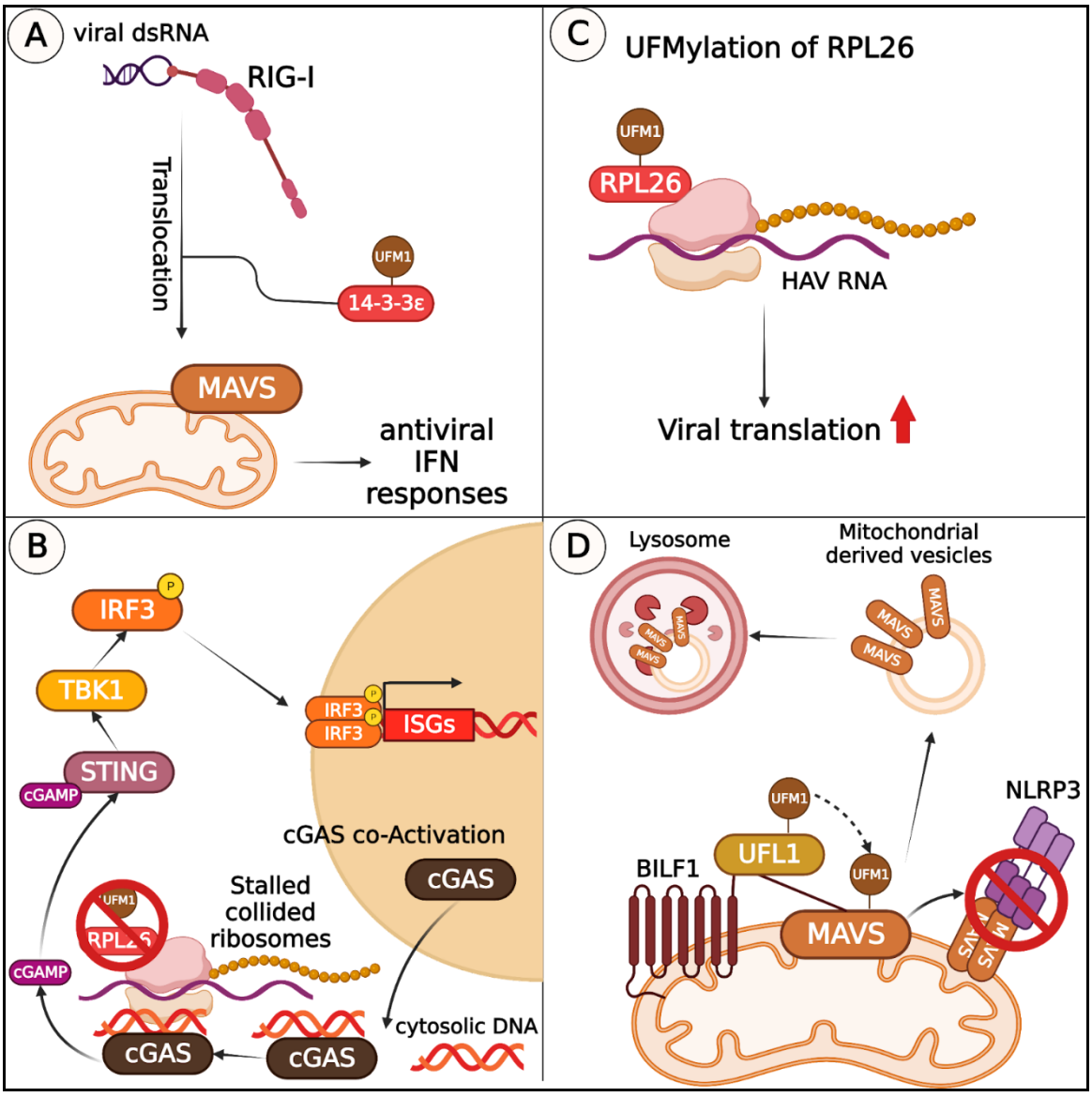

Figure 1-5 (B)). This protein, located near the ribosome exit tunnel, may undergo conformational changes through UFMylation to improve translation of specific sequences or resolve secondary RNA structures. It was suggested that HAV can bear this secondary RNA structures in its mRNAs and this is why RPL26 UFMylation is required for its efficient translation.

Another study that has already shown the importance of UFMylation in the context of viral infection investigates how the Epstein-Barr Virus (EBV) protein BILF1 interacts with host cell mechanisms during the virus's lytic cycle, particularly focusing on the UFMylation pathway and its impact on MAVS (Yiu et al., 2023) (

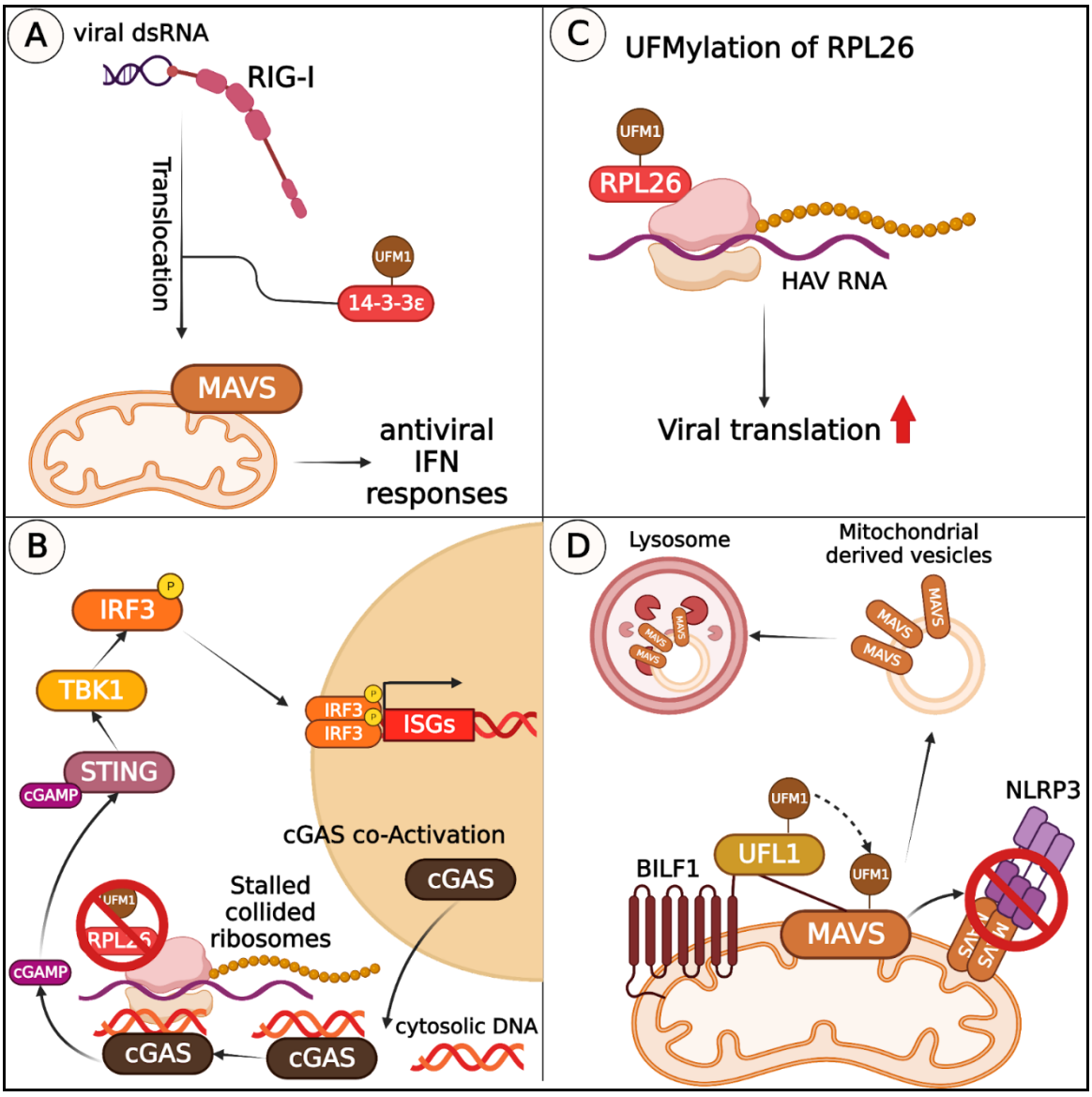

Figure 1-5 (C)). The research identified a strong interaction between EBV protein BILF1 and the host's UFL1. BILF1 expression in cells triggers the UFMylation of MAVS, a key component in the host's antiviral response. This UFMylation was specifically found at lysine 461 of MAVS. The study shows that BILF1-mediated UFMylation of MAVS leads to its dislocation from mitochondria, impairing the activation of downstream interferon responses. BILF1's action was also found to block the activation of the NLRP3 inflammasome, a component of the immune response that can lead to cell death through pyroptosis. The study observes that MAVS, post-UFMylation, traffics via mitochondrial-derived vesicles (MDVs) to lysosomes, indicating a novel pathway for MAVS disposition in EBV-infected cells. MAVS, after being dislocated, was found predominantly in

lysosomes as cleavage products, suggesting its degradation in these organelles. This process occurs without the enrichment of other UFMylation pathway components in the lysosomes. In summary, the study reveals how EBV utilizes BILF1 to manipulate the host's UFMylation pathway, targeting MAVS for dislocation and degradation. This mechanism aids in evading the host's antiviral immune responses, particularly by inhibiting MAVS's role in interferon induction and NLRP3 inflammasome activation.

All three studies mentioned above, showed that UFMylation can play a significant role in both facilitating infection and impairing it. For now, there are no evidence of direct UFMylation of viral proteins. All presented studies highlight important role of UFMylation in regulation of viral infection through affecting different host targets in pathways related to antiviral immune response and ER-RQC.

1.3.6 Rationale and hypothesis

Influenza virus infection can induce ER stress in host cells. The ER is a key organelle in the cell responsible for protein folding, assembly, and trafficking. When a cell is infected by the influenza virus, the increased demand for viral protein production can overwhelm the ER's capacity, leading to an accumulation of misfolded or unfolded proteins in the ER lumen which leads to ER stress. ER stress triggers a cellular adaptive response UPR. UPR aims to restore normal function by halting protein translation, degrading misfolded proteins, and activating signaling pathways that increase the production of molecular chaperones. Some studies suggest that the UPR can be beneficial for influenza virus replication. Certain elements of the UPR, like the IRE1 pathway, can enhance viral replication. At the same time, it was shown that PERK branch of UPR is harmful for IAV. UFMylation pathway – is a regulator of the ER homeostasis. Previously, we discussed how closely UFMylation is connected with different ER related pathways including ER stress, UPR and ER-phagy.

In this study, my investigation of UFMylation and IAV infection is rationalized by UFMylation role in ER-RQC regulation that is crucial for IAV infection due to several viral proteins that are synthesized and proceeded in ER. UFMylation is also an important mechanism of solving the problem of ribosome stalling. Ribosome stalling can be harmful for IAV due to the fact that for influenza virus it is important to have ability to freely usurp host cell ribosomes and produce viral proteins.

My hypothesis is that UFMylation can affect IAV replication as a regulator of ER homeostasis which IAV is known to be sensitive to. I suggest that IAV can also usurp and dysregulate UFMylation pathway transcriptionally and on protein level and by changing its targets to create advantageous ER landscape to facilitate viral protein synthesis and replication.

Figure 1-1 Influenza A virus replication Influenza A virus replication cycle Influenza A Virus replication cycle starts with HA binding to sialic acid receptors on the host cell membrane. Upon binding receptor-mediated endocytosis occurs with endosome formation. Endosomal low pH helps with opening M2 ion channels that acidify the viral core. These events lead to viral particle uncoating and vRNP release to host cell cytosol. Viral proteins that are part of the vRNP complex contain NLS that help vRNP to enter the nucleus. Viral RNA-dependent RNA polymerase handles both viral transcription and replication. Viral genome replication consists of two steps: synthesis of complementary RNA (cRNA) and subsequent synthesis of viral RNA (vRNA) on cRNAs as templates. Viral transcription requires primers to occur which are obtained by a mechanism called cap-snatching. PB2 binds to host mRNAs and PA cleaves 10-13 nucleotides downstream of 5`cap with its endonuclease domain. Synthesized viral mRNAs are exported from the nucleus to the cytosol to be translated on cytosolic ribosomes. Newly translated PB1, PB2, PA, and NP are imported back to the nucleus to be assembled into vRNPs. NA, HA and M2 mRNAs are transported to cytosolic ribosomes, however, the N-terminal sequence of HA and transmembrane domains of NA and M2 recruit ribosome–nascent chain complex to ER. After the synthesis proteins are transported to the Golgi and then trafficked to the host cell plasma membrane. In the late stages of infection, newly synthesized vRNPs are transported to the budding parts of the plasma membrane where NA and HA are colocalized and M2 is located. Figure created in Biorender.

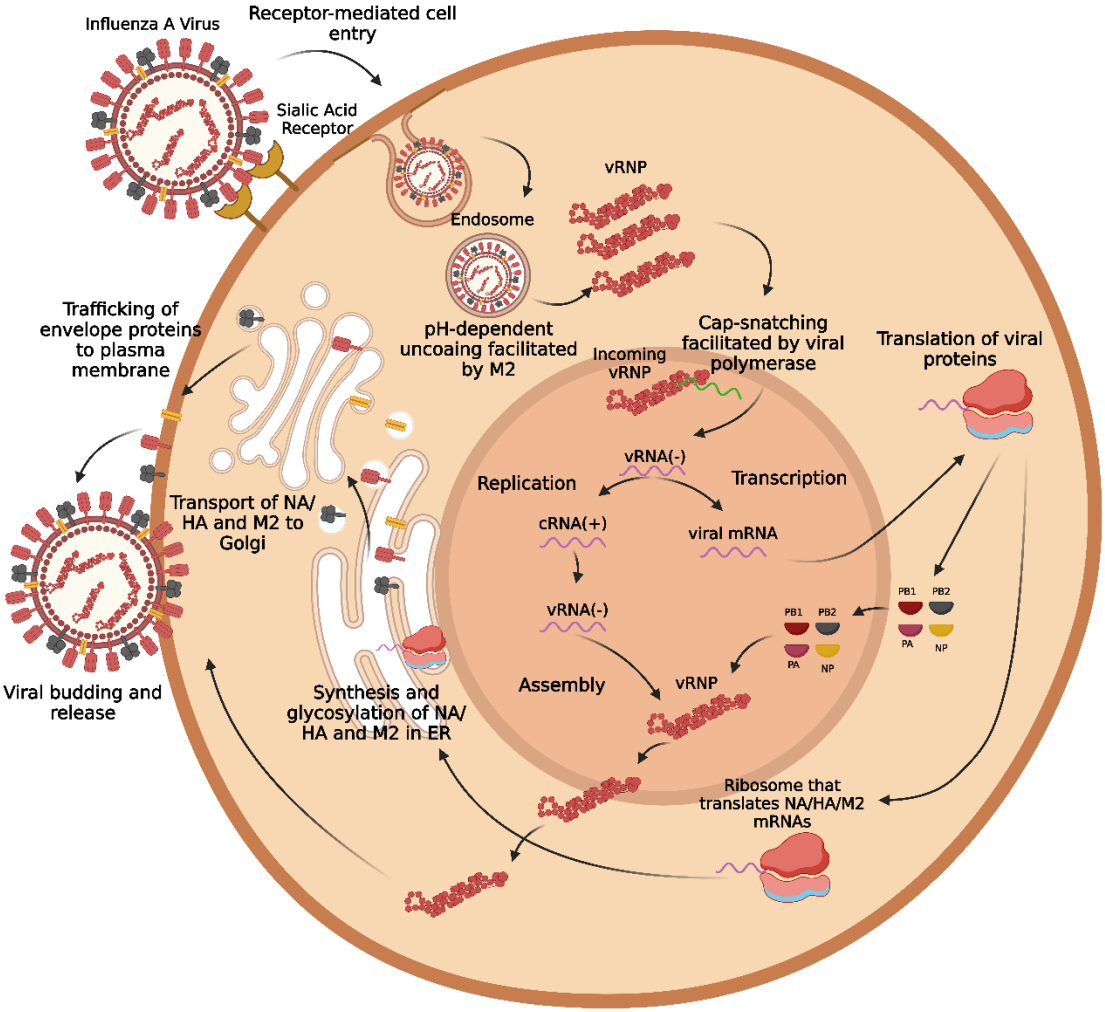
Influenza A Virus
Receptor-mediated cell entry
Sialic Acid Receptor
Endosome
vRNP
pH-dependent uncoaing facilitated by M2
Cap-snatching facilitated by viral polymerase
Translation of viral proteins
Trafficking of envelope proteins to plasma membrane
Incoming vRNP
vRNA(-)
Replication
Transcription
cRNA(+)
viral mRNA
Transport of NA/ HA and M2 to Golgi
PB1
PB2
PA
NP
vRNA(-)
Assembly
vRNP
Viral budding and release
Synthesis and glycosylation of NA/ HA and M2 in ER
Ribosome that translates NA/HA/M2 mRNAs

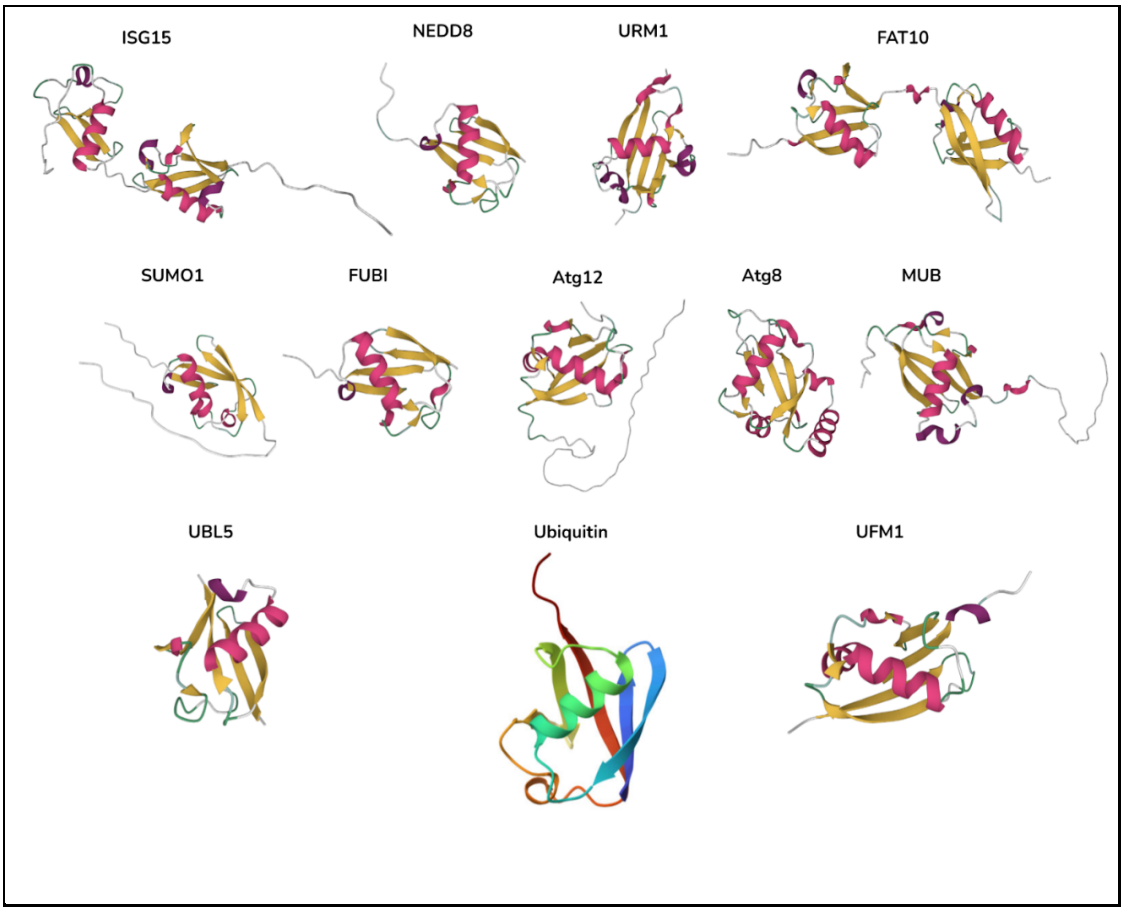

Figure 1-2 Three-dimensional ribbon diagrams of Ubiquitin and Ubiquitin-like proteins. The bottom middle diagram of Ub is located. Ub-like proteins demonstrate similarity in structure to Ub. β-grasps are colored in yellow, and α-helixes colored in pink in Ubls models.

Figure 1-3 Comparison of different types of E3 ligases. HECT E3 ligases contain HECT catalytic domain on its C-terminus. HECT domain has N-lobe for E2 ligase binding and C-lobe with catalytic Cysteine which can bind Ub or Ub-like protein. Ub or Ubl binds HECT C-lobe before transferring to the substrate.

U-box E3 ligases contain U-box catalytic domain at the C-terminal which is required for interaction with E2 ligase charged with Ub or Ubl and stimulating its translocation to the substrate.

RING E3 ligases contain RING zinc-binding domain at the N-terminus. This domain binds E2 ligase charged with Ub or Ubl and stimulates its direct transfer to the substrate.

RBR E3 ligases contain two RING domains (RING1 and RING2) that are linked through the IBR domain. RBR E3 ligases catalyze Ub or Ubl binding to the substrate in a two-step reaction. Firstly, Ub or Ubl is transferred to RING2 domain from E2 located on RING1 domain and then to the substrate.

Multi-subunit RING E3 ligases are subtypes of RING E3 ligases. The figure demonstrates the model of one of the well-studied Cullin-based E3 ligase. It consists of Cullin protein, RING-box small protein which is responsible for E2 binding, adaptor protein, and substrate recognition protein for substrate binding. The complex stimulates the direct transfer of Ub or Ubl to the substrate.

UFMylation E3 ligase complex consists of UFL1 E3 ligase protein which binds both charged with UFM1 E2 (UFC1) and substrate, CDK5RAP3 that is UFMylation regulator, and also binds both UFL1 and DDRGK1 and DDRGK1 that is adaptor protein that recruits the whole complex to cytosolic side of ER.

Domain with similar functions colored in the same colors.

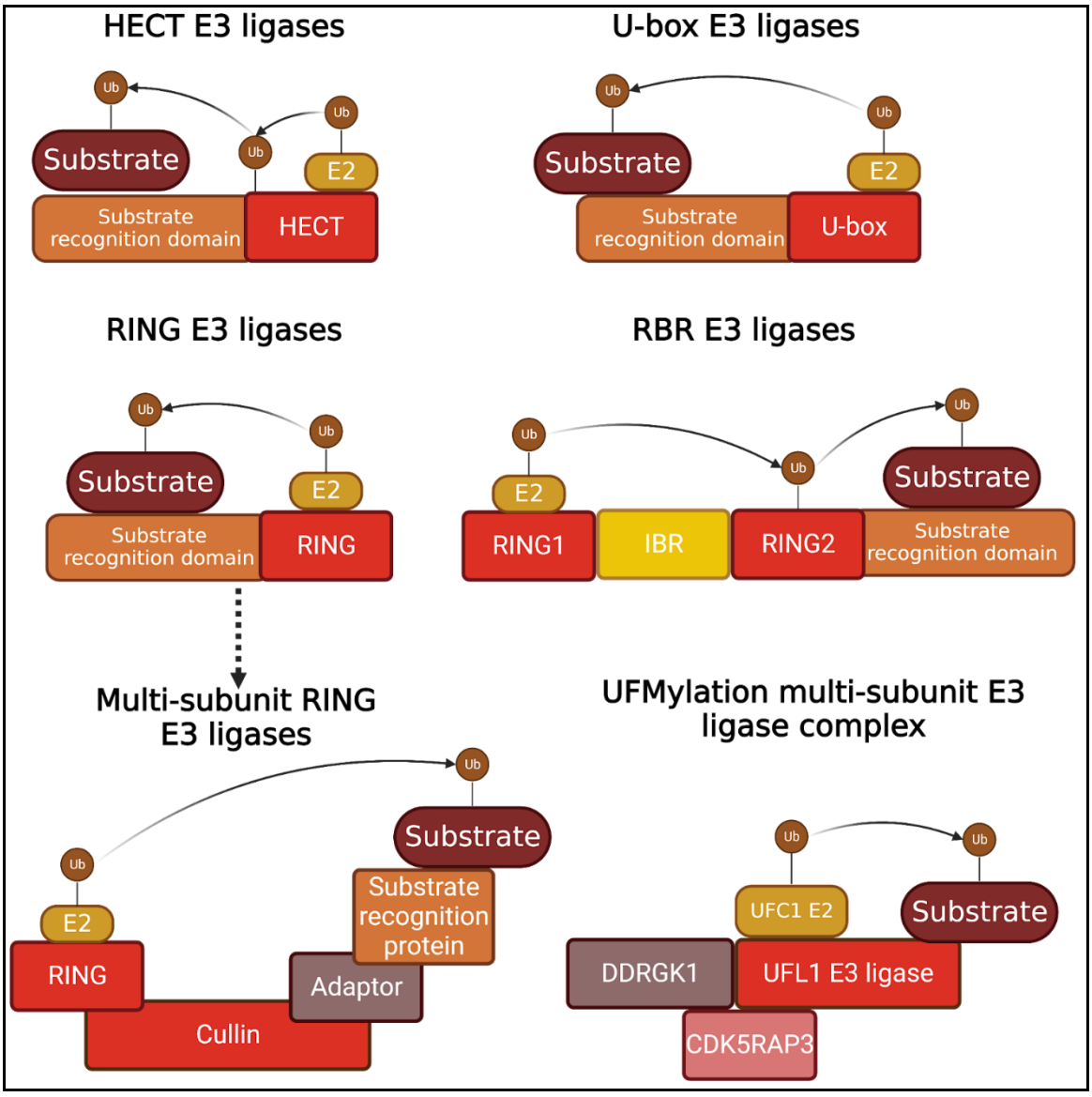
HECT E3 ligases
Ub
Substrate
Ub
Ub
E2
Substrate recognition domain
HECT
U-box E3 ligases
Ub
Substrate
Ub
E2
Substrate recognition domain
U-box
RING E3 ligases
Ub
Substrate
Ub
E2
Substrate recognition domain
RING
RBR E3 ligases
Ub
E2
Ub
Ub
Substrate
RING1
IBR
RING2
Substrate recognition domain
Multi-subunit RING E3 ligases
Ub
Substrate
Ub
E2
Substrate recognition protein
RING
Adaptor
Cullin
UFMylation multi-subunit E3 ligase complex
Ub
Ub
UFC1 E2
Substrate
DDRGK1
UFL1 E3 ligase
CDK5RAP3

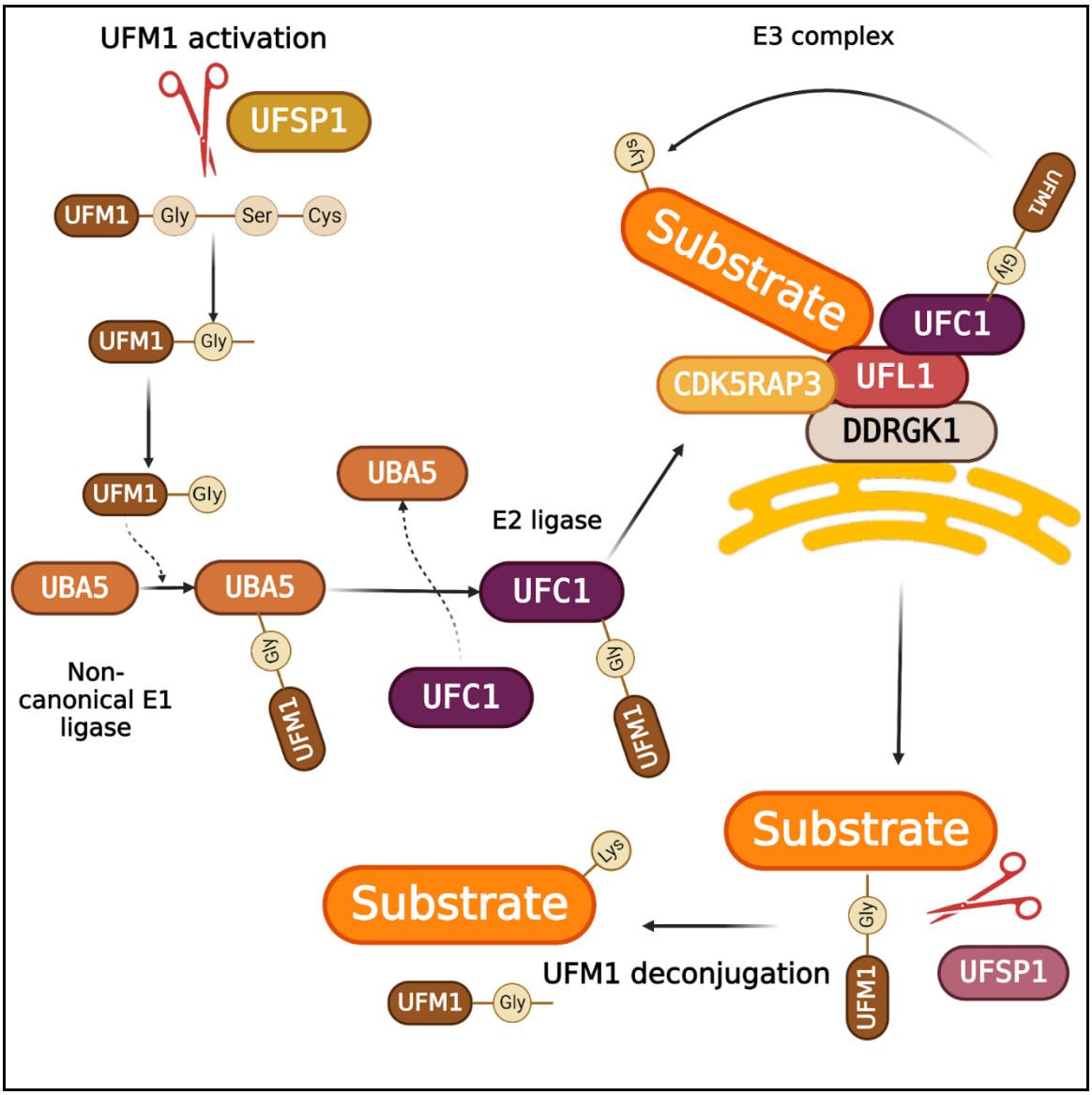

Figure 1-4 Overview of the human UFMylation pathway.UFM1 is activated by UFSP1 protease via cleavage of Cysteine and Serine on its C-terminus and exposing conserved Glycine. Firstly, UFM1 is activated by non-canonical E1 ligase UBA5, forming a high-energy thioester bond with it. Then, activated UFM1 is transferred to UFC1, E2 ligase, forming a similar thioester bond. Next, UFM1 is recruited to the E3 ligase complex that is located on the cytosolic side of ER and consists of UFL1, DDRGK1, and CDK5RAP3. With the help of UFL1, UFM1 is transferred to Lysine of the target protein. UFMylation is a reversible process - UFM1 can be cleaved from target Lysine by UFSP2 protease.

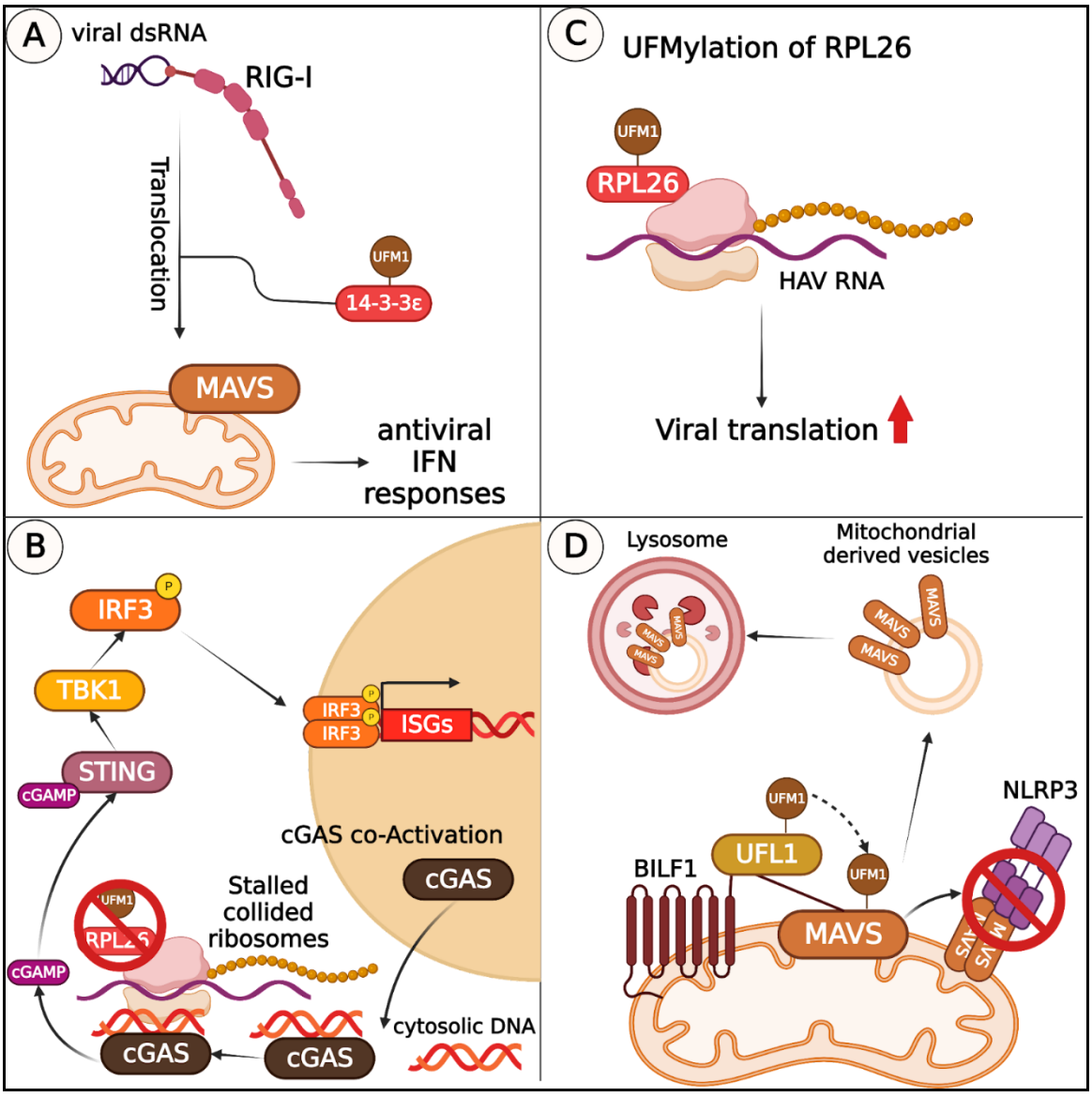

Figure 1-5 Evidence for a role for UFMylation in viral infection. A) 14-3-3ε UFMylation facilitates its interaction with RIG-I with its subsequent translocation to MAVs and activation of antiviral IFN response. B) When cytosolic DNA is presented in the cytoplasm and ribosomes are stalled cGAS-STING pathway is activated which leads to ISGs expression. C) Stalled ribosomes can be degraded by UFMylation of RPL26. This process was shown to enhance HAV translation. D) EBV-encoded G-protein-coupled receptor BILF1 facilitates UFMylation of MAVS leading to its packaging in mitochondrial-derived vesicles with subsequent degradation in lysosomes. Due to this mechanism, MAVS is not able to interact with NLRP3 and form an inflammasome with subsequent activation of antiviral defense.

Materials and Methods

2.1 Cell culture and treatments

UFM1/UFSP2 KO Human lung adenocarcinoma A549 cells were obtained from former McCormick lab honors student - Estelle Samaraweera. To achieve the knockouts of UFM1 and UFSP2, she employed CRISPR/Cas9 using two distinct lentiviral vectors, each carrying a unique guide RNA (gRNA) targeting one of the genes of interest. These vectors were then used to produce lentiviruses. Control lentiviruses, which carried vectors with a non-targeting control sgRNA (designed not to target any protein-coding sequences), were also generated to create a control A549 cell line (NT). The A549 cells were transduced with these lentiviruses, and after selection, monoclonal cell lines were established. Knock out of UFM1 and UFSP2 were confirmed before experiments by immunoblotting. Monoclonal cell lines were used, clone#1 for UFM1 KO A549 cells and clone#2 for UFSP2 KO A549 cells. Madin-Darby canine kidney (MDCK) cells, human embryonic kidney 293T (HEK293T) cells, and human lung adenocarcinoma A549 cells were maintained in Dulbecco's modified Eagle's medium (DMEM, HyClone, Mississauga, ON, Canada) supplemented with 10% heat-inactivated fetal bovine serum (FBS, Life Technologies, Burlington, ON, Canada), 20 μM L-glutamine (Life Technologies, Burlington, ON, Canada), and 100 U/mL penicillin + 100 μg/mL streptomycin + 20 μg/mL glutamine (Pen/Strep/Gln; Wisent Bioproducts, St-Bruno, QC, Canada). Cells were maintained at 37°C in 5% CO_2 atmosphere. Cells were passaged when 70-90% confluence was reached. 1X phosphate-buffered saline (PBS; Wisent Bioproducts, St-Bruno, QC, Canada) was used to wash the monolayer, and 0.05% Trypsin-EDTA (Thermo Fisher Scientific, Burlington, ON, Canada) was used to detach A549 and HEK293T cells during splitting and seeding while 0.5% Trypsin-EDTA (Thermo Fisher Scientific, Burlington, ON, Canada) was used to detach MDCK cells. Cell viability and cell number were determined with Trypan blue (Sigma-Aldrich) staining followed by counting using a hemocytometer. Thapsigargin (Tg) was applied on cells for IAV infection inhibition at a concentration of 100 nM with 24 hours of incubation. It was solubilized in dimethyl sulfoxide (DMSO) and stored at -20℃.

2.2 Transfections For anti-Strep affinity purification, HEK293T cells were transfected using reverse transfection. $4.5x10^6$ cells were seeded in 10 cm dishes, in antibiotic-

free medium with transfection reagent. Transfections of HEK293T cells were performed with a 3:1 ratio (polyethyleneimine (PEI; Warrington, PA) volume in ul: to DNA mass in ug). 12 ug of plasmid DNA were diluted in 0.5 ml OptiMEM (Thermo Fisher Scientific) and left to incubate for 15 minutes at room temperature. The transfection solutions were then added in a drop-wise manner into respective 10 cm dishes. At 12 hours post-transfection, the media was changed and replaced with a culture medium. The cells were incubated at 37°C for a total of 24 h. After 24 h, cells were collected for affinity purification. Similarly, for anti-Strep affinity purification of, A549 NT cells were seeded transfected as above, but using Lipofectamine 3000 (20 ug plasmid DNA, 40 ul of reagent P3000, and 43 ul of reagent Lipofectamine 3000). The DNA mix: 20 ug of PLVX-2XStrep-UFM1 and 40 ul of P3000 were combined with 0.5 mL Opti-MEM (Life Technologies, Burlington, ON, Canada). 43 ul of Lipofectamine 3000 was combined with 0.5 mL Opti-MEM, too. The combined DNA and transfection mix was incubated for 15 minutes and added to the dishes containing 9 mL of culture medium.*Influenza viruses and infections* Viruses used in this study include Amantadine sensitive A/Puerto Rico/8/34/(H1N1) (stPR8) which is a laboratory-adapted strain, A/Puerto Rico/8/34/(H1N1) (rgPR8) was generated using reverse genetics approach by former McCormick lab intern Artem Kichydzhy, A/Udorn/1972(H3N2) (Udorn). PR8 and Udorn stock were propagated in MDCK cells in IAV infection media (DMEM supplemented with 0.5% [w/v] bovine serum albumin (BSA, Sigma, St. Louis, MO, USA) and 20 µg/mL L-glutamine, and 1 µg/ml N-tosyl-L-phenylalanine chloromethyl ketone (TPCK)-treated trypsin) from stocks available in McCormick lab. TPCK-treated trypsin activates IAV HA by cleaving HA0 into HA1 and HA2, liberating the fusion peptide. The supernatant was harvested at 48-72 hpi when cytopathic effects were presented in 90% of the cells, and centrifuged at 2,300 x g for 5 minutes to pellet cellular debris, aliquoted, and stored at -80℃. Plaque forming units (PFU) were calculated by plaque assay as described below. For infections of cultured cells, cell monolayers were washed briefly with 1xPBS twice before inoculation with diluted virus. Infections were conducted at a multiplicity of infection (MOI) of 0.5 and 2

for evaluating viral fitness, MOI of 1 for evaluation of UFMylation pathway genes expression during infection, or MOI of 5 for the affinity purification experiments. The cells were incubated for 1 hour at 37℃ while shaking the inoculum every 10 minutes. After the diluted inoculum was removed, cell monolayers were washed with 1xPBS (Wisent, St-Bruno, QC, Canada), and fresh IAV infection media was added. Supernatants were harvested at 24 hpi unless indicated otherwise. Virus virus-containing supernatant was incubated with TPCK-treated Trypsin at 1.5µg/mL for 1 hour at 37℃ to activate influenza HA and stored at -80℃.*Plaque assay* Plaque assays were performed on 95-100% confluent monolayers of MDCK cells. Six 10-fold serial dilutions of each virus sample were prepared in 0.5% BSA DMEM. Confluent MDCK cells were washed with 1XPBS twice and infected with diluted viral samples for 1 hour at 37℃ shaking every 10 minutes. Viral inoculums were then aspirated off and cells were washed with 1XPBS. Overlay (9 volumes of 2XMEM (Life Technologies, Burlington, ON, Canada), 1 volume 5%BSA in DMEM; 10 volumes 2.6% Avicel supplemented with 1µg/mL TPCK-treated trypsin (Matrosovich et al., 2006)) was added to the wells and incubated for 48h for PR8 and Udorn and 72 hours for Cal7 at 37℃ with 5% CO2 atmosphere providing sufficient time for plaques to form. Cells were washed 3 times with 1XPBS to remove the overlay and fixed with 5% formaldehyde for 30 minutes at room temperature. Cells were washed with 1XPBS for 5 minutes each before adding 1% crystal violet (w/v in 50%methanol:50% dH2O). Crystal violet was washed off after incubating for 5 minutes before counting plaques. Plaques were counted manually from three technical reps to obtain an average. This value was used in the formula to calculate virus titer in pfu/ml: (plaques counted) / (dilution factor x amount of virus plated in ml).*RNA extraction and RT-qPCR* **A549 cells were seeded to the 6-well plate at 200 000 cells/ml, and infected or mock-infected with Influenza A viruses at an MOI of 1. Total cellular/viral RNA was isolated using the RNeasy Plus mini kit (Qiagen Inc., Toronto, ON, Canada) according to the manufacturer's protocol at 8, 16, and 24 hpi. 500 ng of total RNA was reverse transcribed into cDNA using the Maxima H Minus Reverse Transcriptase kit (Thermo Fisher Scientific, Burlington, ON,**

Canada) in separate reactions containing random hexamer primers and the oligo(dT)18 primer for mRNA of cellular targets. 250 ng of total RNA was reverse transcribed into cDNA using the Maxima H Minus Reverse Transcriptase kit in separate reaction tubes containing either the oligo(dT)18 primer for viral mRNA or influenza A virus-specific universal primer Uni12 (5'-AGCAAAAGCAGG-3'), for vRNA. Quantitative PCR analysis was performed after reverse transcription, using 2X GoTaq qPCR Master Mix (Promega), 200 nM of each forward and reverse primers (

Table 3), and 1:40 diluted cDNAs. UFM machinery targeting primers were obtained from former McCormick lab Honors student Trinity Tooley. Primers for viral target genes were designed in Khaperskyy lab and purchased through Thermo Fisher Scientific. The results were analyzed using the ΔΔCq method to calculate fold change and normalized to 18S rRNA levels (Livak & Schmittgen, 2001).

Table 3 Forward and reverse primers used for RT-qPCR.

Gene Target	5'-3' Forward Primer	5'-3'Reverse Primer
Ufm1	TAGAGGAAGTCGTGCTACC	AAGGAAACCTTCGACATGG
Uba5	ACATACTCTGAGGAACATTAATCC	AACCCACCATTACTTATTCTATCC
Ufc1	CCAACAAGGAAGGAACTCG	TGTGATAGGAATGTCAAACTCG
Ufl1	GATATTGCACCTCTGCTACC	CGCTAAAGACTACAGTTGAGG
DDRGK 1	CCAAGGTTGTGCTCTTGG	TCAATCACACCTGTTATAGTCC

Gene Target	5’-3’ Forward Primer	5’-3’Reverse Primer
CDK5RAP3	TCCAGCCTGAAGCGGAAGTGG	TCGCGGATCGTCAGCACCAG
NS1	CTGTGTCAAGCTTTCAGGTAGA	GGTACAGAGGCCATGGTCAT
NP	CCCAGGATGTGCTCTCTGAT	TTCGTCCATTCTCACCCCTC
18S rRNA	TTCGAACGTCTGCCCTATCAA	GATGTGGTAGCCGTTTCTCAGG

2.6 SDS-PAGE and immunoblotting

NT and UFSP2KO A549 cells were seeded 200 000 cells/ml on 6-well plates and infected or not infected at MOI 2 with described before Influenza A viruses. The seeding density was chosen to have sufficient amount of protein at harvesting day. Cell lysates were collected at 8, 16, and 24 hpi. Cell monolayers were washed once with ice-cold PBS and lysed in 2x Laemmli buffer (4% [w/v] sodium dodecyl sulfate [SDS], 20% [v/v] glycerol, 120 mM Tris-HCl [pH 6.8]). DNA was sheared by repeated passage through a 21-gauge needle before 100 mM dithiothreitol (DTT) addition and boiling at 65℃ for 10 minutes. Samples were stored at -80℃ until analysis. Protein concentrations were calculated using the Lowry Protein Assay with DC Protein Assay kit (BioRad). The proteins were diluted with 1X Laemmli to a concentration of 1 ug/uL and 10 ug of protein was loaded per well on polyacrylamide gels. The proteins were resolved at 100V for approximately 1.5 hrs with 1XSDS running buffer. The proteins were then transferred to a methanol-activated PVDF membrane (Bio-Rad) using the Trans-blot Turbo Kit and Transfer System (Bio-Rad). Membranes were blocked in 5% BSA (Bioshop) in TBS-T (Tris-buffered saline, 0.1% Tween) for 1 hour of shaking at room temperature. Membranes then were probed with primary antibodies diluted in 5% BSA in TBS-T overnight at 4℃. Antibodies with concentrations are listed in Table 4. Following incubation, the membranes were washed with TBST 3 times for 5 minutes with rocking.

The membranes were subsequently incubated in a secondary antibody solution, either horseradish peroxidase (HRP)-conjugated goat-anti-rabbit or goat-anti-mouse, diluted 1:5000 in 5 mL of 5% BSA-TBST and incubated for 1 hour at room temperature with rocking. Membranes were again washed 3 times for 5 minutes with TBST. The blots were developed using Clarity Western ECL Substrate (Bio-Rad) for 5 minutes. Blots were visualized using the Bio-Rad ChemiDoc imaging system. Molecular weights were determined using protein standards (New England Biolabs, P7719). Each protein target was probed independently of each other, except cellular actin antibody. For anti-Actin immunoblotting, membranes were washed again 3 times for 5 minutes with TBST and reprobed with actin antibodies.

Table 4 Antibodies and corresponding dilutions used for immunoblotting.

Protein Target	Species	Dilution	Manufacturer and Catalogue Number
Ufm1	Rabbit mAb	1:2000	Abcam/ ab109305
Uba5	Rabbit mAb	1:6000	Abcam/ ab177478
Ufc1	Rabbit mAb	1:2000	Abcam/ ab189252
Ufl1	Rabbit pAb	1:500	Abcam/ ab103047
DDRGK1	Rabbit mAb	1:1000	Proteintech/ 21445-1-AP
CDK5RAP3	Rabbit mAb	1:2000	BETHYL/A300-870A

Protein Target	Species	Dilution	Manufacturer and Catalogue Number
UFSP2	Mouse mAb	1:1000	Santa Cruz/ sc-376804
RPL26	Rabbit mAb	1:1000	Cell Signaling/ 5400
poly IAV	Goat pAb	1:1000	Abcam/ab20841
anti-Strep	Mouse mAb	1:1000	IBA/ 2-1507-001
Anti-mouse HRP	Goat mAb	1:5000	Cell Signaling/ 7076
Anti-rabbit HRP	Goat mAb	1:5000	Cell Signaling/ 7074

2.7 Protein purification and Silver Stain Screening

To obtain cells bearing 2XStrep-tagged UFM1 for affinity purification plasmid pLVX-2XStrep-UFM1delSC was constructed (Figure 2-1). Before conjugation, UFM1 must be activated by cleaving the C-terminal dipeptide Ser-Cys to expose a single glycine residue. pLVX-2XStrep-UFM1delSC was designed with without C-terminal Ser-Cys (2XStrep-UFM1delSC) fragment to enhance conjugation in the cell. 2xStrep tag was located on UFM1 N-terminus to enable anti-Strep affinity purification to extract all proteins that were UFMylated with expressed 2X-Strep-UFM1delSC. 2XStrep-UFM1delSC fragment was synthesized via Invitrogen GeneArt Gene Synthesis. The fragment was codon optimized and flanked with restriction sites: EcoRI on its N-terminus and BamHI on its C-terminus. The synthesized fragment was digested with EcoRI and BamHI, and subcloned into pLVX-EF1alpha-SARS-CoV-2-M-2xStrep-IRES-Puro

(Addgene #141386, a kind gift from Neville Krogan)**.** 2XStrep-UFM1 was pasted into the PLVX backbone via sticky ends ligation under EF1alpha promoter to guarantee a high level of expression. This plasmid can be also used as a plasmid for lentiviruses production, however, in this study it was used for transient transfection. See Figure 2-1 for the plasmid map.

Transfected A549 cells were lysed with lysis buffer (IP buffer) (Gordon et al., 2020) for Strep-tagged protein purification. The buffer content is provided in Table 5. Protein concentrations were calculated using the Lowry Protein Assay with DC Protein Assay kit (BioRad). Samples were diluted equally with lysis buffer to have an equal amount of protein in the experimental sample and control. Afterward, lysates were frozen at -80 and subsequently used for protein purification. Strep-Tactin®XT 4Flow® kit was used for protein purification. The manufacturers' protocol was used with modifications such as Biolock (IBA Lifesciences) application as the first step with the best volume identified as 20 uls to block biotin in lysates and make lysates binding to the columns resin more efficient. Samples were incubated different time with resin to determine the best time for protein binding as 1 hour. 2 washes were applied with subsequent 4 elutions with different conditions:

1 elution - recommended elution due to the manufacturer (5 minutes incubation with elution buffer at RT)

2 elution - recommended elution due to the manufacturer and adding additional amount of biotin as 50 uls of 50 mM biotin

3 elution - 20 minutes incubation time of column with elution buffer with adding of 50 uls of 50 mM biotin

4 elution - 10 minutes incubation time of column with elution buffer at 37°C with adding of 50 uls of 50 mM biotin

Eluted samples were stored at -80 for subsequent analysis. Aliquots of 40 uls were mixed with 2X Laemmli buffer with DTT and Brom Phenol Blue for subsequent Immunoblotting and Silver stain analysis.

Table 5. Lysis buffer for purification of Strep-tagged proteins composition

Reagent	Concentration
Protease Inhibitor Cocktail, cOmplete Tablets, Roche	1 tablet per 10 ml
Tris-HCl, pH 7.4 at 4℃	50 mM
NaCl	150 mM
EDTA	1 mM
NP40 substitute	0.5%

An equal number of experimental samples and control samples (the whole lysate, the flow, 2 washes, and 4 elutions) were loaded on 12% polyacrylamide gels. The proteins were resolved at 100V for approximately 1.5 hrs with a 1XSDS running buffer. Gels were silver stained with Silver Stain Plus Kit from BioRad due to the manufacturer`s instruction. Gels were stained for 60 minutes instead of the recommended 20 minutes to provide better brightness of the bands. Subsequently, gels were imaged with a digital camera and images were obtained in jpeg format or with ChemiDoc (BioRad) and stored in both jpeg and Image Lab Image Document.

2.8 Data analysis

Statistical analysis was performed on values obtained from at least three independent biological replicates with PRISM GraphPad 8. Data obtained from plaque assay were analyzed using logarithmic transformation to normalize data with subsequent one-way ANOVA followed by a Dunnett's multiple comparison test. Data from qPCR experiments was logarithmically transformed and plotted as mean ± SEM from three independent experiments. Significance is indicated with * (p-value of <0.05), ** (p-value of <0.01), *** (p-value of <0.001).

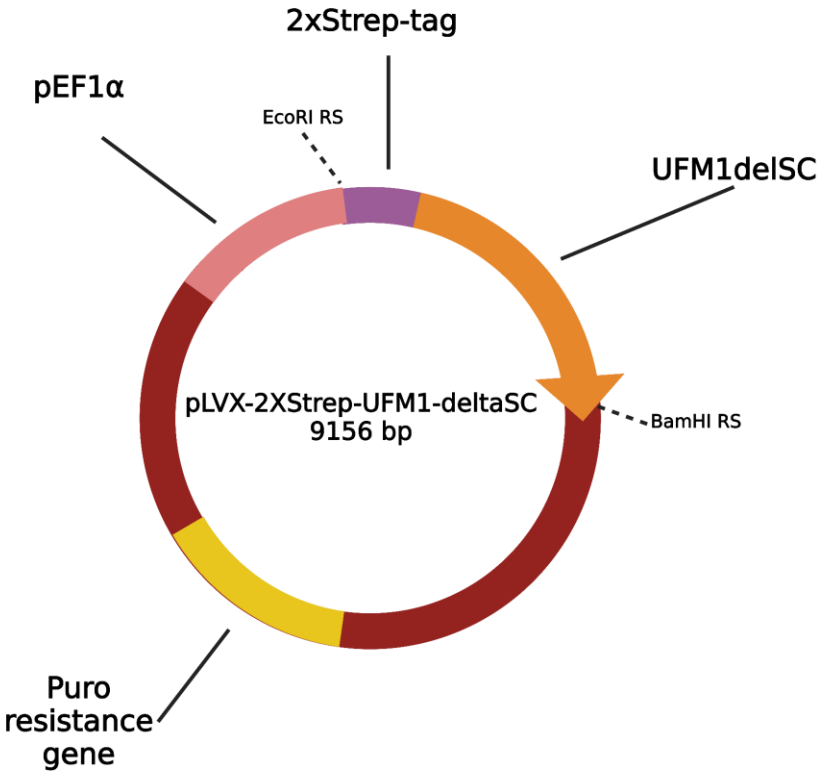

Figure 2-1 Plasmid map of construct pLVX-2XStrep-UFM1delta_SC. Labels: pEF1α - promoter EF1α, 2XStrep-tag - tag for affinity purification, UFM1delSC - preactivated UFM1 with deleted Ser-Cys, dotted lines are showing restriction sites BamHI and EcoRI for cloning the fragment into pLVX backbone. Figure created with Biorender.

Chapter Three - Results

3.1 IAV host shutoff inhibits the accumulation of UFMylation pathway gene products

IAV host shutoff inhibits host gene expression through the action of at least 2 viral proteins that interfere with host mRNA processing and stability. Specifically, NS1 inhibits pre-mRNA 3` end processing and nuclear export, whereas PA-X endonuclease cleaves host mRNAs to prevent their translation and make them susceptible to degradation via the host exonuclease Xrn1 (Khaperskyy D. A. et al., 2016). However, there is mounting evidence for selectivity in IAV host shutoff mechanism, whereby some host transcripts resist host shutoff. There is also evidence that IAVs differ in host shutoff mechanisms, whereby some strains lack host shutoff functions (Twu et al., 2007). For these reasons I investigated whether UFMylation pathway gene products were susceptible to host shutoff.

To evaluate host shutoff influence on UFMylation machinery, I analyzed the level of expression of UFMylation machinery components during IAV infection. Steady-state mRNA levels were assessed for Ufm1 the main player of UFMylation pathway, Uba5 – activator of UFM1, Ufc1 – conjugator of UFM1, Ufl1 – UFMylation pathway ligase, CDK5RAP3 – regulator of the UFMylation, and DDRGK1 - regulator and adaptor. A549 WT cells were infected with PR8 or Udorn IAV viruses that are H1N1 IAV and H3N2 IAV at MOI of 1. I chose these viruses because it can show differences between IAV that have different HA and NA but also because these viruses have different replication rate, different level of host shutoff that they can cause and their PA-X proteins have different turn-over time. After infection, I collected cellular lysates for mRNA extraction, cDNA synthesis and gene-specific qPCR. I conducted time-course experiment with samples collection at 8, 16 and 24 hpi to evaluate changes during all viral replication cycle.

I observed no increase or decrease in mRNA levels during PR8 infection for all UFMylation pathway components despite DDRGK1 (Figure 3-1(B)). DDRGK1 was downregulated (2-fold) during all time-course starting from 8 hpi. These results suggest that UFMylation pathway genes are resistant to host shutoff induced by PR8 IAV and only DDRGK1 is sensitive to host shutoff caused by PR8.

By contrast, drastic changes were observed in the expression of UFMylation machinery during H3N2 Udorn infection. The observed decrease in expression level was

up to 12-fold for CDK5RAP3 and DDRGK1 at 24 hpi, up to 4-fold for UFM1and UFC1, up to 8-fold for UFL1, and up to 10-fold for UBA5 (Figure 3-2 (B)). The pronouncing host shutoff effect on UFMylation pathway genes compared to PR8 infection can be connected with differences in PR8 and Udorn NS1 protein or higher stability of PA-X in the Udorn strain and this will be discussed in the Discussion section. It can be also explained by the higher replication rate of the Udorn strain compared to the PR8 one (Figure 3-1 (A); Figure 3-2 (A)).

3.2 IAV infection decreases the amount of protein for some components of UFMylation machinery

Because IAV affects mRNA level of UFMylation pathway components, I decided to investigate whether these changes were also manifested at the protein level. To identify if IAV PR8 (H1N1) or Udorn (H3N2) infection can affect UFMylation machinery on the protein level, A549 cells were infected with rgPR8 (PR8 obtained by reverse genetics approach) and stPR8 (McCormick lab stock of PR8) or Udorn at MOI of 2. Cell lysates were collected at 8 for PR8 or 4 for Udorn, 16, and 24 hpi with subsequent preparation for immunoblotting. I did not observe any changes in protein levels for UBA5, UFL1, and UFSP2 compared to mock control during PR8 infection. UFC1 was decreased in infected samples compared to mock, but this decrease was inconsistent among 4 replicates so it cannot be considered a valid result (Figure 3-3). At the same time, CDK5RAP3 was strongly decreased at 24 hpi in both stPR8 and rgPR8 infections (Figure 3-4). Subsequent statistical analysis of CDK5RAP3 normalized to Actin intensity values obtained from 3 independent biological replicates confirmed that decrease in protein abundance was significant at all timepoints (Figure 3-5). Due to qPCR data that showed that the number of mRNA transcripts of CDK5RAP3 stayed stable during infection, I hypothesized that PR8 infection can cause degradation of CDK5RAP3 in the late stage of infection via autophagy as CDK5RAP3 is known to play ER-phagy receptor role under ER stress conditions (Mochida & Nakatogawa, 2022). However, it will be discussed further in the Discussion section.

The changes in the amount of DDRGK1 during PR8 infection were identified in the same way as was described for CDK5RAP3 earlier. The amount of DDRGK1 protein was slightly decreased at all time points in infected A549 cells compared to the mock

(Figure 3-3). Subsequent analysis of expression level during infection showed a decrease in expression during infection similar to the one that was observed previously in studies dedicated to host shutoff induced by PA-X (Khaperskyy D. A. et al., 2016). I hypothesized that lower amounts of protein are connected with host shutoff mechanism. The fact that a decrease in the protein amount can be demonstrated starting from 16 hpi are consistent with the data from RT-qPCR that showed DDRGK1 mRNA amounts decreased from 8 hpi. The amount of protein usually starts to decline later than the amount of mRNA due to the effects of longer protein turnover in the cell.

In the case of Udorn infection, no difference compared to mock control was found for UBA5, UFL1, CDK5RAP3, UFC1, and DDRGK1. The amount of UFSP2 protein was decreased at 16 and 24 hpi in infected A549 cells compared to mock during Udorn infection by 39% and 31% of intensity, respectively, due to data from densitometric assay (Figure 3-6 (B)). Interestingly, despite the big effect of host shutoff caused by Udorn infection that was shown by RT-qPCR results, the protein levels were unchanged during Udorn infection with decrease only in UFSP2 protein levels.

3.3 IAV infection alters global patterns of UFMylation

In experiments dedicated to mRNAs and proteins levels of UFMylation machinery during IAV infection, I demonstrated that UFMylation pathway are inhibited by host shutoff caused by IAV H1N1 PR8 and IAV H3N2 Udorn. To determine if IAV PR8 and Udorn infection can change the level of UFMylation of host cell proteins because of UFMylation machinery inhibition I infected NT cells with PR8 or Udorn at MOI of 2. Infected cells were collected at 8 hpi for PR8 and 4 hpi for Udorn, 16 hpi, and 24 hpi and proceeded as previously described for immunoblotting. For immunoblotting with anti-RPL26 antibodies samples were resolved in 10% SDS-PAGE gel and anti-UFM1 - in 12% gel to make it possible free UFM1 to be seen. Samples were infected with 2 PR8 viruses - stPR8 and rgPR8 or Udorn viruses. StPR8 corresponds to the wt PR8 propagated from stock obtained in McCormick lab and rgPR8 corresponds to the wt PR8 generated by reverse genetics approach by former intern student Artem Kichydzhy. Infection with stPR8 resulted in a slight decrease in di-UFMylated RPL26 species while rgPR8, on the contrary, increased its amount (Figure 3-7(A)). At the same time, both PR8 viruses` infections resulted in a decrease of mono-UFMylated species of RPL26 and a

decrease of the general level of cellular RPL26 (Figure 3-7(A)). The question about the differences between mono- and di-UFMylated species of RPL26 and their functions for the host cell is still unanswered in the current literature. The experiments that can answer some questions about 2 different species of RPL26 and their role in the viral replication cycle will be covered in the Discussion section. However, anti-UFM1 immunoblotting showed no difference between bands that correspond to di- and mono-UFMylated species of RPL26 but a strong decrease in the amount of free UFM1 (Figure 3-7(B)). Different results obtained from anti-RPL26 and anti-UFM1 immunoblotting can lead to the thought that in the case of anti-UFM1 immunoblotting more vivid bands that correspond to mono- and di-UFMylated RPL26 can be the result of another UFMylated product of the same molecular weight. However, there is a pronounced decline in the amount of free UFM1 that can be the result of PR8 changing the UFMylaion of host substrates by switching it to other targets, declining UFM1 protein synthesis, or inducing its degradation.

In the case of Udorn infection, anti-UFM1 immunoblotting showed an increase of di-UFMylated RPL26 species in NT cells at 4 hpi. At the same time, the amount of di-UFMylated RPL26 was decreased in NT cells at 16 and 24 hpi. Mono-UFMylated species of RPL26 were not affected during Udorn infection in NT cells. The amount of free UFM1 was increased at 4 and 16 hpi in NT cells (Figure 3-8). The increase in the level of free UFM1 during Udorn infection in NT cells can be the result of inhibition of UFM1 degradation, or inhibition of UFMylation of substrates that are UFMylated in non-infected cells at normal conditions. Another reason can be host shutoff that was shown to be strongly induced by Udorn virus. Host shutoff usually results in the lower number of proteins produced by the cell which leads to a lower protein load in ER and a smaller number of stalled ribosomes. Thus, host shutoff may be expected to result in less RPL26 UFMylation and more free UFM1 in the infected cell.

3.4 UFM1 and UFSP2 affect IAV replication

To determine whether the absence of UFM1 affected IAV replication, the monoclonal KO cell lines along with NT control were infected with stPR8 strain and with Udorn (H3N2) strain with a low multiplicity of infection (MOI) of 0.5. In this and further experiments, UFSP2 KO, UFM1 KO, and NT (not targeted) A549 cells were used where

indicated, genes KO were confirmed by immunoblotting (Figure 3-9). A549 UFSP2KO#2 and UFM1KO#1 were chosen based on immunoblotting results. The NT control cells were treated with thapsigargin (Tg) as a strong positive control. Thapsigargin induces ER stress by inhibiting sarcoendoplasmic reticulum Ca2 ATPase (SERCA). It is an inhibitor of IAV replication (Goulding et al., 2020). The cells were treated with 100 nM Tg solubilized in dimethyl sulfoxide (DMSO) or the DMSO control for 24 hours. Supernatants were collected at 8, 16, and 24 hpi, and viral titers were measured via plaque assays in MDCK cells (Figure 3-10,Figure 3-11). UFM1 KO resulted in an increase in viral titers of PR8 at 16 and 24 hpi. The UFM1 KO increased virus production by 11.3-fold at 16 hpi compared to the NT control (Figure 3-10) and an 8 fold at 24 hpi. The average virus titer for 8hpi was 2.1x10^5 PFU/mL, the average for 16 hpi was 4.26x10^6 PFU/mL and the average virus titer for 24 hpi was 1.02x10^7. The NT control cell line had an average titer of 2.2x10^5 PFU/mL 8 hpi, 3.6x10^5, and 1.2x10^6 16 and 24 hpi, respectively. Tg treatment strongly reduced viral titer as it was expected. These results suggest that UFM1 is antiviral against influenza A virus replication. At the same time, Udorn replication in the UFM1 KO was comparable to the NT control cell line (Figure 3-11). This means that UFM1 likely does not play a role in H3N2 IAV replication and release of infectious progeny viruses.

UFSP2 KO affected the replication of PR8 only at 8 and 24 hpi with the effect of a decrease in viral titer. The UFSP2 KO reduced virus production by 3.5 fold at 8 hpi compared to the NT control (Figure 3-10) and by 2.3 fold at 24 hpi. The average virus titer for 8hpi was 6.2x10^4 PFU/mL, the average for 16 hpi was 4.1x10^5 PFU/mL and the average virus titer for 24 hpi was 5.06x10^5. The NT control cell line had an average titer of 2.2x10^5 PFU/mL 8 hpi, 3.6x10^5, and 1.18x10^6 16 and 24 hpi, respectively.

UFSP2 KO affected the replication of Udorn only at 8 and 24 hpi with the effect of a decrease in viral titer. The UFSP2 KO decreased virus production by 7 fold at 8 hpi compared to the NT control (Figure 3-11) and 9.2 fold at 24 hpi. The average virus titer for 8hpi was 1.2x10^3 PFU/mL, and the average for 24 hpi was 9.96x10^5 PFU/mL. The NT control cell line had an average titer of 8.44x10^3 PFU/mL 8 hpi, and 8.96x10^6 24 hpi. These results suggest that the hyper-UFMylated state of the cell can be harmful to

both H3N2 and H1N1 strains of influenza A virus in the early and late stages of infection with a more pronounced effect on H3N2 IAV.

To elucidate the stage of the viral replication cycle that is affected by UFM1 in PR8 viral infection, I used immunoblotting to evaluate the accumulation of IAV HA and NP and M1 proteins as a measure of protein synthesis, in the UFM1 KO and UFSP2 KO cell lines infected with PR8 IAV. In this study, only a limited number of viral proteins can be observed due to available antibodies in the McCormick lab. The UFM1KO and UFSP2 KO cells and NT control cells were infected with stPR8 with a MOI of 2. At 8, 16, and 24 hpi, cell lysates were collected and prepared as previously described for immunoblotting with goat polyclonal Anti-Influenza A Virus antibody. The blots were imaged on ChemiDoc, Actin was used as loading control (Figure 3-12 (A)). The amount of HA, NP, and M1 protein were comparable to the one observed in infected NT cells.

An experiment with the same design was conducted with the IAV H3N2 Udorn strain. To elucidate the stage of the viral replication cycle that is affected by UFM1in Udorn viral infection, I used immunoblotting to evaluate the accumulation of IAV NP and M1 proteins as a measure of protein synthesis, in the UFM1 KO and UFSP2 KO cell lines infected with Udorn IAV (Figure 3-12(B)). HA protein cannot be observed in this case because these antibodies can detect only H1N1 HA. The amounts of NP and M1 proteins were also comparable to those observed in infected NT cells, the same as for the PR8 virus.

From the obtained results, I concluded that deficiency of UFSP2 and UFM1 do not affect viral protein synthesis for both H1N1 (PR8) and H3N2 (Udorn) IAV. This fact means that when IAV dysregulates UFMylation or inhibits its machinery by the host shutoff mechanism it is not harmful for the virus M1 and NP proteins accumulation and that UFMyltion does not support viral protein synthesis.

3.5 Assay development for detection of Strep-tagged UFMylated proteins during infection

One of the goals of this study was to develop an assay that makes it possible to precisely detect changes in the cell UFMylome while applying infection or other treatments. To develop this assay, I designed and constructed a plasmid (Figure 2-1) that has preactivated UFM1 with 2 deleted amino acids Ser-Cys with active Gly exposed to ensure that exogenous tagged UFM1 will be pre-activated and can compete for

conjugation with endogenous one. UFM1 was Strep-tagged and I cloned it in PLVX backbone under a strong EF1α promoter via restriction-ligation process. The chosen vector is also suitable not only for transient transfection but also for lentivirus production which makes it possible to further use it in lab in different settings. Firstly, I transfected the construct into HEK293T cells with PEI to observe if Strep-tagged UFM1 can be properly expressed and conjugated to RPL26 - the primary substrate of UFMylation. I confirmed that the constructed vector guarantees strong expression and conjugation of exogenous tagged UFM1 to RPL26 in HEK293T cells (Figure 3-13(A, B, C)). My second step was to transfect the construct to A549 NT and UFSP2KO cells as they are less efficient to be transfected but are more relevant for IAV infection studying as IAV infect respiratory epithelial cells and A549 cells are adenocarcinomic human alveolar basal epithelial cells. The transfection efficiency of A549 cells is approximately from 50 to 60% of cells compared to 80-90% for HEK293T cells. This fact affected the results but still Strep-tagged UFM1 was expressed and conjugated to RPL26 (Figure 3-13(A, D)). Next, I optimized Strep-tagged protein purification because the first obtained results showed that tagged-UFM1 was not binding to the columns. Not specific binding can be connected with the appearance of extra biotin in the cell culture media and the cell lysates. Biotin can attach to streptavidin which is used exactly to bind and purify Strep-tagged proteins and block its binding to the targets (Weber et al., 1989). Because of this, I used Biolock – solution containing avidin that block biotin and biotinylated proteins but not Strep-tags, to block biotin in the lysates before its incubation with resin and applied a longer incubation time. At the same time, it was demonstrated that the amount of protein was not enough to be seen on silver stain screening. To optimize cell amounts I decided to seed 22.5 million cells which was 5 times more cells for transfection and subsequent lysis. The amount of protein was increased and the binding was more efficient. The experiments including anti-Strep and anti-UFM1 immunoblotting are required to confirm the efficiency of the developed method further. The next steps also include Mass Spectrometry to evaluate the quality of obtained samples (if they have any contaminants) and the suitability of the method to determine changes in UFMylome during infections.

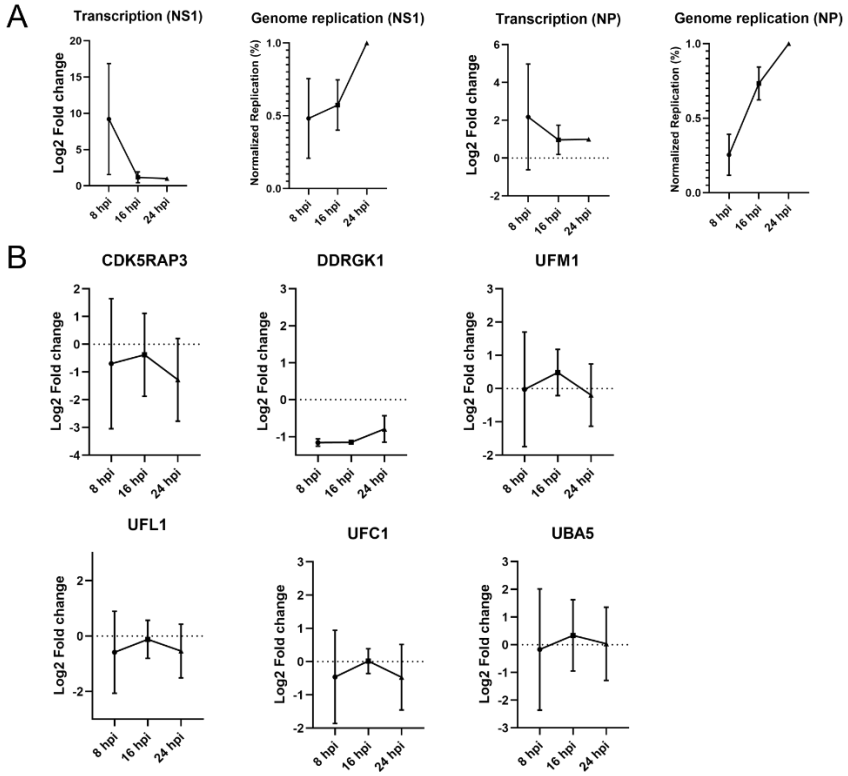

Figure 3-1 UFMylation machinery components genes mRNA levels are not reduced during IAV H1N1 PR8 infection. A) A549 cells were mock infected or infected with PR8 at MOI of 1, and cell lysates were harvested at 8, 16, and 24 hpi. Total mRNA was extracted and steady-state levels of mRNAs encoding UFMylation machinery was analyzed by RT-qPCR. Viral targets were analyzed to evaluate viral genome replication and transcription. The levels of viral genome replication and viral transcripts were normalized to 18S rRNA levels and set relative to transcript levels at 24 hpi. The results were analyzed using the ΔΔCt method **(Livak & Schmittgen, 2001)**. Data was transformed by log transformation. N=3. Data was plotted as mean ± SEM. B) A549 cells were mock infected or infected with PR8 at MOI of 1, and cell lysates were harvested at 8, 16, and 24 hpi. Total mRNA was extracted and steady-state levels of mRNAs encoding UFMylation machinery was analyzed by RT-qPCR. The results were analyzed using the ΔΔCt method **(Livak & Schmittgen, 2001)**. Data was transformed by log transformation to normalize the distribution of data. N=3. Data was plotted as mean ± SEM.

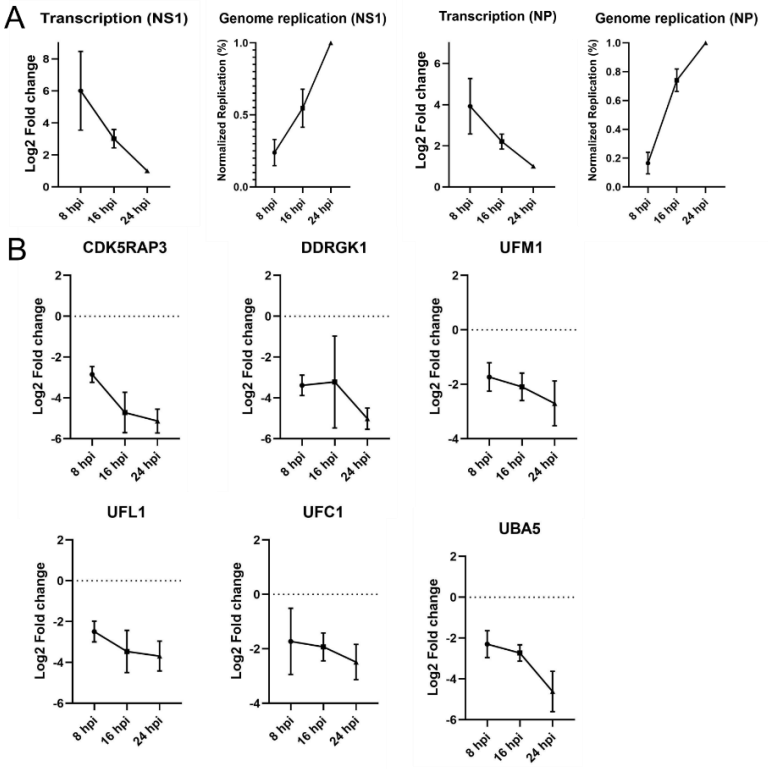

Figure 3-2 IAV H3N2 Udorn infection broadly inhibits accumulation of mRNAs encoding UFMylation machinery. A) A549 cells were mock infected or infected with Udorn at MOI of 1, and cell lysates were harvested at 8, 16, and 24 hpi. Total mRNA was extracted and steady-state levels of mRNAs encoding UFMylation machinery was analyzed by RT-qPCR. Viral targets were analyzed to evaluate viral genome replication and transcription. The levels of viral genome replication and viral transcripts were normalized to 18S rRNA levels and set relative to transcript levels at 24 hpi. The results were analyzed using the ΔΔCt method (Livak & Schmittgen, 2001). Data was transformed by log transformation. N=3. Data was plotted as mean ± SEM. **B)** A549 cells were mock infected or infected with Udorn at MOI of 1, and cell lysates were harvested at 8, 16, and 24 hpi. Total mRNA was extracted and steady-state levels of mRNAs encoding UFMylation machinery was analyzed by RT-qPCR. The results were analyzed using the ΔΔCt method (Livak & Schmittgen, 2001). Data was transformed by log transformation to normalize distribution of data. N=3. Data was plotted as mean ± SEM.

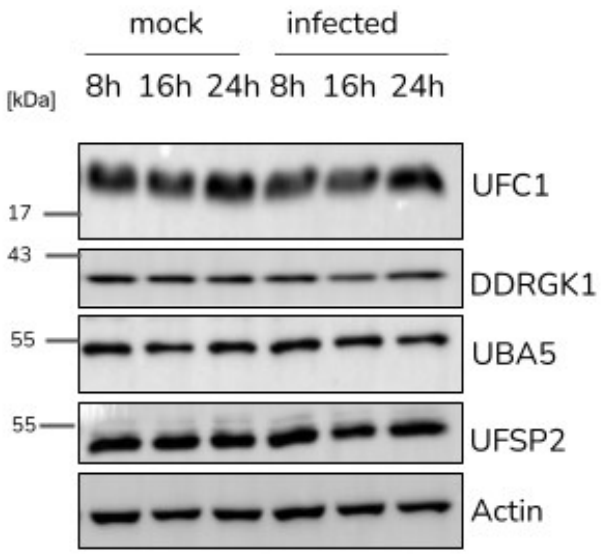

Figure 3-3 IAV PR8 infection slightly decreased DDRGK1 protein levels.A549 cells were infected with IAV H1N1 PR8 at MOI of 2. Cell lysates were harvested at time points 8, 16, and 24h. Proteins amounts were analyzed by Western blotting for antibodies indicated to compare mock infected and PR8 infected samples. Images were captured with BioRad Chemidoc and formatted in Image Lab 6.0.1 software. N=3.

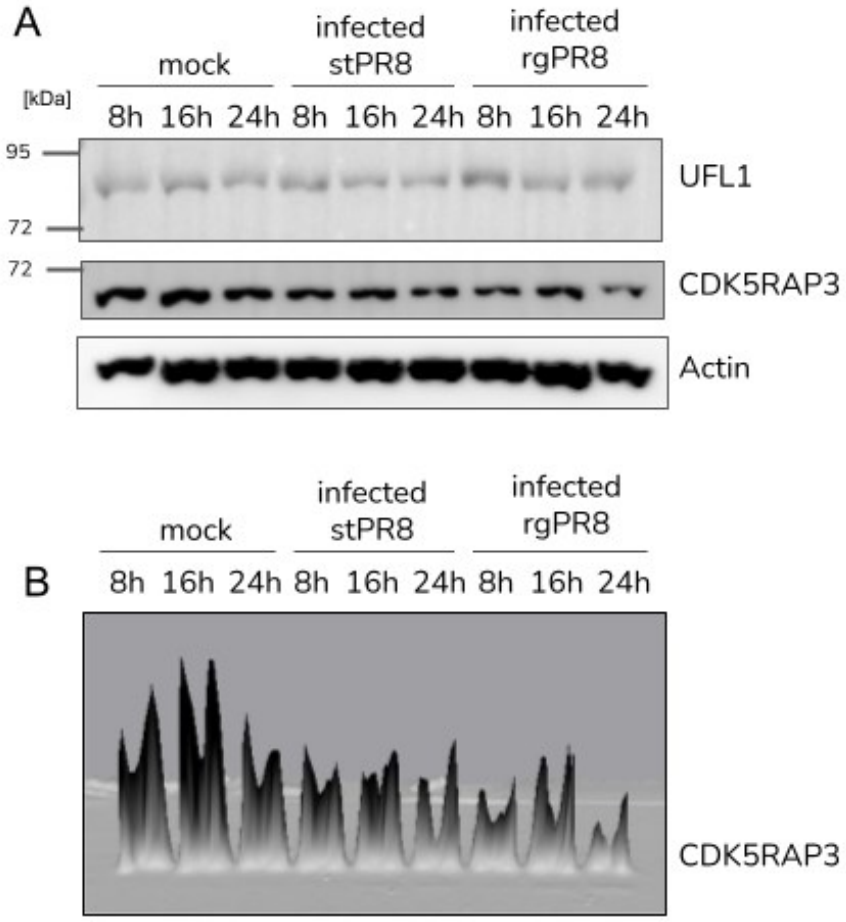

Figure 3-4. IAV PR8 infection reduces CDK5RAP3 protein levels. A) A549 cells were infected with IAV H1N1 stPR8 (lab stock PR8) or rgPR8 (PR8 obtained recently with reverse genetics approach) at MOI of 2. Cell lysates were harvested at time points 8, 16, and 24h. Proteins amounts were analyzed by Western blotting for antibodies indicated to compare mock infected and PR8 infected samples. Images were captured with BioRad Chemidoc and formatted in Image Lab 6.0.1 software. N=3. B) Densitometry figure that corresponds to Western Blot figure (A) with antibodies for CDK5RAP3.

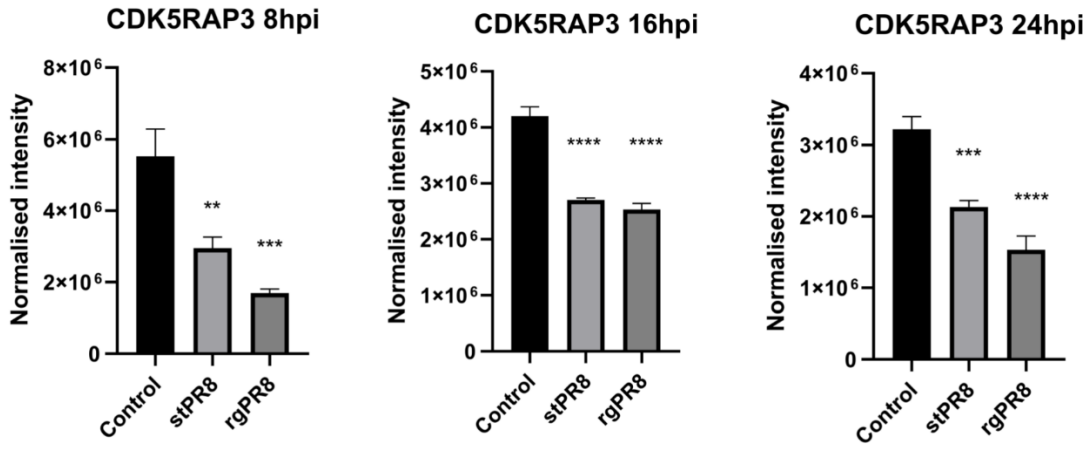

Figure 3-5 CDK5RAP3 Normalized intensity values are decreased during PR8 infection Images of immunoblotted CDK5RAP3 during rgPR8 and stPR8 infection from 3 biological replicates were analyzed by densitometry assay with normalization to Actin. Normalized values were plotted in GraphPad Prism 8.0 and analyzed with one-way ANOVA and Dunnett test. All changes are statistically significant.

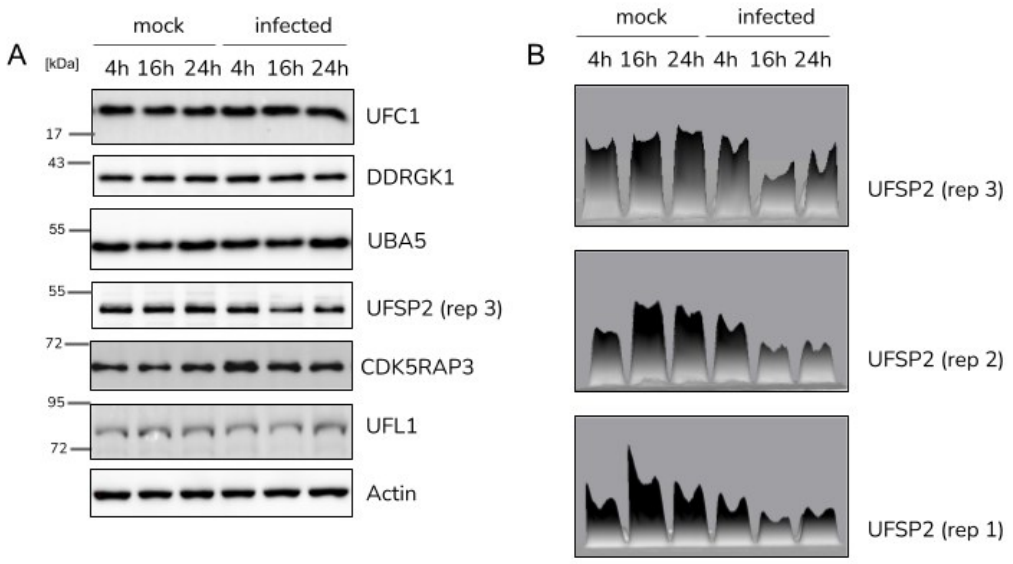

Figure 3-6 IAV Udorn infection reduces UFSP2 protein levels. (A) (B) A549 cells were infected with IAV H3N2 Udorn at MOI of 2. Cell lysates were harvested at time points 4, 16, and 24h. Proteins amounts were analyzed by Western blotting with antibodies indicated to compare mock infected and Udorn infected samples. Images were captured with BioRad Chemidoc and formatted in Image Lab 6.0.1 software. N=3. (B) Densitometry figure that corresponds to Western Blot figure (A) with antibodies for UFSP2 rep3 but also rep2 and rep1 are demonstrated.

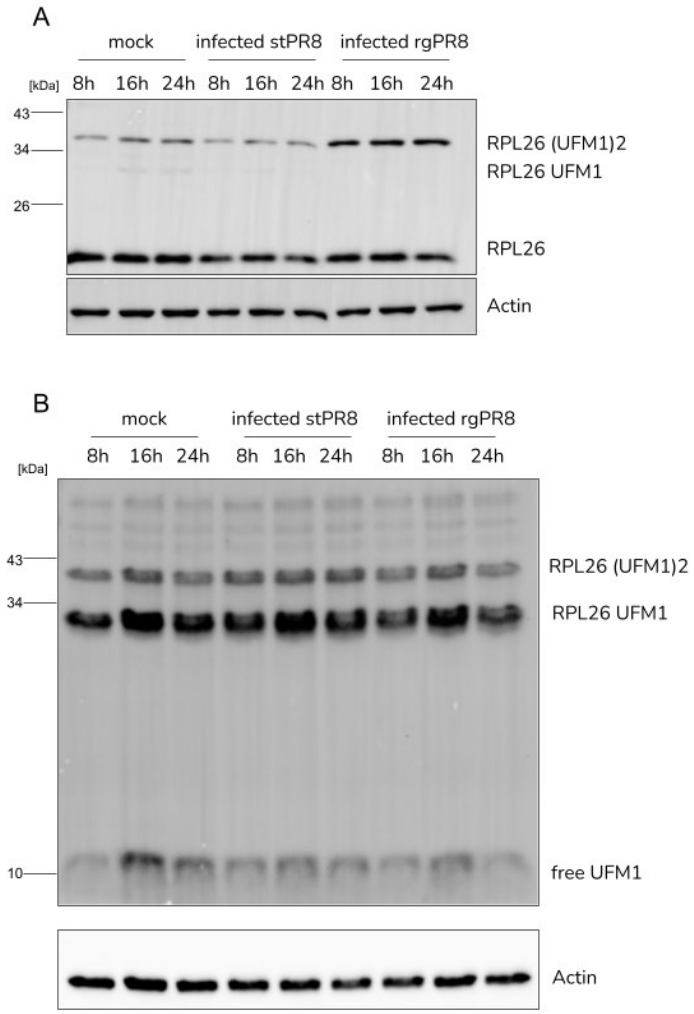

Figure 3-7 IAV PR8 infection decreases the amount of free UFM1 and rgPR8 infection increases the amount of di-UFMylated RPL26. (A) A549 cells were infected with IAV H1N1 stPR8 and rgPR8 at MOI of 2. Cell lysates were harvested at time points 8, 16 and 24h. Protein amounts were analyzed by Western blotting with anti-RPL26 antibodies to compare mock infected and infected samples. Images were captured with BioRad Chemidoc and formatted in Image Lab 6.0.1 software. N=3. (B) A549 cells were infected with IAV H1N1 stPR8 and rgPR8 at MOI of 2. Cell lysates were harvested at time points 8, 16 and 24h. Protein amounts were analyzed by Western blotting with anti-UFM1 antibodies to compare mock infected and infected samples. Images were captured with BioRad Chemidoc and formatted in Image Lab 6.0.1 software. N=3.

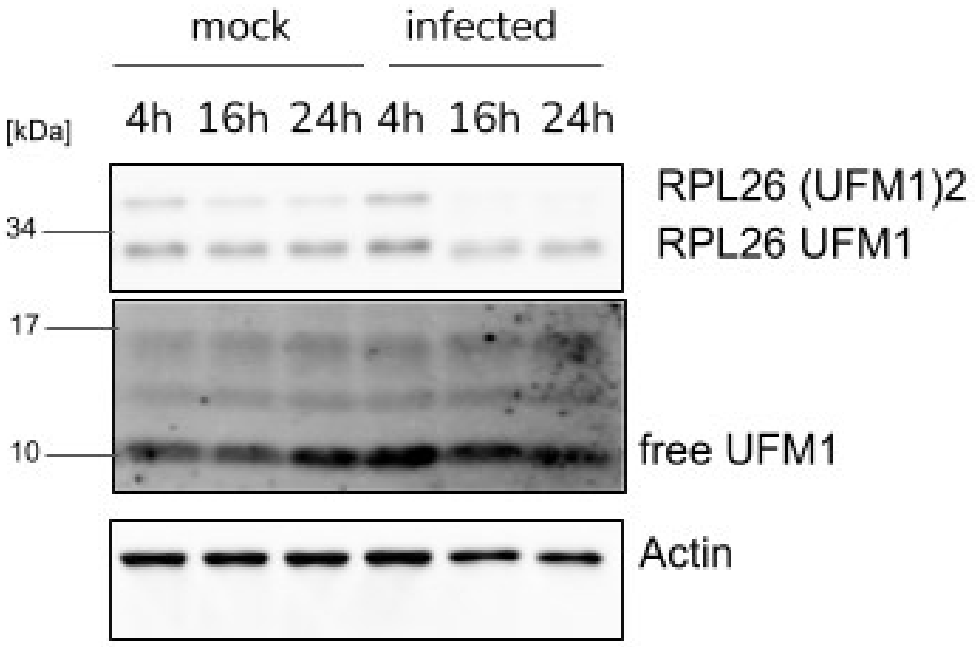

Figure 3-8 IAV Udorn infection decreases levels of di-UFMylated RPL26. A549 cells were infected with IAV H3N2 Udorn at MOI of 2. Cell lysates were harvested at time points 4, 16, and 24h. Protein amounts were analyzed by Western blotting with anti-UFM1 antibodies to compare mock infected and infected samples. Images were captured with BioRad Chemidoc and formatted in Image Lab 6.0.1 software. N=3.

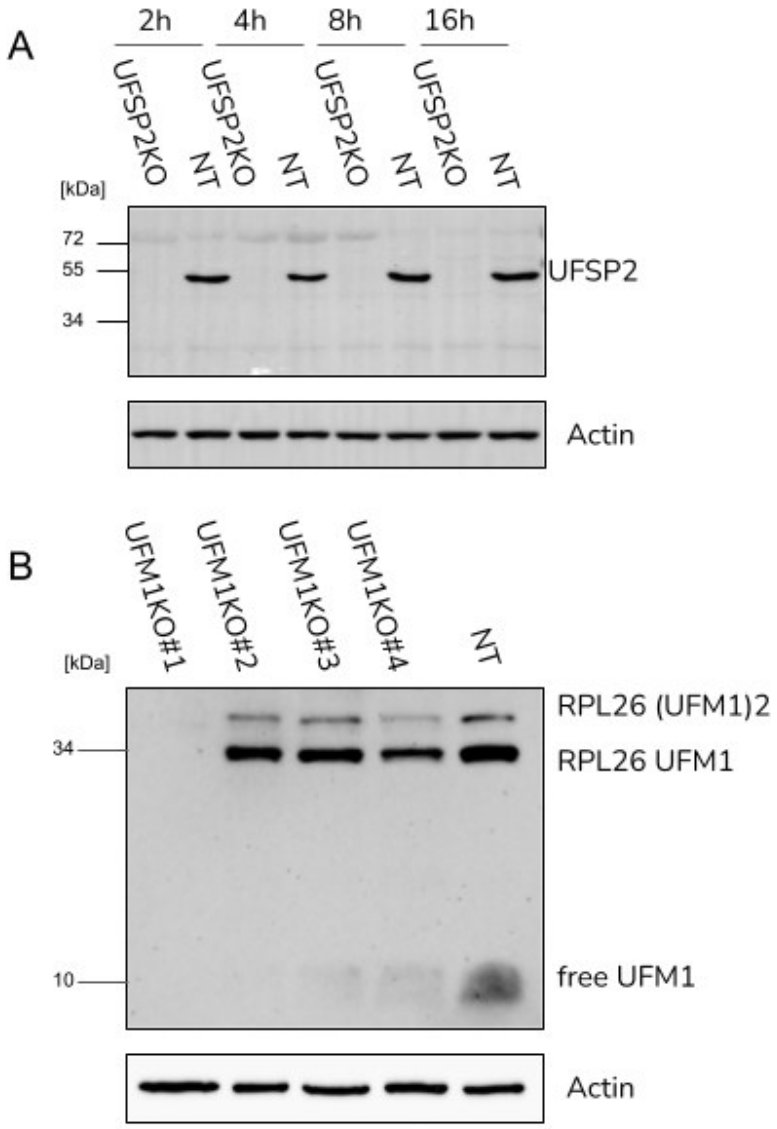

Figure 3-9 Confirmation of UFSP2 and UFM1 KOs in A549 cells.A) A549 UFSP2KO#2 monoclonal and non-targeting (NT) cell lysates were collected from different time points after seeding at 3 passages after thawing and were analyzed by Western blotting for UFSP2. B) 4 monoclonal UFM1KO A549 cell lines were analyzed by immunoblotting with anti-UFM1 antibodies 24h after splitting, and 3 passages after thawing and compared to NT A549 cells. UFM1KO#1 monoclonal was chosen for further experiments

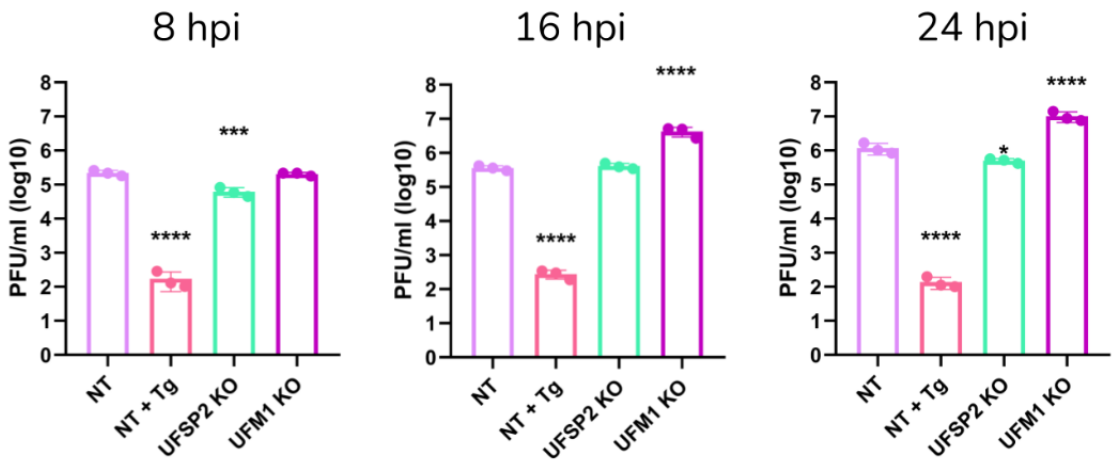

Figure 3-10 IAV PR8 replicates more efficiently in UFM1-deficient cells and less efficiently in UFSP2-deficient cells. A549 cells - UFSP2KO#2 cell line, UFM1KO#1 cell line vs. NT control cell line were infected with IAV H1N1 PR8 strain at a MOI of 0.5. Supernatants were harvested at time points 8, 16, and 24 hpi and infectious viral progeny were enumerated using a plaque assay conducted on MDCK cells. A549 NT cells were treated with thapsigargin at a concentration of 100 nM at 1hpi and were used as a control for viral replication inhibition. Error bars denote the standard deviation of 3 biological replicates (N=3).

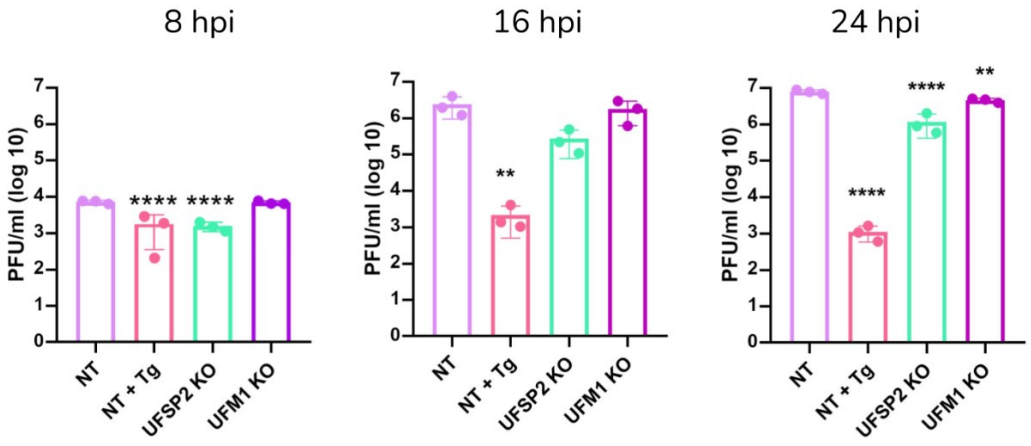

Figure 3-11 UFSP2 deletion inhibits IAV H3N2 Udorn replication. A549 cells - UFSP2KO#2 cell line, UFM1KO#1 cell line vs. NT control cell line were infected with IAV H3N2 Udorn strain at a MOI of 0.5. Supernatants were harvested at time points 8, 16, and 24 hpi and infectious viral progeny were enumerated using a plaque assay conducted on MDCK cells. A549 NT cells were treated with thapsigargin at a concentration of 100 nM at 1hpi and were used as a control for viral replication inhibition. Error bars denote the standard deviation of 3 biological replicates (N=3).

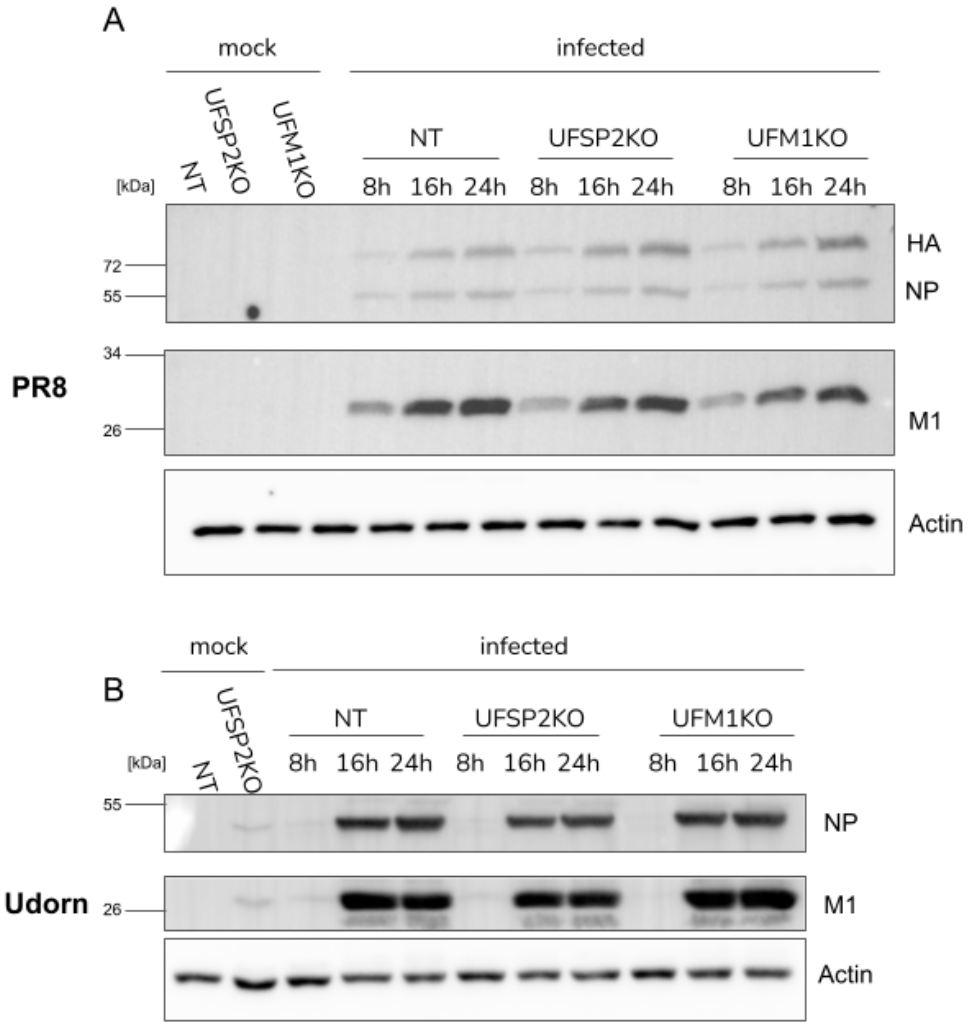

Figure 3-12 The UFMylation pathway does not affect IAV M1 or NP proteins during IAV infection. A) A549 cells - UFSP2KO#2 cell line, UFM1KO#1 cell line vs. NT control cell line were infected with the IAV H1N1 PR8 strain at MOI of 2. Cell lysates were collected at 8, 16, and 24 hpi and analyzed by Immunoblotting with poly-IAV antibodies. Images were captured with BioRad Chemidoc and formatted in Image Lab 6.0.1 software. N=3. B) A549 cells - UFSP2KO#2 cell line, UFM1KO#1 cell line vs. NT control cell line were infected with the IAV H3N2 Udorn strain at MOI of 2. Cell lysates were collected at 8, 16, and 24 hpi and analyzed by Immunoblotting with poly-IAV antibodies. Images were captured with BioRad Chemidoc and formatted in Image Lab 6.0.1 software. N=3.

Figure 3-13 The 2XStrep-UFM1delSC protein accumulates in transfected cells and can be conjugated to primary UFMylation substrate in the cells. A) Expected results for immunoblotting with anti-UFM1 and anti-Strep antibodies of lysates of cells transfected with PLVX-2XStrep-UFM1 vs. PLVX empty vector control. Figure was made in Biorender. B) HEK293T cells were transfected with PLVX-2XStrep-UFM1delsc construct as 3 different clones obtained after *E.coli* transformation or with empty PLVX backbone as empty vector (EV) control. Cell lysates were collected and analyzed by Immunoblotting with anti-Strep antibodies. C) HEK293T cells were transfected with PLVX-2XStrep-UFM1delsc construct as 3 different clones obtained after *E.coli* transformation or with empty PLVX backbone as empty vector (EV) control. Cell lysates were collected and analyzed by Immunoblotting with anti-UFM1 antibodies. D) NT and UFSP2KO A549 cells were transfected with PLVX-2XStrep-UFM1delsc construct (clone 1) or with empty PLVX backbone as empty vector (EV) control. Cell lysates were collected and analyzed by immunoblotting with anti-Strep antibodies.

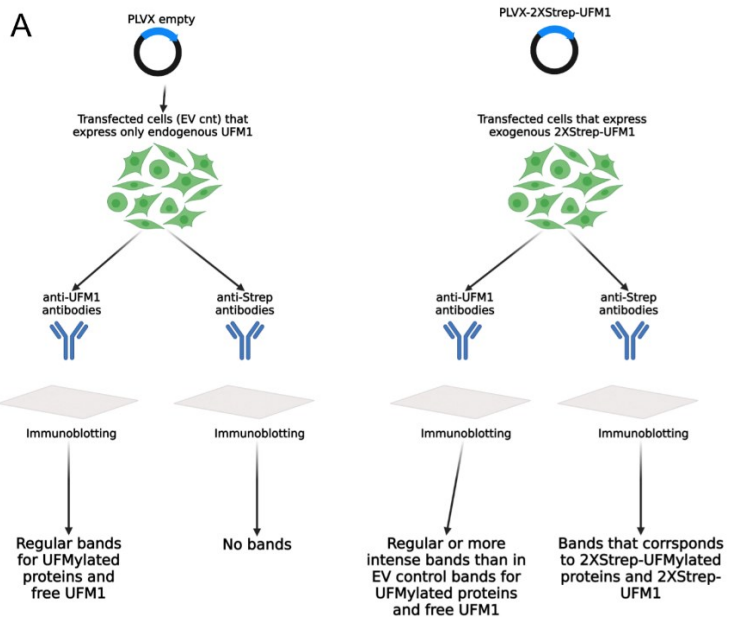
A
PLVX empty
Transfected cells (EV cnt) that express only endogenous UFM1
anti-UFM1 antibodies
anti-Strep antibodies
Immunoblotting
Immunoblotting
Regular bands for UFMylated proteins and free UFM1
No bands
PLVX-2XStrep-UFM1
Transfected cells that express exogenous 2XStrep-UFM1
anti-UFM1 antibodies
anti-Strep antibodies
Immunoblotting
Immunoblotting
Regular or more intense bands than in EV control bands for UFMylated proteins and free UFM1
Bands that corrsponds to 2XStrep-UFMylated proteins and 2XStrep-UFM1

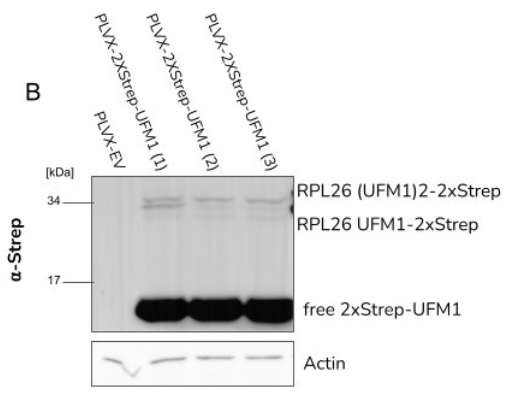
B
PLVX-EV
PLVX-2XStrep-UFM1 (1)
PLVX-2XStrep-UFM1 (2)
PLVX-2XStrep-UFM1 (3)
[kDa]
34
17
α-Strep
RPL26 (UFM1)2-2xStrep
RPL26 UFM1-2xStrep
free 2xStrep-UFM1
Actin

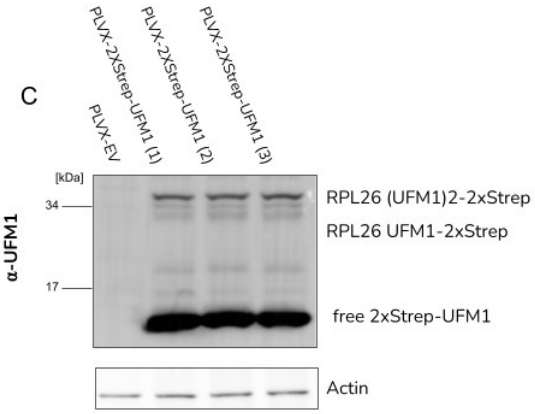
C
PLVX-EV
PLVX-2XStrep-UFM1 (1)
PLVX-2XStrep-UFM1 (2)
PLVX-2XStrep-UFM1 (3)
[kDa]
34
17
α-UFM1
RPL26 (UFM1)2-2xStrep
RPL26 UFM1-2xStrep
free 2xStrep-UFM1
Actin

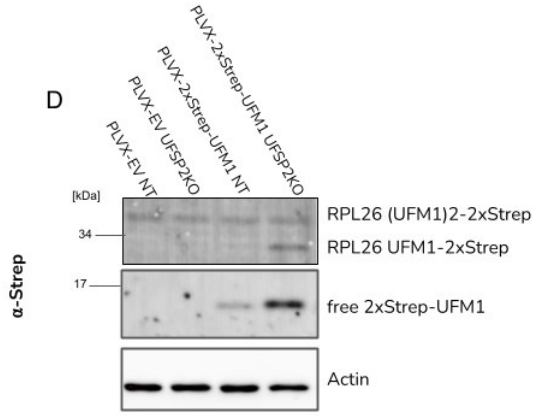
D
PLVX-EV NT
PLVX-EV UFSP2KO
PLVX-2xStrep-UFM1 NT
PLVX-2xStrep-UFM1 UFSP2KO
[kDa]
34
17
α-Strep
RPL26 (UFM1)2-2xStrep
RPL26 UFM1-2xStrep
free 2xStrep-UFM1
Actin

Chapter Four - Discussion

Influenza A viruses are viruses that are dependent on host cell ER - IAV HA, NA, and M2 are synthesized and modified in ER (Manzoor et al., 2017; Hogue & Nayak, 1992). IAV induces ER stress and dysregulate ER homeostasis (Frabutt et al., 2018). At the same time, IAV is affected by ER stress and subsequent UPR as UPR activation inhibits accumulation of IAV glycoproteins (Slaine et al., 2021), but at the same time IRE1 branch of UPR was shown to be required for IAV successful replication (Hassan et al., 2012). These facts together make IAV an exclusively sensitive virus to ER homeostasis – when ER homeostasis is affected – IAV is affected, too. UFMylation is not only important for antiviral immune response but also one of the key regulators of host cell proteostasis and ER homeostasis. Its role in degradation of stalled ribosomes (Walczak et al., 2019), regulation of UPR (Liu et al., 2017), and its interconnection with ER stress (Zhang et al., 2012) and ER-phagy (Liang et al., 2020) provided me a rationale to investigate its relationship with IAV in both ways: my research concentrated on how the UFMylation pathway is regulated by IAV and what changes in host UFMylome are happening during infection, and also how UFMylation can affect virus production and fitness. To investigate this understudied area, I decided to take a comprehensive approach and observe UFMylation machinery during infection on both mRNA and protein levels, evaluate changes in host cell UFMylome during infection, and develop workflow for more precise analysis of UFMylome with a Mass Spectrometry approach. I chose two lab-adapted IAV strains that have a lot of differences in proteins important for host shutoff and different HA that can induce ER stress to different degrees. To investigate how UFMylation affects IAV I used a plaque assay that is regularly applied in virology to evaluate the IAV replication rate (Matrosovich et al., 2006). I also evaluated viral protein synthesis in different UFMylation settings, as protein production is an area where UFMylation plays an important role.

In my thesis work, I found that H3N2 Udorn IAV inhibits all UFMylation machinery gene expression by host shutoff mechanism while UFMylation machinery genes appeared to be mostly resistant to H1N1 PR8 host shutoff with only DDRGK1 showing significant reduction. I also discovered that the CDK5RAP3 protein amount is decreased during H1N1 PR8 infection by an unknown mechanism and this effect is not

connected with downregulation of steady-state mRNA levels. I found that infection with PR8 and Udorn viruses affect cellular UFMylome, but in different ways: both viruses decreased the amount of mono-UFMylated RPL26 but differently affected the amount of di-UFMylated RPL26 and free UFM1.

I evaluated the effects of UFMylation deficiency and hyper-UFMylated state of the cell on virus production of PR8 and Udorn viruses and found that UFMylation is antiviral against H1N1 PR8 while hyper-UFMylated state of the cell has a negative effect on both H1N1 and H3N2 viruses. Interestingly, I demonstrated that these antiviral effects are not connected with viral protein synthesis as it was not affected.

In general, I discovered that IAV interferes with the UFMylation pathway by inducing host shutoff and that UFMylation is antiviral against IAV H1N1 PR8 and that UFSP2 deficiency is antiviral against IAV H3N2 Udorn.

4.1 UFMylation interplay with ER stress and UPR during IAV infection

IAV is strongly linked to ER where HA and NA proteins are synthesized and glycosylated and M2 protein is synthesized (Hogue & Nayak, 1992; Manzoor et al., 2017). When IAV usurp host cell machinery including ER to produce new viral progeny and synthesize its own proteins it overloads host cell machinery and exceed ER limits of proteins folding. This cause accumulation of unfolded proteins in ER and induce ER stress with subsequent UPR activation (Frabutt et al., 2018). Interestingly, different glycosylation patterns of the proteins, HA and NA, can affect UPR activation. It was shown with H5N1 strain that removal of glycans from the HA head led to more inflammation and increased activation of UPR and ER stress (Yin et al., 2020). For H1N1 strain, adding glycosylation sites led to poor activation of ER stress and UPR (Sun et al., 2013). Viruses used in this study have H1 and H3 HA that bear different amount of glycosylation sites which means that they can act differently in ER and induce ER stress to different degrees. However, it was shown that UPR, or at least one of its branches, plays a significant role in IAV replication. IAV was shown to activate the IRE1 branch of UPR during infection, independently of other UPR arms (Schmoldt et al., 2019; Hassan et al., 2012). Another study showed that IAV infection attenuated PERK but had no effect on ATF6 and IRE1 (Landeras-Bueno et al., 2016). This suggested that selective PERK branch activation is harmful for IAV. At the same time, ER stress and the UPR

have clear mechanistic links to the UFMylation pathway that also takes place in ER. Activation of ER stress and UPR with production of transcription factor XBP1s leads to upregulation of UFMylation machinery genes (Zhang et al., 2012), probably because UFMylation can restore ER proteostasis by inducing degradation of stalled ribosomes. At the same time, inhibition of the UFMylation pathway leads to ER stress and the activation of UPR, particularly through the PERK pathway (Figure 4-1). While the PERK pathway generally promotes cell apoptosis and inflammation and has been shown to inhibit influenza virus replication in some studies (Landeras-Bueno et al., Chemical genomics identifies the PERK-mediated unfolded protein stress response as a cellular target for influenza virus inhibition., 2016) I found that a deficiency in UFM1, a key component of the UFMylation pathway, enhances the replication of the PR8 strain of IAV. However, in the case of Udorn H3N2 virus, UFMylation deficiency did not demonstrate such proviral effect which can be linked with different types of HA and NA thus a different profile of ER stress and UPR.

In my work, while studying how H1N1 IAV can influence UFMylation machinery on mRNA and protein level, I found that the only gene from UFMylation machinery components that was not resistant to PR8 host shutoff was DDRGK1. This was intriguing, because DDRGK1 is one of the direct links between UFMylation and UPR (Liu et al., 2017). The studies have shown that depletion of DDRGK1 induces ER stress and increases apoptosis in cancer cells and hematopoietic stem cells (HSCs) through a different mechanism (Cao et al., 2021). Specifically, DDRGK1 depletion hampers the IRE1α-XBP1 signaling pathway and activates the PERK-eIF2α-CHOP pathway, which leads to apoptosis. DDRGK1 appears to stabilize the IRE1α protein by interacting with its kinase domain, a process that depends on UFMylation (Liu et al., 2017). I speculate that inhibition of DDRGK1 expression during H1N1 PR8 infection could be connected to the beneficial role of apoptosis for release of new viral progeny (Figure 4-2).

CDK5RAP3 is simultaneously a key player in the UFMylation process and an ER-phagy receptor. Research indicates that the absence of CDK5RAP3 in hepatocytes leads to increased markers of ER stress, including elevated levels of phospho-PERK, phospho-eIF2α, and cleaved *Xbp-1* (Yang et al., 2020). This association suggests that ER

stress, potentially induced by the lack of CDK5RAP3, could be a factor in premature cell death. Similarly, studies on U2OS cells have shown that removing CDK5RAP3 activates the UPR and causes ER enlargement, further evidencing the critical connection between CDK5RAP3 and ER stress (Klebanovych et al., 2022). I discovered that IAV H1N1 PR8 infection consistently reduced amount of CDK5RAP3 on protein levels. The previous findings underlining that reduction in amounts of CDK5RAP3 in inducing UPR that leads to ER enlargement make me speculate that reduction of CDK5RAP3 by virus can be beneficial for further synthesis and modification of viral proteins and successful release of new viral progeny.

4.2 UFMylation and ER-phagy during IAV infection

Recent research underscores a profound link between the UFMylation pathway, ER-phagy, and the UPR during ER stress conditions (Liang et al., 2020). This study highlights how suppressing ER-phagy by diminishing DDRGK1 UFMylation triggers ER stress and consequently activates the UPR, revealing an interaction where the failure to carry out ER-phagy results in ER stress. This positions ER-phagy as an essential strategy for mitigating ER stress in specific scenarios. The DDRGK1's role in facilitating the UFL1 ligase's attachment to the ER surface is important for ensuring UFMylation-dependent ER-phagy of ER-sheets. Disruption in this mechanism leads to ER stress, indicating the key role of UFMylation in the regulation of ER-phagy and, also in the UPR. Furthermore, the identification of RPN1, a key element of the ER-localized oligosaccharyltransferase (OST) complex, as a novel target for DDRGK1-dependent UFMylation, showed RPN1's critical involvement in ER quality control. It was proposed that UFMylation of ER surface proteins, such as RPN1, serves as a signal for ER-phagy of ER sheets, similar to the role ubiquitylation plays in signaling autophagy for other organelles.

Influenza A viruses (IAV) rely on macroautophagy as a key mechanism to support their replication, specifically by preventing the fusion of autophagosomes with lysosomes (Beale et al., 2014). This strategy is crucial for IAV, as the accumulation of autophagosomes is beneficial for the virus. Despite the extensive use of the endoplasmic reticulum (ER) by IAV during its replication cycle, the significance of ER-phagy for IAV remains unclear. As it was said before, in my thesis work, I discovered that both H1N1

PR8 and H3N2 Udorn inhibit DDRGK1 expression via host shutoff mechanism, and particularly PR8 inhibit only DDRGK1 expression among all UFMylation pathway components. I also noted a minor reduction in DDRGK1 protein levels in the presence of the PR8 strain. It is still unclear if ER-phagy is detrimental for IAV or not but, I can speculate that ER-phagy is not beneficial in terms of continuous synthesis of viral proteins in ER that should not be interrupted by ER-phagy. At the same time, activation of ER stress that happens when DDRGK1-mediated ER-phagy cannot be released can be both harmful and beneficial for IAV.

CDK5RAP3 is an ER-phagy receptor that targets stalled ribosomes, which is facilitated by its interaction with UFL1. Under ER stress conditions, mammalian isoform of ATG8 competitively binds CDK5RAP3 instead of UFM1 to AIM-like sequences in CDK5RAP3's intrinsically disordered region (IDR) (Stephani et al., 2020). ER stress weakens UFM1 interaction with CDK5RAP3 and makes possible for ATG8 to bind. This competition likely plays a regulatory role in the interaction of CDK5RAP3 with ATG8, with implications for the control of ER-phagy under specific conditions. The study emphasizes the switch between CDK5RAP3 as a player of UFMylation pathway and ER-phagy receptor (Figure 4-3). In my work, I found strong decrease in amount of CDK5RAP3 during H1N1 PR8 infection on late stages of infection. Such a decrease can tell us that during PR8 infection ER stress condition is reached which leads to ER-phagy of ER sheets that are decorated with CDK5RAP3, thereby decreasing CDK5RAP3 levels. I speculate that the relatively strong Udorn host shutoff could diminish ER stress relative to PR8 infection leading to lower levels of ER-phagy and leaving CDK5RAP3 protein levels unchanged. Although my results suggest that ER-phagy, influenced by UFMylation, could affect viral replication, they do not conclusively determine whether this mechanism supports or inhibits IAV replication.

4.3 Different IAV strains can induce different changes in host cell UFMylome

The critical role of UFMylation in the degradation of stalled ribosomes, specifically through the UFMylation of RPL26 and regulation of the RQC complex, is a significant aspect of cellular biology, particularly in the context of viral infections. For instance, UFMylation of RPL26, leading to the degradation of stalled ribosomes at ER translocon, has been shown to enhance the replication of HAV (Kulsuptrakul et al.,

2021). This process is relevant as stalled ribosomes often result from the intensive synthesis of viral glycoproteins, which could pose a challenge for IAV. In my research, I encountered contradictory results when studying the PR8 strain of IAV. Anti-RPL26 immunoblotting revealed a decrease in di-UFMylated RPL26 in the case of stPR8, but a notable increase for rgPR8. However, the levels of mono-UFMylated RPL26 were reduced in both instances. The difference between mono- and di-UFMylated species of RPL26 is still unclear and was not covered in literature. However, PR8 infection also induced reduction of RPL26 protein which makes it unclear if the decrease in UFMylated species is connected to reduced UFMylation of RPL26, or reduced amount of RPL26 available for modification. Additionally, anti-UFM1 immunoblotting indicated a minor decrease in mono-UFMylated RPL26 for rgPR8. These findings do not provide a definitive answer regarding the necessity of RPL26 UFMylation for the infection process of the IAV PR8 strain. Anti-UFM1 immunoblotting also provided evidence that the amount of free UFM1 is decreased during viral infection. I speculate that free UFM1 was decreased during H1N1 infection because viral proteins can increase the load on ribosomes and increase number of stalled ribosomes at the ER translocon that leads to more RPL26 to be UFMylated and degraded. This reflects in increased amount of di-UFMylated RPL26 and decrease in general amount of RPL26 that I showed.

H3N2 Udorn infection decreased only di-UFMylated species of RPL26. At the same time the amount of free UFM1 was increased in infected A549 cells. These results are different from those obtained with H1N1 PR8 infection. The differences between results obtained with PR8 and Udorn may be linked to the ability of the viruses to induce host shutoff. PR8 PA-X is less effective at suppressing cellular gene expression than other IAV PA-X proteins. I speculate that relatively strong Udorn host shutoff prevents ER stress and ribosomes stalling resulting in less UFMylated RPL26 and more free UFM1 released (Figure 4-4).

4.4 UFMylation machinery genes can be resistant to host shutoff caused by IAV infection

Host shutoff grants invading viruses considerable advantages by repurposing the host cell's translational machinery and resources, like ribosomes and amino acids, for their own protein synthesis. This process reallocates a significant portion of the cell’s energy, especially ATP—which is normally used about 30% to 40% for mRNA

translation—toward viral replication. Additionally, host shutoff weakens the host's antiviral immune responses, which often rely on the production of new proteins, thus strategically benefiting the virus. Nevertheless, viruses depend on certain host cell functions for their replication and have evolved mechanisms to bypass the limitations host shutoff imposes. This includes ensuring the selective synthesis of specific cellular proteins to mitigate the impact of shutoff (Bercovich-Kinori et al., 2016).

Given UFMylation's critical involvement in various cellular processes such as ER homeostasis, protein quality control, DNA damage response, and ER-phagy (Millrine et al., 2023), it's plausible that UFMylation pathway genes are resistant to host shutoff that was shown with RT-qPCR data of UFMylation machinery genes during H1N1 PR8 infection, similar to how genes responsible for oxidative phosphorylation are affected during PR8 virus infection (Bercovich-Kinori et al., 2016). While the protein levels are mostly maintained during IAV infection as it was shown in this thesis, despite the downregulation of steady-state mRNAs levels during Udorn infection, I can speculate that may be presence of protein is connected with its long turnover in the cell. Furthermore, ribosomes are selectively produced during host shutoff caused by viruses like IAV, suggesting a protective mechanism for ribosome function to ensure viral protein synthesis continues. However, UFMylation machinery genes expression was strongly inhibited during Udorn infection. Additionally, experiments with infected UFM1KO and UFSP2KO A549 cells showed that UFMylation deficiency has no effect on efficient viral protein synthesis which means that both viruses can inhibit UFMylation genes expression without affecting viral protein synthesis.

4.5 Limitations of the study

Current study has some limitation factors that should be removed in further experiments. The observed differences in UFMylated RPL26 levels between rgPR8 and stPR8 might be attributed to mutations that stPR8, having been propagated in the laboratory for some time, could have undergone, potentially altering its behavior. This suggests that the interaction between UFMylation and IAV replication, particularly for the PR8 strain, is complex and may vary depending on viral genetic variations.

Another important limitation that I faced were differences observed in bands with molecular weights that corresponds to mono- and di-UFMylated RPL26 species if

compare anti-UFM1 immunoblots with anti-RPL26 one. Anti-RPL26 immunoblotting is used to detect RPL26, mono- and di-UFMylated species. Anti-UFM1 immunoblotting should also detect mono- and di-UFMylated species. However, during immunoblotting it was found that bands that corresponds to mono- and di-UFMylated RPL26 can differ in their intensity that corresponds to protein amount if compare data obtained with anti-UFM1 and anti-RPL26 antibodies. This can be connected with other UFMylated proteins of the same molecular weight that cannot be differed without specific antibodies of Mass Spectrometry approach.

I also faced limitation in application of anti-IAV proteins antibodies due to availability in lab but also its quality (HA and NA antibodies available demonstrated weak signal) and that fact that PA-X cannot be detected with immunoblotting that was confirmed in both McCormick and Khaperskyy labs. At the same time, goat poly-IAV antibodies that I used in this study cannot detect H3N2 HA. Immunoblotting data that was not shown in this thesis work obtained as preliminary data also showed the inability of immunoblotting method to determine if modified viral protein is UFMylated or has another Ubl modifications. Low sensitivity of immunoblotting method was also a limitation because even UFMylated viral proteins that are present in the cell in low concentration cannot be detected due to low sensitivity of the method. Mass Spectrometry could be a very helpful method that can be used to expand the current study.

The most pronounced limitation was poor binding of Strep-tagged UFM1 and UFMylated proteins to the anti-Strep resin that was used for affinity purification and number of cells required to be seeded and transfected to obtain purified Strep-tagged protein. The protein purification conducted following the manufacturer`s protocol resulted in no Strep-tagged protein in elution fractions due to low binding to the resin. This resulted in long time spent on optimization of the protocol to obtain better results such as application of Biolock, variations in lysates incubation time on the resin. The low transfection efficiency of A549 cells that are regularly used to study IAV infections (50-60% of efficiency) made it more complicated to obtain required amount of both transfected (due to high amounts of transfection reagent Lipofectamine 3000 required) and infected cells (Cal7 that was chosen to be used for this experiments is slow growing

virus that is hard to obtain with titers higher than 5x10^5 pfu/ml) to continue experiments with purified proteins on the stage of Mass Spectrometry.

The absence of any data explaining the difference between mono- and di-UFMylated RPL26 makes it harder to draw conclusions with results obtained with anti-RPL26 immunoblotting.

4.6 Future perspectives

The current study covered only to IAV strains: H1N1 PR8 and H3N2 Udorn. To gather more information about IAV interplay with UFMylation different IAV viruses should be used such as A/California/07/2009(H1N1), H5N1 strains and other subtypes that have different pathogenicity and different glycosylation patterns of HA and NA proteins that directly interact with ER. To further investigate changes in UFMylome connected with IAV infection, Mass Spectrometry of infected and non-infected samples is required to determine proteins that are UFMylated during infection and their roles in the host cell.

Unanswered question is still the role and functions of mono- and di-UFMylated species of RPL26 during infection. To answer this question, I propose experiment with CRISPR-Cas9 mediated substitution of Lysine 132 and 134 to generate cell lines were RPL26 can be only mono-UFMylated by one of the Lysines, only di-UFMylated or not UFMylated at all with subsequent infections to evaluate virus production in these conditions. This kind of experiments will shed light on at least role of mono- or di-UFMylated RPL26 in IAV infection.

As in my work, I showed that IAV PR8 interfere with CDK5RAP3, I think it is important to study the mechanism by which CDK5RAP3 protein amount is decreased. I propose to infect NT A549 cells with IAV PR8 with subsequent drug treatments to elucidate the mechanism. Hydroxychloroquine (Hcq) and Bafilomycin A1 will be used to inhibit autophagy, MG-132 will be used as proteosome inhibitor. Drugs will be applied after 16 hpi as at this time point the amount of CDK5RAP3 was still the same as in the control. Samples should be collected each 2 hours. To elucidate CDK5RAP3 role as ER-phagy receptor, I propose to treat cells with Thapsigargin in low concentration that should be enough to induce ER-stress but at the same time to not inhibit virus production and evaluate virus production in these conditions. Further experiments with inhibitors of

cellular degradation pathways will be required to confirm further that host shutoff can decrease the amount of DDRGK1. Drug treatment with integrated stress response inhibitor (ISRIB) and Tg is proposed for use in this experiment and applied to the host cells at 16 hpi with subsequent lysates collection each 2 hours not to overstimulate cells and induce cell death but also not to miss an effect of ISRIB which can inhibit Integrated Stress Response in the cell and exactly eIF2α phosphorylation and thus inhibit host shutoff (Rabouw et al., 2019). If the protein and mRNA amount of DDRGK1 can be increased and returned to the same in non-infected cells by ISRIB treatment - the shown decrease can be linked to host shutoff confidently. Generation of CDK5RAP3 and DDRGK1 KO A549 cell lines with subsequent infection with IAV and measuring virus production can also help to understand the importance of these UFMylation components in viral infection.

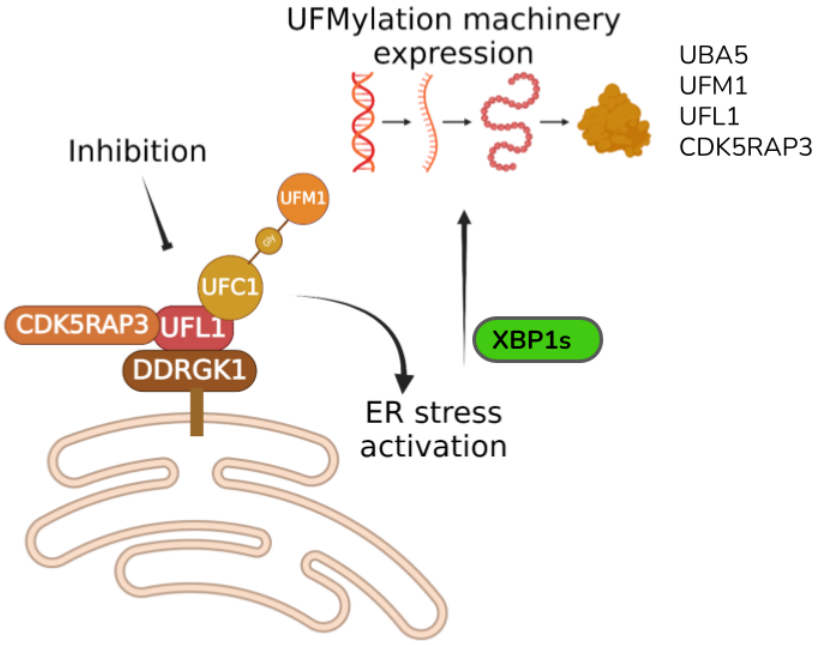

Figure 4-1 The interplay between UFMylation and ER stress. UFMylation pathway inhibition leads to ER stress activation and subsequent UPR activation. IRE1 UPR branch activation resulted in a synthesis of transcriptional factor XBP1s which upregulate expression of UBA5, UFM1, UFL1, and CDK5RAP3. Figure was made with Biorender.

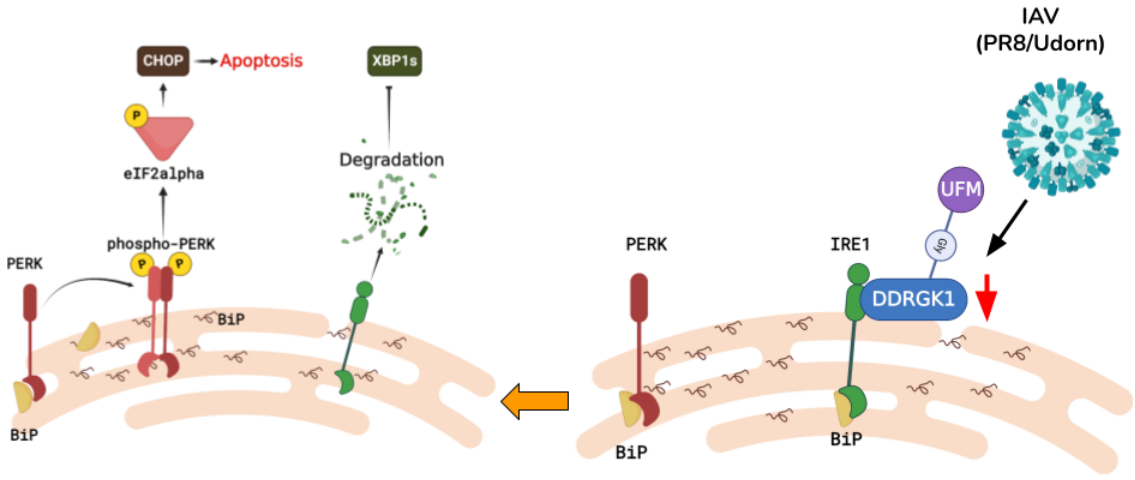

Figure 4-2 IAV infection downregulates DDRGK1 expression by host shutoff. In the thesis work, the downregulation of DDRGK1 expression by host shutoff was demonstrated. In previous studies, it was shown that UFMylated DDRGK1 can interact with IRE1 and stabilize it. When DDRGK1 does not stabilize IRE1 it is degraded and the PERK pathway is activated which leads to apoptosis. Figure was made with Biorender

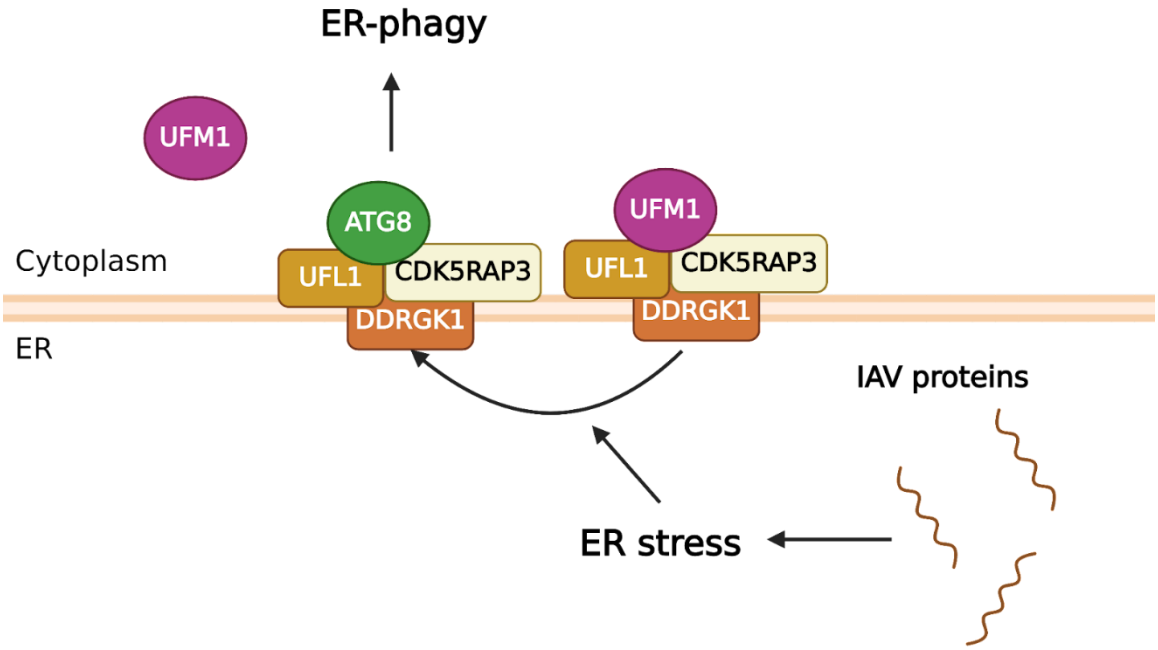

Figure 4-3. CDK5RAP3 as ER-phagy receptor under ER stress conditions. Accumulation of unfolded proteins in ER induced by extensive synthesis of viral proteins induces ER stress. Under ER stress conditions, the binding of UFM1 to CDK5RAP3 weakens and ATG8 competitively binds to CDK5RAP3. It in its turn induces ER-phagy of ER sheets. Figure was made with Biorender

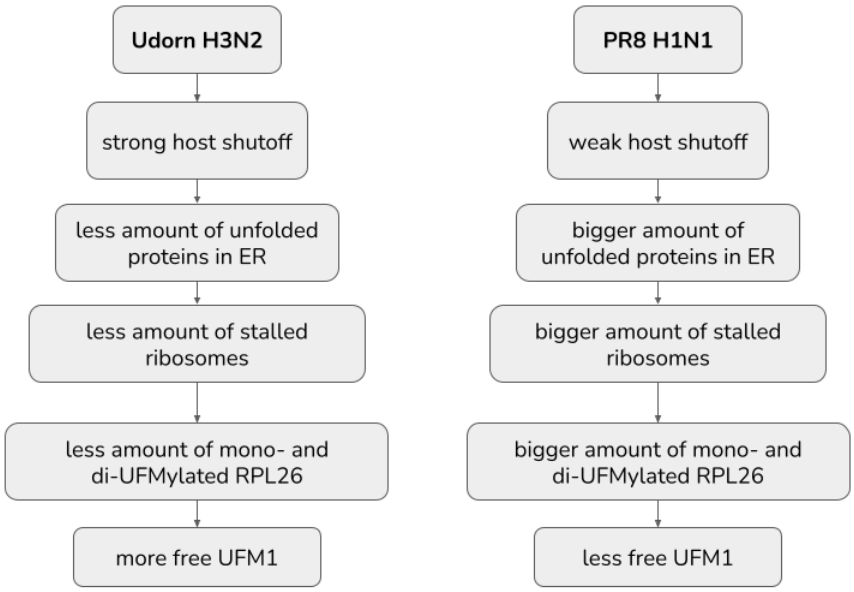

Figure 4-4 Consequences of different types of host shutoff during PR8 and Udorn infections reflected in UFMylome changes of the host cell. Udorn virus induces strong host shutoff while PR8 induce weak host shutoff.

References

Abdullahi, A., Stanojcic, M., Parousis, A., Patsouris, D., & Jeschke, M. G. (2017). Modeling acute ER stress in vivo and in vitro. *Shock, 47(4)*, 506-513.

Aragón, T., de la Luna, S., Novoa, I., Carrasco, L., Ortín, J., & Nieto, A. (2000). Eukaryotic translation initiation factor 4GI is a cellular target for NS1 protein, a translational activator of influenza virus. *Molecular and cellular biology, 20(17)*, 6259-6268.

Artarini, A., Meyer, M., Shin, Y. J., Huber, K., Hilz, N., Bracher, F., & ... Karlas, A. (2019). Regulation of influenza A virus mRNA splicing by CLK1. *Antiviral research, 168*, 187-196.

Banerjee, I., Miyake, Y., Nobs, S. P., Schneider, C., Horvath, P., Kopf, M., & ... & Yamauchi, Y. (2014). Influenza A virus uses the aggresome processing machinery for host cell entry. *Science, 346(6208)*, 473-477.

Banerjee, S., Kumar, M., & Wiener, R. (2020). Decrypting UFMylation: how proteins are modified with UFM1. *Biomolecules, 10(10)*, 1442.

Banerjee, S., Varga, J. K., Kumar, M., Zoltsman, G., Rotem-Bamberger, S., Cohen-Kfir, E., & ... & Wiener, R. (2023). Structural study of UFL1-UFC1 interaction uncovers the role of UFL1 N-terminal helix in ufmylation. *EMBO reports, 24(12)*, e56920.

Bavagnoli, L., Cucuzza, S., Campanini, G., Rovida, F., Paolucci, S., Baldanti, F., & Maga, G. (2015). The novel influenza A virus protein PA-X and its naturally deleted variant show different enzymatic properties in comparison to the viral endonuclease PA. *Nucleic acids research, 43(19)*, 9405-9417.

Beale, R., Wise, H., Stuart, A., Ravenhill, B. J., Digard, P., & & Randow, F. (2014). A LC3-interacting motif in the influenza A virus M2 protein is required to subvert autophagy and maintain virion stability. *Cell host & microbe, 15(2)*, 239-247.

Bercovich-Kinori, A., Tai, J., Gelbart, I. A., Shitrit, A., Ben-Moshe, S., Drori, Y., & ... & Stern-Ginossar, N. (2016). A systematic view on influenza induced host shutoff. *Elife, 5*, e18311.

Bui, M., Whittaker, G., & Helenius, A. (1996). Effect of M1 protein and low pH on nuclear transport of influenza virus ribonucleoproteins. *Journal of virology, 70(12)*, 8391-8401.

Bull, V. H., & Thiede, B. (2012). Proteome analysis of tunicamycin-induced ER stress. *Electrophoresis, 33(12)*, 1814-1823.

Cai, W., & Yang, H. (2016). The structure and regulation of Cullin 2 based E3 ubiquitin ligases and their biological functions. *Cell division, 11*, 1-11.

Calistri, A., Munegato, D., Carli, I., Parolin, C., & Palù, G. (2014). The ubiquitin-conjugating system: multiple roles in viral replication and infection. *Cells, 3(2)*, 386-417.

Cao, Y., Li, R., Shen, M., Li, C., Zou, Y., Jiang, Q., & ... Cai, Y. (2021). DDRGK1, a crucial player of ufmylation system, is indispensable for autophagic degradation by regulating lysosomal function. *Cell Death & Disease, 12(5)*, 416.

Chaimayo, C., Dunagan, M., Hayashi, T., Santoso, N., & Takimoto, T. (2018). Specificity and functional interplay between influenza virus PA-X and NS1 shutoff activity. *PLoS pathogens, 14(11)*, e1007465.

Chang, S., Sun, D., Liang, H., Wang, J., Li, J., Guo, L., & Wang, X. (2015). Cryo-EM structure of influenza virus RNA polymerase complex at 4.3 Å resolution. *Molecular cell, 57(5)*, 925-935.

Chen, Z., Li, Y., & & Krug, R. M. (1999). Influenza A virus NS1 protein targetspoly (A)-binding protein II of the cellular 3′-end processing machinery. *The EMBO journal*.

Chenavier, F., Estrozi, L. F., Teulon, J. M., Zarkadas, E., Freslon, L. L., Pellequer, J. L., & ... & Crépin, T. (2023). Cryo-EM structure of influenza helical nucleocapsid reveals NP-NP and NP-RNA interactions as a model for the genome encapsidation. *Science Advances, 9(50)*, eadj9974.

Chlanda, P., Mekhedov, E., Waters, H., Sodt, A., Schwartz, C., Nair, V., & ... Zimmerberg, J. (2017). Palmitoylation contributes to membrane curvature in influenza A virus assembly and hemagglutinin-mediated membrane fusion. *Journal of virology, 91(21)*, 10-1128.

Ciechanover, A. (2015). The unravelling of the ubiquitin system. *Nature reviews Molecular cell biology, 16(5)*, 322-324.

Cros, J., García-Sastre, A., & P., P. (2005). An unconventional NLS is critical for the nuclear import of the influenza A virus nucleoprotein and ribonucleoprotein. *Traffic, 6(3)*, 205-213.

Cui, L., Zheng, W., Li, M., Bai, X., Yang, W., Li, J., & ... Liu, W. (2019). Phosphorylation status of tyrosine 78 residue regulates the nuclear export and ubiquitination of influenza A virus nucleoprotein. *Frontiers in microbiology, 10*, 1816.

Dawson, A. R., Wilson, G. M., Freiberger, E. C., Mondal, A., Coon, J. J., & Mehle, A. (2020). Phosphorylation controls RNA binding and transcription by the influenza virus polymerase. *PLoS Pathogens, 16(9)*, e1008841.

Deshaies, R. J., & Joazeiro, C. A. (2009). RING domain E3 ubiquitin ligases. *Annual review of biochemistry, 78*, 399-434.

Dias, A., Bouvier, D., Crépin, T., McCarthy, A. A., Hart, D. J., Baudin, F., & ... Ruigrok, R. W. (2009). The cap-snatching endonuclease of influenza virus polymerase resides in the PA subunit. *Nature, 458(7240)*, 914-918.

Díaz-Villanueva, J. F., Díaz-Molina, R., & García-González, V. (2015). Protein folding and mechanisms of proteostasis. *International journal of molecular sciences, 16(8)*, 17193-17230.

Dou, D., Revol, R., Östbye, H., Wang, H., & Daniels, R. (2018). Influenza A virus cell entry, replication, virion assembly and movement. *Frontiers in immunology, 9*, 383042.

Ekiert, D. C., Bhabha, G., Elsliger, M. A., Friesen, R. H., Jongeneelen, M., Throsby, M., & ... Wilson, I. A. (2009). Antibody recognition of a highly conserved influenza virus epitope. *Science, 324(5924)*, 246-251.

Evseev, D., & Magor, K. E. (2021). Molecular evolution of the influenza A virus non-structural protein 1 in interspecies transmission and adaptation. *Frontiers in microbiology, 12*, 693204.

Frabutt, D. A., Wang, B., Riaz, S., Schwartz, R. C., & Zheng, Y. H. (2018). Innate sensing of influenza A virus hemagglutinin glycoproteins by the host endoplasmic

reticulum (ER) stress pathway triggers a potent antiviral response via ER-associated protein degradation. *Journal of Virology, 92(1)*, 10-1128.

Fujiyoshi, Y., Kume, N., Sakata, K., & Sato, B. (1994). Fine structure of influenza A virus observed by electron cryo-microscopy. *The EMBO journal, 13(2)*, 318-326.

Gack, M. U., Albrecht, R. A., Urano, T., Inn, K. S., Huang, I. C., Carnero, E., & ... García-Sastre, A. (2009). Influenza A virus NS1 targets the ubiquitin ligase TRIM25 to evade recognition by the host viral RNA sensor RIG-I. *Cell host & microbe, 5(5)*, 439-449.

Gack, M. U., Shin, Y. C., Joo, C. H., Urano, T., Liang, C., Sun, L., & ... Jung, J. U. (2007). TRIM25 RING-finger E3 ubiquitin ligase is essential for RIG-I-mediated antiviral activity. *Nature, 446(7138)*, 916-920.

Gallagher, P. J., Henneberry, J. M., Sambrook, J. F., & Gething, M. J. (1992). Glycosylation requirements for intracellular transport and function of the hemagglutinin of influenza virus. *Journal of virology, 66(12)*, 7136-7145.

Gannagé, M., Dormann, D., Albrecht, R., Dengjel, J., Torossi, T., Rämer, P. C., & ... Münz, C. (2009). Matrix protein 2 of influenza A virus blocks autophagosome fusion with lysosomes. *Cell host & microbe, 6(4)*, 367-380.

Gao, S., Song, L., Li, J., Zhang, Z., Peng, H., Jiang, W., & ... Huang, W. (2012). Influenza A virus-encoded NS 1 virulence factor protein inhibits innate immune response by targeting IKK. *Cellular microbiology, 14(12)*, 1849-1866.

Gao, S., Wu, J., Liu, R. Y., Li, J., Song, L., Teng, Y., & ... Huang, W. (2015). Interaction of NS2 with AIMP2 facilitates the switch from ubiquitination to SUMOylation of M1 in influenza A virus-infected cells. *Journal of virology, 89(1)*, 300-311.

Gerakis, Y., Quintero, M., Li, H., & Hetz, C. (2019). The UFMylation system in proteostasis and beyond. *Trends in cell biology, 29(12)*, 974-986.

Giese, S., Ciminski, K., Bolte, H., Moreira, É. A., Lakdawala, S., Hu, Z., & ... Schwemmle, M. (2017). Role of influenza A virus NP acetylation on viral growth and replication. *Nature communications, 8(1)*, 1259.

Gordon, D. E., Jang, G. M., Bouhaddou, M., Xu, J., Obernier, K., White, K. M., & ... Krogan, N. J. (2020). A SARS-CoV-2 protein interaction map reveals targets for drug repurposing. *Nature, 583(7816)*, 459-468.

Goulding, L. V., Yang, J., Jiang, Z., Zhang, H., Lea, D., Emes, R. D., & ... Chang, K. C. (2020). Thapsigargin at non-cytotoxic levels induces a potent host antiviral response that blocks influenza A virus replication. *Viruses, 12(10)*, 1093.

Grambas, S., & Hay, A. (1992). Maturation of influenza A virus hemagglutinin—estimates of the pH encountered during transport and its regulation by the M2 protein. *Virology, 190(1)*, 11-18.

Haidari, M., Zhang, W., Ganjehei, L., Ali, M., & Chen, Z. (2011). Inhibition of MLC phosphorylation restricts replication of influenza virus—a mechanism of action for anti-influenza agents. *PLoS One, 6(6)*.

Hale, B. G., Randall, R. E., Ortín, J., & Jackson, D. (2008). The multifunctional NS1 protein of influenza A viruses. *Journal of general virology, 89(10)*, 2359-2376.

Han, Q., Chang, C., Li, L., Klenk, C., Cheng, J., Chen, Y., & ... Xu, K. (2014). Sumoylation of influenza A virus nucleoprotein is essential for intracellular trafficking and virus growth. *Journal of virology, 88(16)*, 9379-9390.

Hänzelmann, P., Stingele, J., Hofmann, K., Schindelin, H., & Raasi, S. (2010). The yeast E4 ubiquitin ligase Ufd2 interacts with the ubiquitin-like domains of Rad23 and Dsk2 via a novel and distinct ubiquitin-like binding domain. *Journal of Biological Chemistry, 285(26)*, 20390-20398.

Hassan, I. H., Zhang, M. S., Powers, L. S., Shao, J. Q., Baltrusaitis, J., Rutkowski, D. T., & ... Monick, M. M. (2012). Influenza A viral replication is blocked by inhibition of the inositol-requiring enzyme 1 (IRE1) stress pathway. *Journal of Biological Chemistry, 287(7)*, 4679-4689.

Hatada, E., & Fukuda, R. (1992). Binding of influenza A virus NS1 protein to dsRNA in vitro. *Journal of General Virology, 73(12)*, 3325-3329.

Hatakeyama, D., Shoji, M., Ogata, S., Masuda, T., Nakano, M., Komatsu, T., & ... Kuzuhara, T. (2022). Acetylation of the influenza A virus polymerase subunit PA in the N-terminal domain positively regulates its endonuclease activity. *The FEBS Journal, 289(1)*, 231-245.

Hatakeyama, S., & Kei-ichi, I. N. (2003). U-box proteins as a new family of ubiquitin ligases. *Biochemical and biophysical research communications, 302(4)*, 635-645.

Hayashi, T., MacDonald, L. A., & Takimoto, T. (2015). Influenza A virus protein PA-X contributes to viral growth and suppression of the host antiviral and immune responses. *Journal of virology, 89(12)*, 6442-6452.

Hershko, A., & Ciechanover, A. (1998). The ubiquitin system. *Annual review of biochemistry, 67(1)*, 425-479.

Hetz, C., Zhang, K., & Kaufman, R. J. (2020). Mechanisms, regulation and functions of the unfolded protein response. *Nature reviews Molecular cell biology, 21(8)*, 421-438.

Hochstrasser, M. (2009). Origin and function of ubiquitin-like proteins. *Nature, 458(7237)*, 422-429.

Hogue, B. G., & Nayak, D. P. (1992). Synthesis and processing of the influenza virus neuraminidase, a type II transmembrane glycoprotein. *Virology*.

Hrincius, E. R., Liedmann, S., Finkelstein, D., Vogel, P., Gansebom, S., Samarasinghe, A. E., & ... McCullers, J. A. (2015). Acute lung injury results from innate sensing of viruses by an ER stress pathway. *Cell reports, 11(10)*, 1591-1603.

Hsiang, T. Y., Zhou, L., & Krug, R. M. (2012). Roles of the phosphorylation of specific serines and threonines in the NS1 protein of human influenza A viruses. *Journal of virology, 86(19)*, 10370-10376.

Hui, X., Cao, L., Xu, T., Zhao, L., Huang, K., Zou, Z., & ... Jin, M. (2022). PSMD12-mediated M1 ubiquitination of influenza A virus at K102 regulates viral replication. *Journal of Virology, 96(15)*.

Hurtley, S. M., Bole, D. G., Hoover-Litty, H., Helenius, A., & Copeland, C. S. (1989). Interactions of misfolded influenza virus hemagglutinin with binding protein (BiP). *The Journal of cell biology, 108(6)*, 2117-2126.

Husain, M., & Cheung, C. Y. (2014). Histone deacetylase 6 inhibits influenza A virus release by downregulating the trafficking of viral components to the plasma membrane via its substrate, acetylated microtubules. *Journal of virology, 88(19)*, 11229-11239.

Ishimura, R., El-Gowily, A. H., Noshiro, D., Komatsu-Hirota, S., Ono, Y., Shindo, M., & ... Komatsu, M. (2022). The UFM1 system regulates ER-phagy through the ufmylation of CYB5R3. *Nature Communications, 13(1)*, 7857.

Ishimura, R., Ito, S., Mao, G., Komatsu-Hirota, S., Inada, T., Noda, N. N., & Komatsu, M. (2023). Mechanistic insights into the roles of the UFM1 E3 ligase complex in ufmylation and ribosome-associated protein quality control. *Science Advances, 9(33)*.

Jagger, B. W., Wise, H. M., Kash, J. C., Walters, K. A., Wills, N. M., Xiao, Y. L., & ... Digard, P. (2012). An overlapping protein-coding region in influenza A virus segment 3 modulates the host response. *Science, 337(6091)*, 199-204.

Kamata, T., & Watanabe, Y. (1977). Role for nucleocapsid protein phosphorylation in the transcription of influenza virus genome. *Nature, 267(5610)*, 460-462.

Karim, M., Biquand, E., Declercq, M., Jacob, Y., van Der Werf, S., & Demeret, C. (2020). Nonproteolytic K29-linked ubiquitination of the PB2 replication protein of influenza A viruses by proviral cullin 4-based E3 ligases. *Mbio, 11(2)*, 10-1128.

Kathum, O. A., Schräder, T., Anhlan, D., Nordhoff, C., Liedmann, S., Pande, A., & ... Ludwig, S. (2016). Phosphorylation of influenza A virus NS1 protein at threonine 49 suppresses its interferon antagonistic activity. *Cellular microbiology, 18(6)*, 784-791.

Khaperskyy, D. A., & McCormick, C. (2015). Timing is everything: coordinated control of host shutoff by influenza A virus NS1 and PA-X proteins. *Journal of virology, 89(13)*, 6528-6531.

Khaperskyy, D. A., Emara, M. M., Johnston, B. P., Anderson, P., Hatchette, T. F., & McCormick, C. (2014). Influenza a virus host shutoff disables antiviral stress-induced translation arrest. *PLoS pathogens, 10(7)*.

Khaperskyy, D. A., Schmaling, S., Larkins-Ford, J., McCormick, C., & Gaglia, M. M. (2016). Selective Degradation of Host RNA Polymerase II Transcripts by Influenza A Virus PA-X Host Shutoff Protein. *PLoS pathogens, 12(2)*.

Khaperskyy, D. A., Schmaling, S., Larkins-Ford, J., McCormick, C., & Gaglia, M. M. (2016). Selective degradation of host RNA polymerase II transcripts by influenza A virus PA-X host shutoff protein. *PLoS pathogens, 12(2)*.

Kim, H., Webster, R. G., & Webby, R. J. (2018). Influenza virus: dealing with a drifting and shifting pathogen. *Viral immunology, 31(2)*, 174-183.

Kirui, J., Mondal, A., & Mehle, A. (2016). Ubiquitination upregulates influenza virus polymerase function. *Journal of virology, 90(23)*, 10906-10914.

Klebanovych, A., Vinopal, S., Dráberová, E., Sládková, V., Sulimenko, T., Sulimenko, V., & ... Dráber, P. (2022). C53 interacting with UFM1-protein ligase 1 regulates microtubule nucleation in response to ER stress. *Cells, 11(3)*, 555.

Koliopoulos, M. G., Lethier, M., van der Veen, A. G., Haubrich, K., Hennig, J., Kowalinski, E., & ... Rittinger, K. (2018). Molecular mechanism of influenza A NS1-mediated TRIM25 recognition and inhibition. *Nature communications, 9(1)*, 1820.

Komatsu, M., Chiba, T., Tatsumi, K., Iemura, S. I., Tanida, I., Okazaki, N., & ... Tanaka, K. (2004). A novel protein-conjugating system for Ufm1, a ubiquitin-fold modifier. *The EMBO journal, 23(9)*, 1977-1986.

Košík, I., Praznovska, M., Košíková, M., Bobišová, Z., Hollý, J., Varečková, E., & ... Russ, G. (2015). The ubiquitination of the influenza A virus PB1-F2 protein is crucial for its biological function. *PLoS One, 10(4)*.

Kulsuptrakul, J., Wang, R., Meyers, N. L., Ott, M., & Puschnik, A. S. (2021). A genome-wide CRISPR screen identifies UFMylation and TRAMP-like complexes as host factors required for hepatitis A virus infection. *Cell reports, 34(11)*.

Kumar, M., Padala, P., Fahoum, J., Hassouna, F., Tsaban, T., Zoltsman, G., & ... Wiener, R. (2021). Structural basis for UFM1 transfer from UBA5 to UFC1. *Nature communications, 12(1)*, 5708.

Kuo, R. L., Zhao, C., Malur, M., & Krug, R. M. (2010). Influenza A virus strains that circulate in humans differ in the ability of their NS1 proteins to block the activation of IRF3 and interferon-β transcription. *Virology, 408(2)*, 146-158.

Lamb, R. A., & Choppin, P. W. (1979). Segment 8 of the influenza virus genome is unique in coding for two polypeptides. *Proceedings of the National Academy of Sciences, 76(10)*, 4908-4912.

Landeras-Bueno, S., Fernández, Y., Falcón, A., Oliveros, J. C., & & Ortín, J. (2016). Chemical genomics identifies the PERK-mediated unfolded protein stress response as a cellular target for influenza virus inhibition. *MBio, 7(2)*, 10-1128.

Landeras-Bueno, S., Fernández, Y., Falcón, A., Oliveros, J. C., & Ortín, J. (2016). Chemical genomics identifies the PERK-mediated unfolded protein stress response as a cellular target for influenza virus inhibition. *MBio*.

Li, J., Yu, M., Zheng, W., & Liu, W. (2015). Nucleocytoplasmic shuttling of influenza A virus proteins. *Viruses, 7(5)*, 2668-2682.

Li, S., Min, J. Y., Krug, R. M., & Sen, G. C. (2006). Binding of the influenza A virus NS1 protein to PKR mediates the inhibition of its activation by either PACT or double-stranded RNA. *Virology, 349(1)*, 13-21.

Li, Y., Sun, L., Zheng, W., Li, J., Bi, Y., Wang, H., & ... Luo, T. R. (2018). Phosphorylation and dephosphorylation of threonine 188 in nucleoprotein is crucial for the replication of influenza A virus. *Virology, 520*, 30-38.

Liang, J. R., Lingeman, E., Luong, T., Ahmed, S., Muhar, M., Nguyen, T., & ... Corn, J. E. (2020). A genome-wide ER-phagy screen highlights key roles of mitochondrial metabolism and ER-resident UFMylation. *Cell, 180(6)*, 1160-1177.

Liao, T. L., Wu, C. Y., Su, W. C., Jeng, K. S., & Lai, M. M. (2010). Ubiquitination and deubiquitination of NP protein regulates influenza A virus RNA replication. *The EMBO journal, 29(22)*, 3879-3890.

Lin, C. Y., Shih, M. C., Chang, H. C., Lin, K. J., Chen, L. F., Huang, S. W., & ... Ling, P. (2021). Influenza a virus NS1 resembles a TRAF3-interacting motif to target the RNA sensing-TRAF3-type I IFN axis and impair antiviral innate immunity. *Journal of biomedical science, 28*, 1-17.

Liu, C. H., Zhou, L., Chen, G., & Krug, R. M. (2015). Battle between influenza A virus and a newly identified antiviral activity of the PARP-containing ZAPL protein. *Proceedings of the National Academy of Sciences, 112(45)*, 14048-14053.

Liu, J., Guan, D., Dong, M., Yang, J., Wei, H., Liang, Q., & ... Cong, Y. S. (2020). UFMylation maintains tumour suppressor p53 stability by antagonizing its ubiquitination. *Nature cell biology, 22(9)*, 1056-1063.

Liu, J., Wang, Y., Song, L., Zeng, L., Yi, W., Liu, T., & ... Cong, Y. S. (2017). A critical role of DDRGK1 in endoplasmic reticulum homoeostasis via regulation of IRE1α stability. *Nature communications, 8(1)*, 14186.

Livak, K. J., & Schmittgen, T. D. (2001). Analysis of relative gene expression data using real-time quantitative PCR and the 2− ΔΔCT method. *methods, 25(4)*, 402-408.

Luo, G., Luytjes, W., Enami, M., & Palese, P. (1991). The polyadenylation signal of influenza virus RNA involves a stretch of uridines followed by the RNA duplex of the panhandle structure. *Journal of virology, 65(6)*, 2861-2867.

Ma, J., Wu, R., Xu, G., Cheng, Y., Wang, Z., Wang, H. A., & ... Sun, J. (2020). Acetylation at K108 of the NS1 protein is important for the replication and virulence of influenza virus. *Veterinary research, 51*, 1-10.

Mamelund, S. (2008). Influenza, historical. *Medicine, 54*, 361-371.

Manzoor, R., Igarashi, M., & Takada, A. (2017). Influenza A virus M2 protein: roles from ingress to egress. *International journal of molecular sciences, 18(12)*, 2649.

Marques, M., Ramos, B., Soares, A. R., & Ribeiro, D. (2019). Cellular proteostasis during influenza A virus infection—friend or foe? *Cells, 8(3)*, 228.

Marreiros, R., Müller-Schiffmann, A., Trossbach, S. V., Prikulis, I., Hänsch, S., Weidtkamp-Peters, S., & ... Korth, C. (2020). Disruption of cellular proteostasis by H1N1 influenza A virus causes α-synuclein aggregation. *Proceedings of the National Academy of Sciences, 117(12)*, 6741-6751.

Martínez-Alonso, M., Hengrung, N., & Fodor, E. (2016). RNA-free and ribonucleoprotein-associated influenza virus polymerases directly bind the serine-5-phosphorylated carboxyl-terminal domain of host RNA polymerase II. *Journal of virology, 90(13)*, 6014-6021.

Matrosovich, M., Matrosovich, T., Garten, W., & Klenk, H. D. (2006). New low-viscosity overlay medium for viral plaque assays. *Virology journal, 3*, 1-7.

Matsuoka, Y., Matsumae, H., Katoh, M., Eisfeld, A. J., Neumann, G., Hase, T., & ... Kawaoka, Y. (2013). A comprehensive map of the influenza A virus replication cycle. *BMC systems biology, 7*, 1-18.

Mazel-Sanchez, B., Iwaszkiewicz, J., Bonifacio, J. P., Silva, F., Niu, C., Strohmeier, S., & ... Schmolke, M. (2021). Influenza A viruses balance ER stress with host protein synthesis shutoff. *Proceedings of the National Academy of Sciences, 118(36)*.

Millrine, D., Peter, J. J., & Kulathu, Y. (2023). A guide to UFMylation, an emerging posttranslational modification. *The FEBS Journal, 290(21)*, 5040-5056.

Min, J. Y., & Krug, R. M. (2006). The primary function of RNA binding by the influenza A virus NS1 protein in infected cells: Inhibiting the 2′-5′ oligo (A) synthetase/RNase L pathway. *Proceedings of the National Academy of Sciences, 103(18)*, 7100-7105.

Mizushima, T., Tatsumi, K., Ozaki, Y., Kawakami, T., Suzuki, A., Ogasahara, K., & ... Yamane, T. (2007). Crystal structure of Ufc1, the Ufm1-conjugating enzyme. *Biochemical and biophysical research communications, 362(4)*, 1079-1084.

Mochida, K., & Nakatogawa, H. (2022). ER-phagy: selective autophagy of the endoplasmic reticulum. *EMBO reports, 3(3)*, 285-287.

Moeller, A., Kirchdoerfer, R. N., Potter, C. S., Carragher, B., & Wilson, I. A. (2012). Organization of the influenza virus replication machinery. *Science, 338(6114)*, 1631-1634.

Momose, F., Basler, C. F., O'Neill, R. E., Iwamatsu, A., Palese, P., & Nagata, K. (2001). Cellular splicing factor RAF-2p48/NPI-5/BAT1/UAP56 interacts with the influenza virus nucleoprotein and enhances viral RNA synthesis. *Journal of virology, 75(4)*, 1899-1908.

Mondal, A., Potts, G. K., Dawson, A. R., Coon, J. J., & Mehle, A. (2015). Phosphorylation at the homotypic interface regulates nucleoprotein oligomerization and assembly of the influenza virus replication machinery. *PLoS pathogens, 11(4)*.

Monto, A. S., Gravenstein, S., Elliott, M., Colopy, M., & Schweinle, J. (2000). Clinical signs and symptoms predicting influenza infection. *Archives of internal medicine, 160(21)*, 3243-3247.

Morreale, F. E., & Walden, H. (2016). Types of ubiquitin ligases. *Cell, 165(1)*, 248-248.

Nakada, R., Hirano, H., & Matsuura, Y. (2015). Structure of importin-α bound to a non-classical nuclear localization signal of the influenza A virus nucleoprotein. *Scientific reports, 5(1)*, 15055.

Nakagawa, Y., Oda, K., & Nakada, S. (1996). The PB1 subunit alone can catalyze cRNA synthesis, and the PA subunit in addition to the PB1 subunit is required for viral

RNA synthesis in replication of the influenza virus genome. *Journal of virology, 70(9)*, 6390-6394.

Nemeroff, M. E., Barabino, S. M., Li, Y., Keller, W., & Krug, R. M. (1998). Influenza virus NS1 protein interacts with the cellular 30 kDa subunit of CPSF and inhibits 3′ end formation of cellular pre-mRNAs. *Molecular cell, 1(7)*, 991-1000.

Neumann, G., Castrucci, M. R., & Kawaoka, Y. (1997). Nuclear import and export of influenza virus nucleoprotein. *Journal of virology, 71(12)*, 9690-9700.

Nie, T., Zhu, L., & Yang, Q. (2021). The classification and basic processes of autophagy. *Autophagy: Biology and Diseases: Technology and Methodology*, 3-16.

O'Neill, R. E., Talon, J., & Palese, P. (1998). The influenza virus NEP (NS2 protein) mediates the nuclear export of viral ribonucleoproteins. *The EMBO journal*.

Oweis, W., Padala, P., Hassouna, F., Cohen-Kfir, E., Gibbs, D. R., Todd, E. A., & ... Wiener, R. (2016). Trans-binding mechanism of ubiquitin-like protein activation revealed by a UBA5-UFM1 complex. *Cell reports, 16(12)*, 3113-3120.

Ozato, K., Shin, D. M., Chang, T. H., & Morse III, H. C. (2008). TRIM family proteins and their emerging roles in innate immunity. *Nature reviews immunology, 8(11)*, 849-860.

Padala, P., Oweis, W., Mashahreh, B., Soudah, N., Cohen-Kfir, E., Todd, E. A., & ... Wiener, R. (2017). Novel insights into the interaction of UBA5 with UFM1 via a UFM1-interacting sequence. *Scientific reports, 7(1)*, 508.

Panthu, B., Terrier, O., Carron, C., Traversier, A., Corbin, A., Balvay, L., & ... Ohlmann, T. (2017). The NS1 protein from influenza virus stimulates translation initiation by enhancing ribosome recruitment to mRNAs. *Journal of Molecular Biology, 429(21)*, 3334-3352.

Parsons, L. M., An, Y., de Vries, R. P., de Haan, C. A., & Cipollo, J. F. (2017). Glycosylation characterization of an influenza H5N7 hemagglutinin series with engineered glycosylation patterns: implications for structure–function relationships. *Journal of proteome research, 16(2)*, 398-412.

Peter, J. J., Magnussen, H. M., DaRosa, P. A., Millrine, D., Matthews, S. P., Lamoliatte, F., & ... Kulathu, Y. (2022). A non-canonical scaffold-type E3 ligase complex mediates protein UFMylation. *The EMBO Journal, 41(21)*.

Poon, L. L., Pritlove, D. C., Fodor, E., & Brownlee, G. G. (1999). Direct evidence that the poly (A) tail of influenza A virus mRNA is synthesized by reiterative copying of a U track in the virion RNA template. *Journal of virology, 73(4)*, 3473-3476.

Potter, C. (2001). A history of influenza. *Journal of applied microbiology, 91(4)*, 572-579.

Protter, D. S., & Parker, R. (2016). Principles and properties of stress granules. *Trends in cell biology, 26(9)*, 668-679.

Pumroy, R. A., Ke, S., Hart, D. J., Zachariae, U., & Cingolani, G. (2015). Molecular determinants for nuclear import of influenza A PB2 by importin α isoforms 3 and 7. *Structure, 23(2)*, 374-384.

Qiu, Y., & Krug, R. (1994). The influenza virus NS1 protein is a poly (A)-binding protein that inhibits nuclear export of mRNAs containing poly (A). *Journal of virology, 68(4)*, 2425-2432.

Qiu, Y., Nemeroff, M., & Krug, R. M. (1995). The influenza virus NS1 protein binds to a specific region in human U6 snRNA and inhibits U6-U2 and U6-U4 snRNA interactions during splicing. *Rna, 1(3)*, 304-316.

Rabouw, H. H., Langereis, M. A., Anand, A. A., Visser, L. J., de Groot, R. J., Walter, P., & van Kuppeveld, F. J. (2019). Small molecule ISRIB suppresses the integrated stress response within a defined window of activation. *Proceedings of the National Academy of Sciences, 116(6)*, 2097-2102.

Rajsbaum, R., & García-Sastre, A. (2013). Viral evasion mechanisms of early antiviral responses involving regulation of ubiquitin pathways. *Trends in microbiology, 21(8)*, 421-429.

Roberson, E. C., Tully, J. E., Guala, A. S., Reiss, J. N., Godburn, K. E., Pociask, D. A., & ... Anathy, V. (2012). Influenza induces endoplasmic reticulum stress, Caspase-12–dependent apoptosis, and c-jun n-terminal kinase–mediated transforming growth factor–β release in lung epithelial cells. *American journal of respiratory cell and molecular biology, 46(5)*, 573-581.

Sala, A. J., Bott, L. C., & Morimoto, R. I. (2017). Shaping proteostasis at the cellular, tissue, and organismal level. *Journal of Cell Biology, 216(5)*, 1231-1241.

Samji, T. (2009). Influenza A: understanding the viral life cycle. *The Yale journal of biology and medicine, 82(4)*, 153.

Santos, A., Pal, S., Chacón, J., Meraz, K., Gonzalez, J., Prieto, K., & Rosas-Acosta, G. (2013). SUMOylation affects the interferon blocking activity of the influenza A nonstructural protein NS1 without affecting its stability or cellular localization. *Journal of virology, 87(10)*, 5602-5620.

Sasakawa, H., Sakata, E., Yamaguchi, Y., Komatsu, M., Tatsumi, K., Kominami, E., & ... Kato, K. (2006). Solution structure and dynamics of Ufm1, a ubiquitin-fold modifier 1. *Biochemical and biophysical research communications, 343(1)*, 21-26.

Satterly, N., Tsai, P. L., Van Deursen, J., Nussenzveig, D. R., Wang, Y., Faria, P. A., & ... Fontoura, B. M. (2007). Influenza virus targets the mRNA export machinery and the nuclear pore complex. *Proceedings of the National Academy of Sciences, 104(6)*, 1853-1858.

Scavone, F., Gumbin, S. C., Da Rosa, P. A., & Kopito, R. R. (2023). RPL26/uL24 UFMylation is essential for ribosome-associated quality control at the endoplasmic reticulum. *Proceedings of the National Academy of Sciences, 120(16)*.

Schmoldt, C., Vazquez-Armendariz, A. I., Shalashova, I., Selvakumar, B., Bremer, C. M., Peteranderl, C., & ... Herold, S. (2019). IRE1 signaling as a putative therapeutic target in influenza virus–induced pneumonia. *American Journal of Respiratory Cell and Molecular Biology, 61(4)*, 537-540.

Schulze, I. (1972). The structure of influenza virus: II. A model based on the morphology and composition of subviral particles. *Virology, 47(1)*, 181-196.

Selman, M., Dankar, S. K., Forbes, N. E., Jia, J. J., & Brown, E. G. (2012). Adaptive mutation in influenza A virus non-structural gene is linked to host switching and induces a novel protein by alternative splicing. *Emerging microbes & infections, 1(1)*, 1-10.

Shapiro, G. I., Gurney Jr, T., & Krug, R. M. (1987). Influenza virus gene expression: control mechanisms at early and late times of infection and nuclear-cytoplasmic transport of virus-specific RNAs. *Journal of virology, 61(3)*, 764-773.

Slaine, P. D., Kleer, M., Duguay, B. A., Pringle, E. S., Kadijk, E., Ying, S., & ... Khaperskyy, D. A. (2021). Thiopurines activate an antiviral unfolded protein response that blocks influenza A virus glycoprotein accumulation. *Journal of Virology, 95(11)*, 10-1128.

Smit, J. J., & Sixma, T. K. (2014). RBR E3-ligases at work. *EMBO reports, 15(2)*, 142-154.

Snider, D. L., Park, M., Murphy, K. A., Beachboard, D. C., & Horner, S. M. (2022). Signaling from the RNA sensor RIG-I is regulated by ufmylation. *Proceedings of the National Academy of Sciences, 119(15)*.

Stebbins, C. E., Kaelin Jr, W. G., & Pavletich, N. P. (1999). Structure of the VHL-ElonginC-ElonginB complex: implications for VHL tumor suppressor function. *Science, 284(5413)*, 455-461.

Stephani, M., Picchianti, L., Gajic, A., Beveridge, R., Skarwan, E., Sanchez de Medina Hernandez, V., & ... Dagdas, Y. (2020). A cross-kingdom conserved ER-phagy receptor maintains endoplasmic reticulum homeostasis during stress. *elife, 9*.

Su, W. C., Chen, Y. C., Tseng, C. H., Hsu, P. W., Tung, K. F., Jeng, K. S., & Lai, M. M. (2013). Pooled RNAi screen identifies ubiquitin ligase Itch as crucial for influenza A virus release from the endosome during virus entry. *Proceedings of the National Academy of Sciences, 110(43)*, 17516-17521.

Su, W. C., Yu, W. Y., Huang, S. H., & Lai, M. M. (2018). Ubiquitination of the cytoplasmic domain of influenza A virus M2 protein is crucial for production of infectious virus particles. *Journal of virology, 92(4)*, 10-1128.

Sun, X., Jayaraman, A., Maniprasad, P., Raman, R., Houser, K. V., Pappas, C., & ... Tumpey, T. M. (2013). N-linked glycosylation of the hemagglutinin protein influences virulence and antigenicity of the 1918 pandemic and seasonal H1N1 influenza A viruses. *Journal of virology, 87(15)*, 8756-8766.

Talon, J., Horvath, C. M., Polley, R., Basler, C. F., Muster, T., Palese, P., & García-Sastre, A. (2000). Activation of interferon regulatory factor 3 is inhibited by the influenza A virus NS1 protein. *Journal of virology, 74(17)*, 7989-7996.

Tatsumi, K., Sou, Y. S., Tada, N., Nakamura, E., Iemura, S. I., Natsume, T., & ... Komatsu, M. (2010). A novel type of E3 ligase for the Ufm1 conjugation system. *Journal of biological chemistry, 285(8)*, 5417-5427.

Tatu, U., Hammond, C., & Helenius, A. (1995). Folding and oligomerization of influenza hemagglutinin in the ER and the intermediate compartment. *The EMBO Journal, 14(7)*, 1340-1348.

Tran, V., Ledwith, M. P., Thamamongood, T., Higgins, C. A., Tripathi, S., Chang, M. W., & ... Mehle, A. (2020). Influenza virus repurposes the antiviral protein IFIT2 to promote translation of viral mRNAs. *Nature microbiology, 5(12)*, 1490-1503.

Twu, K., Kuo, R., Marklund, J., & Krug, R. (2007). The H5N1 influenza virus NS genes selected after 1998 enhance virus replication in mammalian cells. *Journal of virology, 81(15)*, 8112-8121.

Ueda, M., Yamate, M., Du, A., Daidoji, T., Okuno, Y., Ikuta, K., & Nakaya, T. (2008). Maturation efficiency of viral glycoproteins in the ER impacts the production of influenza A virus. *Virus research, 136(1-2)*, 91-97.

van der Veen, A. G., & Ploegh, H. L. (2012). Ubiquitin-like proteins. *Annual review of biochemistry, 81*, 323-357.

Varga, Z. T., Grant, A., Manicassamy, B., & Palese, P. (2012). Influenza virus protein PB1-F2 inhibits the induction of type I interferon by binding to MAVS and decreasing mitochondrial membrane potential. *Journal of virology, 86(16)*, 8359-8366.

Varga, Z. T., Ramos, I., Hai, R., Schmolke, M., García-Sastre, A., Fernandez-Sesma, A., & Palese, P. (2011). The influenza virus protein PB1-F2 inhibits the induction of type I interferon at the level of the MAVS adaptor protein. *PLoS pathogens, 7(6)*.

Vester, D., Lagoda, A., Hoffmann, D., Seitz, C., Heldt, S., Bettenbrock, K., & ... Reichl, U. (2010). Real-time RT-qPCR assay for the analysis of human influenza A virus transcription and replication dynamics. *Journal of virological methods, 168(1-2)*, 63-71.

Walczak, C. P., Leto, D. E., Zhang, L., Riepe, C., Muller, R. Y., DaRosa, P. A., & ... Kopito, R. R. (2019). Ribosomal protein RPL26 is the principal target of

UFMylation. *Proceedings of the National Academy of Sciences, 116(4)*, 1299-1308.

Wang, L., Xu, Y., Rogers, H., Saidi, L., Noguchi, C. T., Li, H., & ... Ye, Y. (2020). UFMylation of RPL26 links translocation-associated quality control to endoplasmic reticulum protein homeostasis. Cell research, 30(1), 5-20. *Cell research, 30(1)*, 5-20.

Wang, S., Zhao, Z., Bi, Y., Sun, L., Liu, X., & Liu, W. (2013). Tyrosine 132 phosphorylation of influenza A virus M1 protein is crucial for virus replication by controlling the nuclear import of M1. *Journal of virology, 87(11)*, 6182-6191.

Wang, Y., Argiles-Castillo, D., Kane, E. I., Zhou, A., & Spratt, D. E. (2020). HECT E3 ubiquitin ligases–emerging insights into their biological roles and disease relevance. *Journal of cell science, 133(7)*.

Weber, P. C., Ohlendorf, D. H., Wendoloski, J. J., & Salemme, F. R. (1989). Structural origins of high-affinity biotin binding to streptavidin. *Science, 243(4887)*, 85-88.

Webster, R. G. (1999). Antigenic variation in influenza viruses. *In Origin and evolution of viruses. Academic Press.*, 377-390.

Wei, D., & Sun, Y. (2010). Small RING finger proteins RBX1 and RBX2 of SCF E3 ubiquitin ligases: the role in cancer and as cancer targets. *Genes & cancer, 1(7)*, 700-707.

Wise, H. M., Foeglein, A., Sun, J., Dalton, R. M., Patel, S., Howard, W., & ... Digard, P. (2009). A complicated message: Identification of a novel PB1-related protein translated from influenza A virus segment 2 mRNA. *Journal of virology, 83(16)*, 8021-8031.

Wise, H. M., Hutchinson, E. C., Jagger, B. W., Stuart, A. D., Kang, Z. H., Robb, N., & ... Digard, P. (2012). Identification of a novel splice variant form of the influenza A virus M2 ion channel with an antigenically distinct ectodomain. *PLoS pathogens, 8(11)*.

Witting, K. F., & Mulder, M. P. (2021). Highly specialized ubiquitin-like modifications: shedding light into the UFM1 enigma. *Biomolecules, 11(2)*, 255.

Wu, C. Y., Jeng, K. S., & Lai, M. M. (2011). The SUMOylation of matrix protein M1 modulates the assembly and morphogenesis of influenza A virus. *Journal of virology, 85(13)*, 6618-6628.

Yang, S., Yang, R., Wang, H., Huang, Y., & Jia, Y. (2020). CDK5RAP3 deficiency restrains liver regeneration after partial hepatectomy triggering endoplasmic reticulum stress. *The American Journal of Pathology, 190(12)*, 2403-2416.

Yin, Y., Yu, S., Sun, Y., Qin, T., Chen, S., Ding, C., & ... Liu, X. (2020). Glycosylation deletion of hemagglutinin head in the H5 subtype avian influenza virus enhances its virulence in mammals by inducing endoplasmic reticulum stress. *Transboundary and Emerging Diseases, 67(4)*, 1492-1506.

Yiu, S. P., Zerbe, C., Vanderwall, D., Huttlin, E. L., Weekes, M. P., & Gewurz, B. E. (2023). An Epstein-Barr virus protein interaction map reveals NLRP3 inflammasome evasion via MAVS UFMylation. *Molecular cell, 83(13)*, 2367-2386.

Yoo, H. M., Kang, S. H., Kim, J. Y., Lee, J. E., Seong, M. W., Lee, S. W., & ... Chung, C. H. (2014). Modification of ASC1 by UFM1 is crucial for ERα transactivation and breast cancer development. *Molecular cell, 56(2)*, 261-274.

Yoshimura, A., Kuroda, K., Kawasaki, K., Yamashina, S., Maeda, T., & Ohnishi, S. I. (1982). Infectious cell entry mechanism of influenza virus. *Journal of Virology, 43(1)*, 284-293.

Zhang, T., Ye, Z., Yang, X., Qin, Y., Hu, Y., Tong, X., & ... Ye, X. (2017). NEDDylation of PB2 reduces its stability and blocks the replication of influenza A virus. *Scientific Reports, 7(1)*, 43691.

Zhang, Y., Zhang, M., Wu, J., Lei, G., & Li, H. (2012). Transcriptional regulation of the Ufm1 conjugation system in response to disturbance of the endoplasmic reticulum homeostasis and inhibition of vesicle trafficking. *PloS one, 7(11)*.

Zhao, C., Hsiang, T. Y., Kuo, R. L., & Krug, R. M. (2010). ISG15 conjugation system targets the viral NS1 protein in influenza A virus–infected cells. *Proceedings of the National Academy of Sciences, 107(5)*, 2253-2258.

Zhao, N., Sebastiano, V., Moshkina, N., Mena, N., Hultquist, J., Jimenez-Morales, D., & ... Marazzi, I. (2018). Influenza virus infection causes global RNAPII termination defects. *Nature structural & molecular biology, 25(9)*, 885-893.

Zheng, W., Cao, S., Chen, C., Li, J., Zhang, S., Jiang, J., & ... Liu, W. (2017). Threonine 80 phosphorylation of non-structural protein 1 regulates the replication of influenza A virus by reducing the binding affinity with RIG-I. *Cellular microbiology, 19(2)*.

Zheng, W., Li, J., Wang, S., Cao, S., Jiang, J., Chen, C., & ... Liu, W. (2015). Phosphorylation controls the nuclear-cytoplasmic shuttling of influenza A virus nucleoprotein. *Journal of virology, 89(11)*, 5822-5834.